

**APPLICATION OF STOCHASTIC SIMULATION FOR  
HYDROCARBON IN PLACE ESTIMATION**



Miss Patchalalai Isarangkura

A Thesis Submitted in Partial Fulfillment of the Requirements  
for the Degree of Master of Engineering in Petroleum Engineering  
Department of Mining and Petroleum Engineering

Faculty of Engineering  
Chulalongkorn University

Academic Year 2004

ISBN 974-17-7062-6

Copyright of Chulalongkorn University

การประยุกต์ใช้แบบจำลองการเฟ้นสุ่มในการประมาณค่าปริมาณไฮโดรคาร์บอนในแหล่งกักเก็บ

นางสาวพัชราลัย อิศรางกูร ณ อยุธยา

สถาบันวิทยบริการ

วิทยานิพนธ์นี้เป็นส่วนหนึ่งของการศึกษาตามหลักสูตรปริญญาวิศวกรรมศาสตรมหาบัณฑิต  
สาขาวิชาวิศวกรรมปิโตรเลียม ภาควิชาวิศวกรรมเหมืองแร่และปิโตรเลียม

คณะวิศวกรรมศาสตร์ จุฬาลงกรณ์มหาวิทยาลัย

ปีการศึกษา 2547

ISBN 974-17-7062-6

ลิขสิทธิ์ของจุฬาลงกรณ์มหาวิทยาลัย

Thesis Title            APPLICATION OF STOCHASTIC SIMULATION FOR  
HYDROCARBON IN PLACE ESTIMATION  
By                        Patchalalai Isarangkura  
Field of Study        Petroleum Engineering  
Thesis Advisor        Suwat Athichanagorn, Ph.D.  
Thesis Co-advisor    Sunthorn Pumjan, Ph.D.

---

Accepted by the Faculty of Engineering, Chulalongkorn University in  
Partial Fulfillment of the Requirements for the Master's Degree

..... Dean of the Faculty of Engineering  
(Professor Direk Lavansiri, Ph.D.)

#### THESIS COMMITTEE

..... Chairman  
(Associate Professor Yingyos Khemayodhin)

..... Thesis Advisor  
(Assistant Professor Suwat Athichanagorn, Ph.D.)

..... Thesis Co-advisor  
(Sunthorn Pumjan, Ph.D.)

..... Member  
(Jirawat Chewaroungroj, Ph.D.)

พัชรลาชัย อิศรางกูร ณ อยุธยา: การประยุกต์ใช้แบบจำลองการ फैนสุ่มในการประมาณค่าปริมาณไฮโดรคาร์บอนในแหล่งกักเก็บ (APPLICATION OF STOCHASTIC SIMULATION FOR HYDROCARBON IN PLACE ESTIMATION) อาจารย์ที่ปรึกษา: ผศ. ดร. สุวัฒน์ อธิษณากร, อาจารย์ที่ปรึกษาร่วม: ดร. สุนทร พุ่มจันทร์ จำนวนหน้า 123 หน้า, ISBN 974-17-7062-6

การประมาณค่าปริมาณไฮโดรคาร์บอนในแหล่งกักเก็บมีความสำคัญอย่างมากต่อการพัฒนาแหล่งกักเก็บ วิธีการประมาณค่าทางปริมาตรซึ่งต้องใช้ความพรุนของหินและความอิ่มตัวของน้ำเป็นวิธีการหนึ่งของการประมาณค่าปริมาณไฮโดรคาร์บอนในแหล่งกักเก็บ ในงานวิจัยนี้มุ่งเน้นการประมาณการกระจายตัวของความพรุนของหินและความอิ่มตัวของน้ำโดยอ้างอิงจากข้อมูลจริงในแหล่งกักเก็บที่หาได้ โดยใช้แบบจำลองการ फैนสุ่มที่แตกต่างกันคือ Monte Carlo Simulation (MCS), Sequential Gaussian Simulation (SGS), และ Sequential Gaussian Cosimulation (SGCOSIM) ความพรุนของหินและความอิ่มตัวของน้ำสามารถประมาณค่าได้ในรูปแบบของฟังก์ชันความน่าจะเป็น (probability distribution function) และนำค่าดังกล่าวไปใช้ในการประมาณค่าปริมาณไฮโดรคาร์บอนในแหล่งกักเก็บ รวมถึงสามารถประมาณความไม่แน่นอนของค่าปริมาณไฮโดรคาร์บอนในแหล่งกักเก็บได้อีกด้วย

ข้อมูลของลักษณะต่างๆในแหล่งกักเก็บที่ใช้ในงานวิจัยนี้ได้มาจากหลุมเจาะจำนวนสามหลุมที่เจาะในแหล่งก๊าซธรรมชาติ ข้อมูลค่าความพรุนของหินและความอิ่มตัวของน้ำ ถูกนำมาใช้เป็นข้อมูลสำหรับแบบจำลองการ फैนสุ่มทั้งสามวิธี เพื่อใช้ในการประมาณค่าปริมาณก๊าซธรรมชาติเริ่มต้นในแหล่งกักเก็บก๊าซ ผลจากค่าปริมาณก๊าซธรรมชาติเริ่มต้นในแหล่งกักเก็บก๊าซที่ได้จากทั้งสามวิธี ถูกนำมาเปรียบเทียบเพื่อหาวิธีที่ดีที่สุด และเมื่อพิจารณาจากค่าความแปรปรวนที่ต่ำที่สุดของค่าปริมาณก๊าซธรรมชาติเริ่มต้นในแหล่งกักเก็บก๊าซพบว่า วิธี SGCOSIM ให้ผลลัพธ์ที่ดีที่สุด

ในการวิเคราะห์ความไวต่อการเปลี่ยนแปลงของค่าตัวแปรลักษณะโครงสร้างของพื้นที่ ได้แก่ nugget, search distance, และ correlation coefficient ซึ่งหากพิจารณาจากค่าเฉลี่ย และค่าความความแปรปรวนที่เกิดขึ้นเมื่อมีการเปลี่ยนแปลงตัวแปรทั้งสามดังกล่าวพบว่า ค่า nugget มีผลกระทบต่อเปลี่ยนแปลงค่าปริมาณก๊าซธรรมชาติเริ่มต้นในแหล่งกักเก็บก๊าซมากที่สุด รองลงมาคือ correlation coefficient และ search distance ตามลำดับ

ภาควิชาวิศวกรรมเหมืองแร่และปิโตรเลียม  
สาขาวิชาวิศวกรรมปิโตรเลียม  
ปีการศึกษา 2547

ลายมือชื่อนิติ.....  
ลายมือชื่ออาจารย์ที่ปรึกษา.....  
ลายมือชื่ออาจารย์ที่ปรึกษาร่วม.....

## 4571607221: MAJOR PETROLEUM ENGINEERING

KEY WORD: /HYDROCARBON IN PLACE ESTIMATION/STOCHASTIC  
SIMULATION

PATCHALALAI ISARANGKURA. THESIS TITLE: APPLICATION OF  
STOCHASTIC SIMULATION FOR HYDROCARBON IN PLACE  
ESTIMATION. THESIS ADVISOR: SUWAT ATHICHANAGORN, Ph.D.  
THESIS CO-ADVISOR: SUNTHORN PUMJAN, Ph.D. 123 pp.  
ISBN 974-17-7062-6

Original hydrocarbon in place estimation is very important in oil field development. The volumetric method which requires the estimates of porosity and water saturation is one of the techniques to determine original hydrocarbon in place. This study focuses on the estimation of porosity and water saturation distributions based on available data. Using three different stochastic simulation techniques which are Monte Carlo Simulation (MCS), Sequential Gaussian Simulation (SGS), and Sequential Gaussian Cosimulation (SGCOSIM), porosity and water saturation probability distribution functions were generated and used to estimate original hydrocarbon in place and quantify its uncertainty.

A set of field data obtain from locations along three directional wells drilled in a gas reservoir was selected for this study. Then, the three stochastic methods were used to determine original gas in place (OGIP) for the selected area of gas field. Results from the three methods were compared to determine the best method. Based on the criterion that the best algorithm should provide the least variance of OGIP estimate, SGCOSIM was determined to be the best method.

To quantify the influence of spatial structure variables on hydrocarbon in place estimation, variogram parameters such as nugget value, search distance, and correlation coefficient were varied. Considering the mean and variance of OGIP, the most sensitive spatial structure variables is the nugget value followed by correlation coefficient and search distance.

Department of Mining and Petroleum Engineering Student's signature.....

Field of study: Petroleum Engineering Advisor's signature.....

Academic year: 2004 Co-advisor's signature.....

## Acknowledgments

I would like to express my gratitude to Dr. Suwat Athichanagorn, my advisor, and Dr. Sunthorn Pumjan, my co-advisor for accessibility for discussion, suggestion, and invaluable advice. I would like to gratefully thank Mr. Kevin Perry, Petrophysicist and Mr. Nuttapon Nampratchayakul, Petroleum Engineer (Unocal Thailand Ltd.) for providing the field data for this study and recommendations.

I am grateful to my family for their love, encouragement, and support which helped me so much throughout the hard time during this study.

I would like to thank the thesis committee members for providing comments and suggestions.



สถาบันวิทยบริการ  
จุฬาลงกรณ์มหาวิทยาลัย

# Contents

	<b>Pages</b>
<b>Abstract (in Thai)</b> .....	<b>iv</b>
<b>Abstract (in English)</b> .....	<b>v</b>
<b>Acknowledgements</b> .....	<b>vi</b>
<b>Table of Contents</b> .....	<b>vii</b>
<b>List of Tables</b> .....	<b>ix</b>
<b>List of Figures</b> .....	<b>xi</b>
<b>Nomenclature</b> .....	<b>xiii</b>
<b>Chapter</b>	
<b>1. Introduction and Literatures</b> .....	<b>1</b>
1.1 Introduction .....	1
1.2 Literature review .....	4
1.3 Thesis outline .....	9
<b>2. Theories and Concepts</b> .....	<b>10</b>
2.1 Monte Carlo method .....	10
2.1.1 Statistical convergence of sequences .....	10
2.1.2 The law of large numbers .....	11
2.1.3 Central Limit Theorem .....	11
2.1.4 Monte Carlo Simulation (MCS) .....	15
2.2 Geostatistical Method of Conditional Simulation .....	16
2.2.1 MultiGaussian Model .....	17
2.2.2 Normal Score Transform .....	19
2.2.3 Checking for bivariate normality .....	20
2.2.4 Sequential simulation approach .....	21
2.3 Sequential Gaussian Simulation (SGS) .....	22
2.4 Sequential Gaussian Cosimulation (SGCOSIM) .....	25
2.4.1 The Bayesian framework .....	25
2.4.2 Collocated Cokriging Model .....	26
2.4.3 Makrov Model .....	28
2.4.4 Collocated Cokriging with Makrov Model .....	29



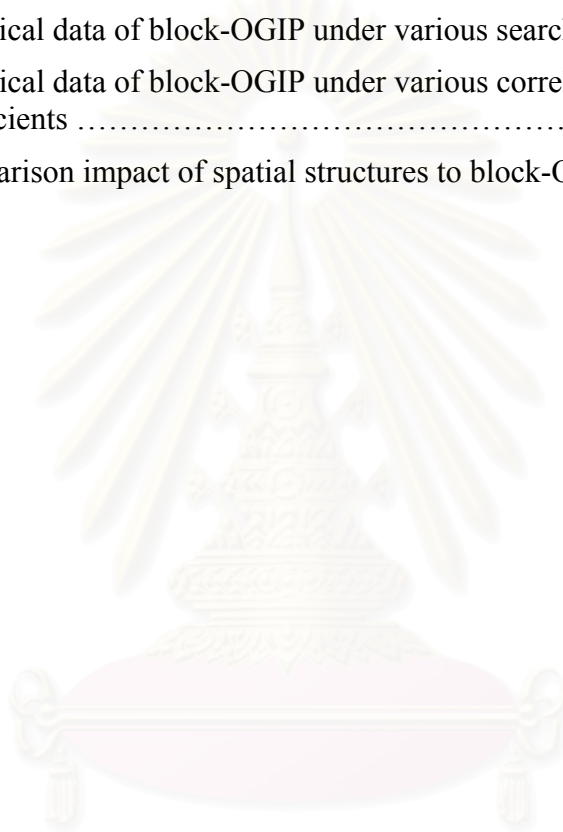
<b>Chapter</b>	<b>Pages</b>
<b>3. Data Preparation .....</b>	<b>32</b>
3.1 General information of data set .....	32
3.2 Statistical analysis of petrophysical variables .....	35
3.3 Related parameters for volumetric OGIP calculation .....	42
<b>4. Application of Stochastic Simulation in Estimation of Hydrocarbon in Place Data Preparation .....</b>	<b>44</b>
4.1 Monte Carlo Simulation (MCS) .....	44
4.1.1 Probability distribution of input variables .....	44
4.1.2 OGIP calculation .....	45
4.1.3 Sensitivity analysis .....	49
4.2 Sequential Gaussian Simulation (SGS) .....	51
4.2.1 Structural analysis (Variogram model) .....	52
4.2.2 Sequential Gaussian Simulation .....	64
4.3 Sequential Gaussian Cosimulation (SGCOSIM) .....	69
4.3.1 Structural analysis (Variogram model) .....	69
4.3.2 Sequential Gaussian Cosimulation .....	79
4.4 Comparison of simulation methods .....	84
4.5 Sensitivity analysis .....	91
4.5.1 Nugget value .....	92
4.5.2 Search distance .....	95
4.5.3 Correlation coefficient .....	97
<b>5. Conclusions and Recommendations .....</b>	<b>102</b>
<b>References .....</b>	<b>108</b>
<b>Appendices .....</b>	<b>110</b>
<b>Vitae .....</b>	<b>123</b>



## List of Tables

<b>Table</b>	<b>Page</b>
3.1 General information from well A, B, and C .....	33
3.2 Porosity, water saturation, permeability, formation resistivity, and locations of Formation I .....	36
3.3 Statistics of well log data in Formation I .....	39
3.4 Correlation among variables in Formation I .....	39
3.5 Gas formation volume factor for three wells located in Formation I	43
4.1 Percentage error in variance for various numbers of realization .....	45
4.2 Comparison between statistics of original and random data .....	46
4.3 The OGIP statistics from MCS .....	47
4.4 OGIP at various percentiles from MCS .....	47
4.5 Sensitivity analysis of input variables to OGIP output .....	50
4.6 Porosity and water saturation normal score transform .....	53
4.7 Variogram parameters in omni and south-east (SE) directions of porosity and water saturation .....	57
4.8 Statistics of the 50 <sup>th</sup> realization of porosity and water saturation generated by SGS-local and global distribution .....	65
4.9 The OGIP statistics from SGS-local and global distribution .....	68
4.10 OGIP at various percentiles from SGS-local and global distribution	68
4.11 Permeability and resistivity normal score transform .....	70
4.12 Parameters for omni-directional variograms of permeability and resistivity .....	75
4.13 Statistics of the 50 <sup>th</sup> realization of porosity and water saturation generated by SGCOSIM-local and global distribution .....	80
4.14 The OGIP statistics from SGCOSIM-local and global distribution	83
4.15 OGIP at various percentiles from SGCOSIM-local and global distribution .....	83
4.16 Statistics of simulated porosity by Conventional MCS, Modified MCS, SGS, and SGCOSIM .....	86

<b>Table</b>	<b>Page</b>
4.17 Statistics of simulated water saturation by Conventional MCS, Modified MCS, SGS, and SGCOSIM .....	86
4.18 Statistics of OGIP obtained from Conventional MCS, Modified MCS, SGS, and SGCOSIM .....	90
4.19 Statistical data of block-OGIP under various nugget values .....	94
4.20 Statistical data of block-OGIP under various search distances .....	97
4.21 Statistical data of block-OGIP under various correlation coefficients .....	100
4.22 Comparison impact of spatial structures to block-OGIP .....	100



สถาบันวิทยบริการ  
จุฬาลงกรณ์มหาวิทยาลัย

## List of Figures

<b>Figure</b>	<b>Page</b>
2.1 Monte Carlo Simulation (MCS) flow chart .....	16
2.2 Sequential Gaussian Simulation (SGS) flow chart .....	24
2.3 Sequential Gaussian Cosimulation (SGCOSIM) flow chart .....	31
3.1 Schematic of Well A, B and C .....	33
3.2 Location map of well log data in Formation I .....	34
3.3 Porosity histogram and cumulative distribution .....	40
3.4 Water saturation histogram and cumulative distribution .....	40
3.5 Permeability histogram and cumulative distribution .....	41
3.6 Resistivity histogram and cumulative distribution .....	41
4.1 OGIP probability distribution function from MCS .....	48
4.2 OGIP cumulative distribution function from MCS .....	48
4.3 Histogram of normal score transform for porosity and water saturation .....	56
4.4 Omni-directional variograms of the original data and normal score transform of porosity .....	58
4.5 Omni-directional variograms of the original data and normal score transform of water saturation .....	59
4.6 Variograms in the south-east (SE) direction of the original data and normal score transform of porosity .....	60
4.7 Variograms in the south-east (SE) direction of the original data and normal score transform of water saturation .....	61
4.8 Experimental and Gaussian model-derived indicator variograms for porosity at median cutoff (0.5 cdf value) .....	63
4.9 Experimental and Gaussian model-derived indicator variograms for water saturation at median cutoff (0.5 cdf value) .....	63
4.10 Example of porosity realization generated by SGS-local and global distribution at layer # 50 .....	66
4.11 Example of water saturation realization generated by SGS-local and global distribution at layer # 50 .....	66

<b>Figure</b>	<b>Page</b>
4.12 Histogram of OGIP obtained from SGS-local and global distribution variables .....	67
4.13 Histogram of original and normal score transform of permeability	73
4.14 Histogram of original and normal score transform of resistivity ....	74
4.15 Omni –directional variograms of the original data and normal score transform of permeability .....	76
4.16 Omni –directional variograms of the original data and normal score transform of resistivity .....	77
4.17 Experimental and Gaussian model-derived indicator variograms for permeability at median cutoff (0.5 cdf value) .....	78
4.18 Experimental and Gaussian model-derived indicator variograms for resistivity at median cutoff (0.5 cdf value) .....	79
4.19 Example of porosity realization generated by SGCOSIM-local and global distribution at layer # 50 .....	81
4.20 Example of water saturation realization generated SGCOSIM-local and global distribution at layer # 50 .....	82
4.21 Histogram of OGIP obtain from SGCOSIM-local and global distribution variables .....	84
4.22 Histogram of simulated porosity by Conventional MCS, Modified MCS, SGS, and SGCOSIM .....	87
4.23 Histogram of simulated water saturation by Conventional MCS, Modified MCS, SGS, and SGCOSIM .....	88
4.24 Cumulative distribution of simulated porosity and water saturation by Conventional MCS, Modified MCS, SGS, and SGCOSIM .....	89
4.25 The well locations and positions of drawn sample for sensitivity analysis .....	93
4.26 Histogram of porosity in block for different nugget values .....	93
4.27 Histogram of porosity in block for different search distances .....	96
4.28 Histogram of porosity in block for different correlation coefficients	99

## Nomenclature

$A$	area
$Ac$	accuracy
$B_g$	gas formation volume factor
$B_o$	oil formation volume factor
$C$	confidence
$C(h)$	stationary covariance between any two random variables separated by vector $h$
$C_Y(u)$	correlogram
cdf	cumulative distribution function
$E$	Expectation
$F^{-1}(p)$	inverse cumulative distribution function for the probability value
$F_Y(y)$	cumulative distribution function of a random variable $Y$
$F_Z(z)$	cumulative distribution function of a random variable $Z$
$f(u)$	uniform probability density function
$\bar{f}(u)$	average value of uniform probability density function
$G(y)$	standard normal cumulative distribution function
$G^{-1}(p)$	standard normal $p$ -quantile function
$h$	thickness
$I$	intergral
$I(u ; p)$	Binary indicator random function at location $u$ and for cutoff $z$
$k$	permeability
$m(u)$	mean at location $u$
$N$	number of sample size
$OGIP$	original gas in place
$OOIP$	original oil in place
$Prob$	probability
$p$	pressure
pdf	probability distribution function

RF	Random function
$Rt$	resistivity
RV	Random variables
$S_w$	water saturation
$T$	temperature
$u_n$	uniform probability density at $n$ random variables
$Y(u)$	generic variable function of location $u$
$Z$	gas compressibility factor
$Z_i$	joint distribution
$Z(u)$	generic random variable at location $u$
$z(u)$	generic variable function of location $u$
$z^{(l)}(u)$	$l$ -th realizations of the random function $Z(u)$ at location $u$

### GREEK LETTERS

$\phi$	porosity
$\infty$	infinity
$\sigma$	standard deviation
$\sigma^2$	variance
$\rho(h)$	stationary correlogram function
$\omega_\alpha$	Kriging weight associated to datum $\alpha$
$\lambda_\alpha$	Kriging weight associated to datum $\alpha$
$\lambda_\beta$	Kriging weight associated to datum $\beta$
$\nu_l$	Kriging weight associated to datum $l$
$\gamma(h)$	variogram function
$\gamma_I(h; p)$	stationary indicator semivariogram for lag vector $h$ and cutoff $p$ -quantile
$\mu(u)$	Lagrange parameter for Kriging at location $u$

**SUBSCRIPTS**

<i>COSK</i>	cokriging
<i>OK</i>	ordinary Kriging
<i>SK</i>	simple Kriging
<i>sc</i>	standard condition



สถาบันวิทยบริการ  
จุฬาลงกรณ์มหาวิทยาลัย



# CHAPTER I

## INTRODUCTION AND LITERATURES

### 1.1 Introduction

The original hydrocarbon in place can be estimated from several methods. These include volumetric and material balance methods. The accuracy of the estimate varies with the quality and quantity of raw data available and estimation method. The volumetric method is the most commonly used since it does not rely on production data. Original hydrocarbon in place is directly calculated from the following equation.

$$\text{OGIP} = \frac{43560 A h \phi (1 - S_w)}{B_g} \quad (1.1)$$

$$\text{STOOIP} = \frac{7758 A h \phi (1 - S_w)}{B_o} \quad (1.2)$$

where OGIP = Original gas in place, scf

STOOIP = Original oil in place, stb

$A$  = area, acre

$h$  = thickness, ft

$\phi$  = porosity, fraction

$S_w$  = water saturation, fraction

$B_g$  = gas formation volume factor, res cu.ft./scf

$B_o$  = oil formation volume factor, res bbl/stb

The data used in estimating original hydrocarbon in place are geophysical and geological data of reservoir rock and its fluid content. These data are obtained from direct and indirect measurements. Successful original hydrocarbon in place estimation requires sufficient and realistic reservoir description. Various sources of data are useful in making original hydrocarbon in place estimates. Such data are porosity, permeability, and fluid saturations of the reservoir rocks (obtained directly from core analysis or from various types of measurement taken from a well or

several wells); geological maps of the areal extent, thickness, and continuity of reservoir rock (inferred from well logs, geophysical, and geological data). However, the most important aspect in the volumetric method is reservoir descriptions: volume, porosity and water saturation. It has been clearly demonstrated in the past that heterogeneities associated with these parameters have a large impact on connectivity pattern and dynamic behavior of the field. Therefore, a fair estimate of original hydrocarbon in place has to be based on geological model that represents explicitly these heterogeneities.

During exploration or early field development stage, quantification of original hydrocarbon in place has to be conducted due to economic viability assessment. At that time, very small amount of data is available because much of the geological data are measured only at well locations such as data obtained from well logging of which locations are far apart. Sparse sampling can only provide a picture of the general trends of reservoir properties, not their variations. Thus, for reservoir with high geological complexity, estimation of oil or gas in place will contain much more uncertainties. In the past, deterministic methods have been used to estimate original hydrocarbon in place. However, these techniques have shown limitations in cases where reservoirs are heterogeneous or have complex structures. Such failure is due to their deterministic nature which cannot handle uncertainties on geological parameters. This is why stochastic techniques such as Monte-Carlo simulation and Geostatistics have been gradually used for original hydrocarbon in place quantification.

Stochastic method can describe complexity that deterministic methods cannot which is expressed in term of probability distribution function (pdf) for uncertainty assessment in reservoir engineering problems. It can be used to generate variable distribution from a small amount of regional well data availability with ability to preserve the original data and integrate more conditions to enhance reservoir description. Stochastic method is well accepted in the petroleum industry as it has been successfully proven in the mining industry for decades.

The Monte-Carlo simulation is a typical method of stochastic simulation because it is a probabilistic approach. Much of uncertainty analyses consist of an estimation variable under study with a range of values rather than with a single value. It allows a full mapping of uncertainty in model input-output, expressed as probability distribution function. Uncertainty in the model outcome is quantified via multiple model calculations using parameter values drawn randomly from probability distribution function specified for uncertain input. A simulation is a succession of hundreds or thousands of repeated trials. Monte-Carlo simulation takes many simulations to determine the probability distribution function of the output. The inputs are modeled as random variables without taking into account of spatial correlation.

Geostatistics is another methodology with an emphasis on describing and modeling the spatial variability of reservoir properties and the spatial correlation between related properties. The method can be used to construct spatial distribution of reservoir properties from some sampled locations. The key feature of such techniques is its ability to account for spatial character of the data and incorporate many types of geological and engineering data. Spatial continuity is known to be important in describing reservoir parameters since reservoir properties are correlated in space. Lack of spatial information seriously decreases the accuracy of estimated properties. In general, it is likely to increase the accuracy of reservoir properties when using Geostatistics.

In addition, the important characteristic of geostatistical modeling is its probabilistic aspect which can describe more heterogeneity in reservoir model as well as generating a number of equiprobable images of the distribution of the reservoir parameters. Another aspect of geostatistical modeling is the estimation of petrophysical properties at unsampled location. This means geostatistical modeling can recognize and preserve spatial relationships of sample data for estimation of data values or describe uncertainty at unsampled locations.

In some geostatistics applications, the reservoir properties may be simulated independently or interdependently. In reservoir modeling, the most critical

parameters are porosity which is related to reservoir storage, permeability which is related to reservoir flow and flow unit which is related to reservoir connectivity. These parameters are spatially interdependent. Porosity and water saturation may be related as well. These spatial interdependent characteristics can be incorporated into the simulation model. By taking account correlated variables into simulation model, stochastic images which are generated from model of covariance and cross-variance between parameters, are obtained from joint simulation approach.

## 1.2 Literature Review

Stochastic methods for reservoir characterization have been used in many applications. An ultimate goal of reservoir characterization is improved prediction of future performance of the reservoir. Stochastic methods have been developed from a conceptually simple model to a complex model. Monte Carlo Simulation (MCS) methodology is a simple stochastic method used at the early stage of field development. Volumetric calculation of original hydrocarbon in place is one of its applications. Behrenbruch (1985) used MCS to estimate the gross rock volume in reserves estimation. He demonstrated that the probability distribution function of gross rock volume could be constructed by dividing the formation into substructure details, i.e., faults, unconformity surface, and intra-reservoir horizon. Using MCS, a large number of maps for each individual specific reservoir were constructed related to these uncertainties.

When performing Monte Carlo Simulation, probability distribution function has to be defined. Murtha (1997) illustrated the application of MCS by assigning appropriate probability distribution for each input. He stated that some specific probability distribution functions of parameters for the volumetric estimation of original hydrocarbon in place are typical. Normal distribution function can be used to describe data of porosity, percent of minerals in rock. Lognormal distribution function is often used for many of the volumetric model inputs such as net-to-gross ratio and hydrocarbon saturation. Oil or gas formation volume factor typically appears in uniform distribution. Alternatively, some literatures stated that porosity is best represented by lognormal distribution function and reservoir area is fairly

defined by triangular distribution. In addition, original hydrocarbon in place obtained from MCS typically has a lognormal distribution. Therefore, uncertainty analysis can be evaluated by distribution of output.

Moreover, MCS can be applied in case that when there are only few data available. Nakayama (2000) used MCS to generate many pseudo wells in order to make the sample data set bigger. For each of the simulated pseudo wells, seismic attributes were generated and used as sample data in addition to the actual well data, and then the reserves were evaluated. He also claimed that when there are too small numbers of known data points, the usual geostatistics method is hardly applied. Hence, defining the range and distribution of uncertainty inputs are unlikely to be precise when data availability is an issue. Alternative methods are proposed as more suitable when information regarding parameter uncertainty is limited (Mishra 1996). First-order second moment method (FOSM), pointed estimated method, and first-order reliability method were proposed for the assessment of uncertainty in volumetric reserves estimation. Even the result showed that the alternative methods are efficient in computing model output, MCS is still reliable when there is a sufficient number of realizations.

Monte Carlo Simulation is a resampling with replacement from the original sample data. Hence, the only statistics that MCS uses is the sample probability. The original sample data set is a subset of the global population. Ideally, one would want to resample from the entire population (reservoir). Monte Carlo Simulation resamples from the sampled data (subset of a population) instead of resampling from the entire population. Every time a new value is resampled, it is resampled from exactly the same distribution no matter what the previously resampled values are. Because of this, MCS procedure would not be able to correct any bias in the original sample data. It approximates the variability in the entire population by the variability in the sample data (Bitanov 2003). Furthermore, Monte Carlo Simulation implicitly assumes all variables to be independent. In reality, many models contain parameters that depend on each other. For instance, porosity and water saturation may depend on each other, i.e., rock with higher porosity tends to have smaller water saturation (Thanh 2002). This assumption creates a potential risk of producing too narrow



range of possible outcomes. If dependency exists between the data, the output range would miss taking dependency into account. Independent sampling cannot account for such spatial continuity effects. Thus, the application of MCS when spatial dependence prevails is questionable.

Geostatistics is capable of taking into account the spatial continuity and integrating geological data. It also offers a collection of deterministic and statistical tools, aims at understanding and modeling spatial variability. Geostatistical method provides two kinds of prediction which are estimation and simulation. Kriging is known as a linear estimation technique, providing unbiased estimates with minimum variances. It is deterministic, leading to a single reservoir model, which has smooth estimate values. A smooth map, as provided by Kriging, is appropriate for showing the global trends. The presence of a few very high and low values tends to inflate local average, and simple interpolation may mislead interpretation and decision. In that case, the linear estimators may not be the best to reflect the degree of local variability.

Simulation technique was initially developed to correct for the smoothing effect shown on maps produced by Kriging algorithm. It is composed of two steps: (1) calculation of an unconditionally simulated value at each point in an area and (2) adjustment of these values to honor sampled values. Hohn (1998) stated that when simulation honors the sampled values, it said to be “conditional”. Examples of conditional simulation are Sequential Gaussian Simulation (SGS), Sequential Indicator Simulation (SIS), Gaussian Truncated simulation, and Annealing simulation. This type of techniques allows more heterogeneity that is sensitive to local variability. Conditional simulation is different from Kriging estimation in its ability to create a number of equiprobable images of the distribution. Conditional simulated maps also provide a measure of uncertainty which is defined in term of distribution. Murray (1992) used both Kriging and simulation methods, i.e., Sequential Gaussian Simulation (SGS) and Sequential Indicator Simulation (SIS) to address hydrocarbon pore volume (HPV) area. He found that both conditional simulation methods (SGS and SIS) could clearly indicate high and low HPV area

which means indication of spatial uncertainty while Kriging gave a smooth interpolated map of HPV.

Conditional techniques have been applied on reproduction of reservoir parameters. Sequential Gaussian Simulation (SGS) is commonly used to generate the distribution of petrophysical properties, i.e., porosity and permeability. Sahin *et al.* (2001) indicated that reservoir simulation model using the average value of porosity from several realizations which were derived from SGS as an input appeared to have more realistic levels of heterogeneity when compared with Kriging techniques. Likewise, Petit *et al.* (1994) demonstrated that hydrocarbon in place can be quantified in the case of very heterogeneous field where the complex fluid patterns prevent us from using deterministic or probabilistic methods. When geostatistical model for petrophysical attributes such as porosity generated by SGS and static connectivity technique to locate gas water contact pattern, the model provides relatively reliable and realistic heterogeneity. Also, he indicated that geostatistical model is an alternative to quantify total uncertainty of hydrocarbon in place.

Commonly, we have to perform conditional simulation of petrophysical properties by adapting a two-stage approach. In the first stage, the geological description is simulated using a conditional simulation technique such as Sequential Indicator Simulation or Gaussian Truncated Simulation. Secondly, petrophysical properties are simulated for each type of geological facies using a conditional simulation technique such as Sequential Gaussian Simulation or Simulated Annealing. The simulated petrophysical properties are then filtered using the generated geological simulation to produce the final simulation result. The drawback of this approach is its intensive computation time since it requires several simulations.

In typical reservoir modeling, petrophysical properties that are correlated cannot be simulated independently (Landa *et al.* 2002). It seems reasonable that the addition of cross-correlated information will produce good estimates. The effort to jointly simulate or cosimulate interdependent attributes such as porosity and permeability has been discussed by several authors using several methods. However,



these techniques require tedious inference and modeling of covariances and cross covariances, full cokriging. Although Gaussian simulation with full cokriging is made conditional to all secondary data, instability of cokriging matrix will occur if the secondary data are numerous and smoothly vary in space. Another co-simulation technique that eliminates the requirement of solving the full cokriging system has been proposed by Xu *et al.* (1992). The technique is based on a collocated cokriging and a Markov-type hypothesis. This hypothesis simplifies the inference and modeling of the cross covariances. When the collocated technique is used, an assumption of a linear relationship among the attributes needs to be applied. The technique is based on a combination of simultaneous sequential Gaussian simulation and a conditional distribution technique. Using this technique, the user is free from developing cross variograms.

However, the collocated technique makes an assumption that the primary and secondary data points have the same spatial continuity. Bahar *et al.* (2000) applied the cosimulation technique to generate petrophysical properties such as porosity and permeability. They demonstrated the capability of cosimulation through a known reference system. The simulated petrophysical properties are consistent with the underlying reference. Furthermore, as in any conditional simulation methodology, the authors emphasized that conditioning data plays a very important role in determining the result of this cosimulation technique. Ayoub *et al.* (2002) compared several stochastic modeling techniques: Kriging, SGS, Kriging with external 3D drift and collocated cokriging, to build porosity, permeability, and saturation models. Results showed that the collocated cokriging with external drift as the soft data gave the best match with well data and fit with the geology of reservoir. Also, in water saturation modeling by collocated cokriging using 3D-depth as soft data, the impact of water saturation on original oil in place was reduced. Almeida (1993) proved that simulated value honors local statistics when it is conditioned with sampled data and previously simulated data. The study showed that when using collocated co-simulation through Sequential Gaussian Cosimulation (SGCOSIM) to simulate core porosity and permeability which are highly correlated, the sample correlation values

compared to the simulated correlation values were seen to be reasonable. In addition, cosimulation technique has been proven to be successful in several applications.

### **1.3 Thesis Outline**

This thesis paper consists of five chapters.

Chapter 1 outlines introduction and previous works of stochastic simulation, i.e., Monte Carlo Simulation, Sequential Gaussian Simulation, and Sequential Gaussian Cosimulation which have been conducted in order to estimate original hydrocarbon via the volumetric method and also other applications.

Chapter 2 describes the theories and concepts of Monte Carlo Simulation, Sequential Gaussian Simulation, and Sequential Gaussian Cosimulation. These include steps to conduct in each stochastic simulation.

Chapter 3 discusses data preparation in various stochastic simulations. This chapter introduces the general information of Formation I which was selected to be case study and illustrates statistical data of Formation I. The last section in this chapter describes how to estimate parameters needed for original hydrocarbon in place which is used throughout this study.

Chapter 4 discusses application of stochastic simulation. First, Monte Carlo Simulation is applied on real field data prepared in Chapter 3. Sensitivity analysis is presented to quantify impact of input variables: porosity and water saturation to original hydrocarbon in place output. Other conditional simulations: Sequential Gaussian Simulation and Sequential Gaussian Cosimulation are conducted for the same field. Finally, three stochastic simulations are compared and evaluated. The best simulation result is selected for sensitivity study of spatial behavior variables such as nugget, range, and correlation.

Chapter 5 makes conclusion and provides recommendation for future works.

## CHAPTER II

### THEORIES AND CONCEPTS

#### 2.1 Monte Carlo method

The Monte Carlo method can be regarded as a computational tool for solving a problem with statistical methods. The term “Monte Carlo” was apparently first used by Stanislav Ulam and John von Neumann as a Los Alamos code word for the stochastic simulations which was applied to build better atomic bombs. The Monte Carlo method has no formal definition but several general definitions have been offered. For instances, *“A monte Carlo technique is any technique making use of random numbers to solve a problem”* or *“A Monte Carlo method represents the solution of a problem as a parameter of a hypothetical population, and using a random sequence of numbers to construct a sample of the population, from which statistical estimates of the parameter can be obtained”*.

The definition of Monte Carlo method is not important to Monte Carlo Theory. What is really important are the two theorems on which Monte Carlo theory is based: the Law of Large Numbers and the Central Limited theorem. Another way to think of Monte Carlo method is the application of these two theorems to solve a problem using random numbers.

##### 2.1.1 Statistical convergence of sequences

The definition of statistical convergence is stated that *“A sequence of points  $x_1, x_2, \dots, x_n$  in  $X^n$  is said to statistically converge to  $x \in X^n$  if  $\forall \varepsilon > 0 \exists M$  when  $m > M \exists$  a probability  $P$ , with  $0 < P < 1$ , that  $|x_m - x| < \varepsilon$ . We then say the sequence  $x_1, x_2, \dots, x_n$  has the probability  $P$  of converging to  $x$ ”*. From the definition of statistical convergence it means when a sequence statistically converge to some  $x \in X^n$ , it may converge to  $x$  but there is a chance it does not. Thus, values obtained by Monte Carlo method will be given with a confidence  $C$ , and accuracy  $A$ .

### 2.1.2 The law of large numbers

The law of large numbers is a theorem that deals with the behavior of sums of large numbers of random variables. The theorem is stated as followed: “ Let  $u_1, u_2, \dots, u_n$  be  $n$  random variables with uniform probability densities on the interval  $(a, b) \in X$ . Let  $f: X \rightarrow X$  be a piecewise continuous function on the interval  $(a, b) \in X$  ”. Then the limit

$$\lim_{n \rightarrow \infty} \frac{1}{n} \sum_{i=1}^n f(u_i) = \frac{1}{b-a} \int_a^b f(u) du \quad (2.1)$$

Following the law, if the defined function is taken on some interval  $(a, b)$  and  $n$  random points are chosen in  $(a, b)$ , when evaluate  $f$  at each of these points and take the average of evaluations, then as  $n \rightarrow \infty$ , the average of evaluation will be approached the average value of  $f$  on  $(a, b)$ . When integral are evaluated the function at an infinite number of points are evaluated in a certain interval and multiply by the infinitesimally small differential.

It must be noted that using Eq. 2.1 can be obtained a Monte Carlo estimate of an integral. When take part  $\lim_{n \rightarrow \infty}$  out of the equation, then for  $n$  sufficiently large

$$\frac{b-a}{a} \sum_{i=1}^n f(u_i) \approx \int_a^b f(u) du \quad (2.2)$$

Eq. 2.2 can now be used to estimate the value of integral. However, it can't tell how accurate and how much confidence to have in the estimate value. The confidence and accuracy must certainly depend on  $n$ . To determine the accuracy and confidence, Central Limit theorem is used.

### 2.1.3 Central Limit Theorem

This spectacular theorem, which was first proved by Laplace, and later extended by Chebyshev and again by Markov, permeates nearly all of probability theory. It concerns the distribution of the average of large number of independent

random variables. The theorem is stated as follows: “If an experiment and a random variable have an expectation  $E$  and standard deviation  $\sigma$ , then if the experiment is repeated  $n$  times, with average result  $\bar{x}$ , the probability at  $\bar{x}$  is between

$$E + \frac{\sigma}{\sqrt{n}}a \text{ and } E + \frac{\sigma}{\sqrt{n}}b \text{ is approximately } \frac{1}{\sqrt{2\pi}} \int_a^b e^{-y^2/2} dy ”.$$

To better understand this theorem, consider the general example. Suppose random variables with expectation  $E$  and standard deviation  $\sigma$  were repeated this experiment  $n$  times with results  $x_1, x_2, \dots, x_n$ . The Central Limit theorem tells that the distribution of the average  $\bar{x} = \frac{1}{n}(x_1 + \dots + x_n)$  will be approached the normal distribution as  $n \rightarrow \infty$ . The theorem also tells that the distribution of average  $\bar{x}$  will have expectation  $E$  and standard deviation  $\frac{\sigma}{\sqrt{n}}$ . The content of the Central Limit theorem is absolutely remarkable. The fact that the average of any number of trials of an experiment will always be normally distributed permits to solve an unimaginable number of problems. Essentially, any problem that involves sampling can be solved using the Central Limit theorem.

To determine the accuracy  $Ac$  and confidence  $C$  of a Monte Carlo estimate of an integral, firstly the accuracy must be decided, i.e. what the maximum error to allow, and on the confidence. Suppose certain accuracy  $Ac$  and confidence  $C$  is determined to evaluate an integral. Recall that the confidence is merely the probability  $P$ , with  $0 < P < 1$ , that estimate of the integral is within  $Ac$  of the true answer. Recall also that estimate of an integral can be obtained from Eq. 2.2. What to determine now is how large  $n$  must be to evaluate an integral to accuracy  $Ac$  with confidence  $C$ .

Starting with confidence  $C$ , this is corresponding to a certain number  $N$  of standard deviations of the normal distribution curve. The normal distribution curve,  $\mu(x) = \frac{1}{\sqrt{2\pi}} e^{-y^2/2}$ , is continuous at all  $x \in X$ . If integrating the normal distribution  $\mu(x)$  over  $X$ , the area underneath the curve is exactly equal to 1.



Furthermore, the standard deviation of  $\mu(x)$  is 1. These are the reasons why the Gaussian distribution is called the normal distribution. Suppose integrating  $\mu(x)$  over  $(-a, a)$  so that the area underneath the curve is then equal to confidence  $C$ . To find the number  $N$  of standard deviations that correspond to confidence  $C$ , this is what we must to do. Since the standard deviation of  $\mu(x)$  is 1, problem reduces to finding the interval  $(-N, N)$  over which the integral of  $\mu(x)$  equal  $C$ , that is to solve the following equation for  $N$ :

$$C = \frac{1}{\sqrt{2\pi}} \int_{-N}^N e^{-y^2/2} dy \quad (2.3)$$

For example, if desired confidence is 95%, the corresponding number of standard deviations is 2. If desired confidence is 99.7%, the corresponding number of standard deviations is 3. To solve the Eq.2.3, Taylor series is used by integrating Taylor series of  $e^{-y^2/2}$ . Using Taylor series, Eq.2.3 can be rewritten as a polynomial equation that it can be solved using numerical polynomial root-finding methods.

$$e^{-y^2/2} = 1 - \frac{y^2}{2} + \frac{y^4}{8} - \frac{y^6}{48} + \dots \quad (2.4)$$

Eq.2.4 is Taylor series for  $e^{-y^2/2}$ . Using the sixth-degree Taylor polynomial, it should be able to get an estimate for the integral that is accurate enough. Eq.2.3 becomes

$$C \approx \frac{1}{\sqrt{2\pi}} \int_{-N}^N \left( \frac{-y^6}{48} + \frac{y^4}{8} - \frac{y^2}{2} + 1 \right) dy \quad (2.5)$$

$$\text{Integrating Eq. 2.5 } C \approx \frac{1}{\sqrt{2\pi}} \left[ \frac{-y^7}{336} + \frac{y^5}{40} - \frac{y^3}{6} + y \right]_{-N}^N$$

$$\text{which becomes } C \approx \frac{1}{\sqrt{2\pi}} \left( \frac{-N^7}{168} + \frac{N^5}{20} - \frac{N^3}{3} + 2N \right) \quad (2.6)$$

Eq.2.6 can be solved for  $N$  using polynomial root-finding methods. Now that we have the number of standard deviations, we turn to determine the number of points  $n$ , we must evaluate a function to attain the certain accuracy and confidence. Recall from Eq.2.1 that the expectation  $E$  of a function  $f$  is

$$E = \lim_{n \rightarrow \infty} \frac{1}{n} \sum_{i=1}^n f(u_i) = \frac{1}{a-b} \int_a^b f(u) du$$

Let  $\bar{f}(u) \approx \frac{1}{n} \sum_{i=1}^n f(u_i)$  with  $n < \infty$  be the estimate of  $E$ ,

$$I = \lim_{n \rightarrow \infty} \frac{a-b}{n} \sum_{i=1}^n f(u_i) = \int_a^b f(u) du \text{ be the value of integral of } f \text{ over}$$

the interval  $(a, b)$ ,

$$\text{and } i \approx \frac{a-b}{n} \sum_{i=1}^n f(u_i) \text{ be the estimate of integral.}$$

When accuracy  $Ac$  is needed, it means  $|I - i| \leq Ac$ . Clearly  $I = E(a-b)$  and  $i = \bar{f}(u)(a-b)$ . Thus  $|E(a-b) - \bar{f}(u)(a-b)| \leq Ac$ , which is the same as  $|a-b||E - \bar{f}(u)| \leq Ac$ . Thus  $|E - \bar{f}(u)| \leq \frac{Ac}{|a-b|}$ . The Central Limit theorem tells that

the standard deviation of our estimates for the average value of  $f$ , that is  $\bar{f}(u)$ , will be  $\frac{\sigma}{\sqrt{n}}$ . The confidence in estimate for  $\bar{f}(u)$  corresponds to the number of standard

deviations that calculated earlier,  $N$ . To attain a certain confidence in an estimate of  $\bar{f}(u)$  to a certain accuracy, we want the product of our number of standard deviations

$N$  and the standard deviation of  $\bar{f}(u)$ , that is  $\frac{\sigma}{\sqrt{n}}$ , to be less than the desired

accuracy. As already shown that we want  $|E - \bar{f}(u)| \leq \frac{Ac}{|a-b|}$ , thus  $\frac{N\sigma}{\sqrt{n}} \leq \frac{Ac}{|a-b|}$ .

Therefore,  $n^2 \geq \frac{N^2 \sigma^2 (a-b)^2}{Ac^2}$ . This equation tells the minimum number of points



that must evaluate the function  $f$  at to attain a certain accuracy and confidence. However, standard deviation  $\sigma$  of  $f$  is not known. To solve this problem, let  $n$  be sufficiently large, on order of several thousand, and estimate  $\sigma$  via the equation for the variance which equals  $\sigma^2$  ( $\sigma^2 \approx \frac{1}{n} \sum_{i=1}^n (f(u_i) - \bar{f}(u))^2$ ). We can use our estimate for  $\sigma$  to estimate how large  $n$  must be to get a good estimate of the integral  $I$ . Note that we will not know how accurate initial estimate of  $\sigma$  is or how much confidence to have in estimate. However, initial  $\sigma$  and  $\sigma$  obtained using computed value of  $n$  will be compared. If there is not too much difference between two  $\sigma$ 's, it concludes that estimate for the integral  $I$  is accurate enough.

#### 2.1.4 Monte Carlo Simulation (MCS)

Monte Carlo Simulation (MCS) uses statistical sampling techniques in order to estimate parameters of unknown distribution, which is in term of stochastic model. The model is selected such that the value of a quantity of interest is related to the expected value of an estimator for that quantity, which itself is a function of random variables that are part of the model. If the expected value equals the quantity of interest, the estimator is called unbiased. Otherwise it is biased.

The method uses the probability density function (pdf) of the model random variables. The expected value is estimated by averaging the estimator over a large sample of values, which means its pdf has to be determined. A random number generator is used to generate a value for each random variable with probability according to its pdf. From these values the estimator is computed and its value stored (e.g. in a histogram). This process is repeated until the sample is large enough to estimate the properties of the estimator pdf (e.g. mean, variance) to a desired statistical precision. As stated above in two theorems on MCS that is justified by the Law of Large Numbers and Central Limit Theory, namely that the sample mean will approach the expected value with increasing sample size,  $N$ , and its variance will decrease as  $1/N$ .

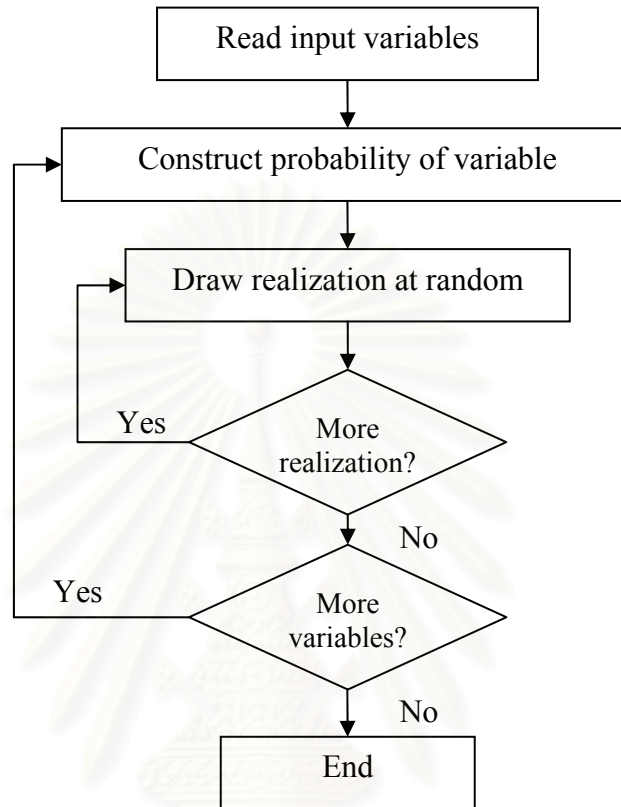


Figure 2.1: Monte Carlo Simulation (MCS) flow chart.

## 2.2 Geostatistical method of conditional simulation

Geostatistical prediction (Kriging) provides the best local estimation of each unsampled value and a measure of its variability (Kriging variance). Stochastic simulation differs from geostatistical prediction (kriging) or any interpolation algorithm. Stochastic simulation is the process of building alternative, equally probable, high resolution model of the spatial distribution. The realizations  $\{z^{(l)}(u), u \in A\}$   $l = 1, \dots, L$  represent  $L$  possible images of the spatial distribution of the attribute value  $z(u)$  over the field  $A$ . Each realization also called a “stochastic image”. The simulation is said to be conditional (to the data) if the resulting realizations honor the primary/hard data values at their location. Conditional simulation was developed to correct for the smoothing effect produced

by kriging algorithm. Each model is representation of reality in some global sense. Each spatial model is different from the others. Each honors the measured samples and previously simulated values, and each is a statistically possible solution. Many alternative models provide a measure of joint spatial uncertainty. Therefore, conditional simulation provide not only the probabilistic structures of variable under the study (a measure of joint spatial uncertainty), but also the natural variability and spatial fluctuation are preserved.

The application of conditional simulation starts the same way as geostatistical estimation, involving structural analysis of spatial variability and the selection of a suitable estimation model. But for now on, the approach diverge. Once the conditional joint probability density function (pdf) is determined, simulated values are uniformly drawn from the estimated joint pdf. These simulated values have two important properties. First, the simulated values equal the sample values at the point where sampling has taken place, and are conditioned to the available sample data and previously simulated data in their local area of influence. Second, the simulated values have the same spatial distribution as the same data. Then, if many simulated values are drawn, the statistical measure of joint spatial uncertainty can be applied.

### 2.2.1 MultiGaussian Model

The main part of the conditional simulation process involves building the conditional cumulative distribution function, ccdf, at point or volume to be simulated. The derivation of ccdf requires joint multivariate distribution of variable involved. The simplest model is being MultiGaussian model which has been applied successfully for modeling continuous variables with little or no continuity of extreme values. Multivariate Gaussian Random Function model is defined through its characteristic properties below:

The RF  $Y(u) = \{Y(u), u \in A\}$  is multivariate normal if and only if:

- All subsets of the RF, for example  $\{Y(u), u \in B \subset A\}$  are also multivariate normal.

- All linear combinations of the RV components of  $Y(u)$  are (univariate) normally distributed, e.g.,

$$X = \sum_{\alpha=1}^n \omega_{\alpha} Y(u_{\alpha}) = \text{normal distribution} \quad (2.7)$$

Whatever the weight,  $\omega_{\alpha}$ , as long as  $u_{\alpha} \in A$

- Zero covariance (or correlation) entail full independence:

If  $Cov\{Y(u), Y(u')\} = 0$ , the two RV's  $Y(u)$  and  $Y(u')$  are not only uncorrelated, they are also independent.

- All conditional distributions of any subset of the RF  $Y(u)$ , given realizations of any other subset, are (multivariate) normal. For example, the conditional distribution  $K$  RV's  $\{Y_k(u'_k), k=1, \dots, K, u'_k \in A\}$  given the realizations  $y(u_{\alpha}) = 1, \dots, n$ , is  $K$ -variate normal,  $\forall k, \forall u'_k, \forall u_{\alpha}, \forall y_{\alpha}$ .

When  $K = 1$ ,  $u'_1 = u_0$  where the RV  $Y(u_0)$  models the uncertainty about a specific unsampled value  $y(u_0)$  is of particular interest: the ccdf of  $Y(u_0)$ , given the  $n$  data  $y_{\alpha}$ , is normal and fully characterized by

a) its mean, or conditional expectation, identified to the SK (Simple Kriging) or linear regression estimates of  $y(u_0)$ .

$$E\{Y(u_0)|y(u_{\alpha}) = y_{\alpha}, \alpha = 1, \dots, n\} \equiv [y(u_0)]^*_{SK} = m(u_0) + \sum_{\alpha=1}^n \lambda_{\alpha} [y_{\alpha} - m(u_{\alpha})] \quad (2.8)$$

where  $m(u) = E\{Y(u)\}$  is the expected value of the not necessarily stationary RV  $Y(u)$ . The  $n$  weights  $\lambda_{\alpha}$  are given by SK system:

$$\sum_{\beta=1}^n \lambda_{\beta} C(u_{\beta}, u_{\alpha}) = C(u_0, u_{\alpha}), \alpha = 1, \dots, n \quad (2.9)$$

where  $C(u, u') = \text{Cov}\{Y(u), Y(u')\}$  is the covariance, not necessarily stationary, of the RF  $Y(u)$ .

b) its variance, or conditional variance, is the SK variance:

$$\text{Var}\{Y(u_0)|y(u_\alpha) = y_\alpha, \alpha = 1, \dots, n\} = C(u_0, u_0) - \sum_{\alpha=1}^n \lambda_\alpha C(u_0, u_\alpha) \quad (2.10)$$

### 2.2.2 Normal score transform

The first necessary condition for the stationary RF  $Y(u)$  to be multivariate normal is that its univariate cdf be normal, i.e.,

$$\text{Prob}\{Y(u) \leq y\} = G(y) \quad \forall y \quad (2.11)$$

where  $G(*)$  is the standard Gaussian cdf;  $Y(u)$  is assumed to be standardized, i.e., with a zero mean and unit variance.

In earth science most data do not present even a normal univariate distribution. Therefore, a necessary condition to apply the algorithm is first to transform the original data into univariate normally distribution values. Simulation is then performed on these values and the result is back transformed into values of the original attribute.

Consider two RV's  $Z$  and  $Y$  with cdf's  $F_Z(z)$  and  $F_Y(y)$  respectively. The transform  $Y = \varphi(Z)$  should identify the cumulative probabilities corresponding to equal  $p$ -quantiles for  $Z$  and  $Y$ ;

$$F_Y(y_p) = F_Z(z_p) = p, \quad \forall p \in [0, 1], \text{ hence, } F_Y^{-1}(F_Z(z)) \quad (2.12)$$

with  $F_Y^{-1}(*)$  being the inverse cdf, or quantile function, of the RV  $Y$ :

$$y_p = F_Y^{-1}(p), \quad \forall p \in [0, 1] \quad (2.13)$$

If  $Y$  is standard normal with cdf  $F_Y(y) = G(y)$ , the transform  $G^{-1}(F_Z(*))$  is the normal score transform.

In practice, the procedure consists of ranking the  $n$   $Z$ -sample data in increasing order:

$$z^{(1)} \leq z^{(2)} \leq \dots \leq z^{(k)} \leq \dots \leq z^{(n)} \quad (2.14)$$

The cumulative frequency corresponding to the  $k^{\text{th}}$  largest  $z$  datum is  $F_Z(z^{(k)}) = k/n$ , or  $F_Z(z^{(k)}) = \sum_{j=1}^k \omega_j \in [0, 1]$  if a set of declustering weights  $\omega_j$  have been applied to the  $n$  data. Then the normal score transform of  $z^{(k)}$  is the  $k/n$ -quantile of the standard normal cdf, i.e.:

$$y_k = G^{-1}\left(\frac{k}{n}\right) \quad (2.15)$$

### 2.2.3 Checking for bivariate normality

The normal score transform defines a new variable  $Y$  which is univariate normally distributed by construction. The Gaussian algorithm requires that this new variable be also multivariate normally distributed. Therefore, before applying algorithm it is recommended to check if the variable  $Y$  is at least bivariate normally distributed.

There are several ways the check for bivariate normality of a data set. One method consists in verifying that the bivariate of cdf of any pairs of values  $Y(u)$ ,  $Y(u+h)$ ,  $\forall h$  is normal. To implement this check, experimental indicator variogram corresponding to specific cut offs are compared to Gaussian theoretical ones obtained through analytical and tabulated relation such as:

$$Pr ob \left\{ Y(u) \leq y_p, Y(u+h) \leq y_p \right\} = p^2 + \frac{1}{2\pi} \int_0^{\arcsin C_Y(h)} \exp\left(-\frac{y_p^2}{1+\sin \theta}\right) d\theta \quad (2.16)$$

where  $y_p = G^{-1}(p)$  is the standard normal  $p$ -quantile and  $C_Y(u)$  is the correlogram of the standard normal RF  $Y(u)$ . The bivariate probability Eq.2.16 is the non-centered indicator covariance for the threshold  $y_p$ :



$$Pr ob \{ Y(u) \leq y_p, Y(u+h) \leq y_p \} = E \{ I(u; p) \cdot I(u+h; p) \} = p - \gamma_I(h; p) \quad (2.17)$$

where  $I(u; p) = 1$ , if  $Y(u) \leq y_p$ , zero, if not; and  $\gamma_I(h; p)$  is the indicator semivariogram for the  $p$ -quantile threshold  $y_p$ .

The comparison between the experimental and Gaussian model derived indicator variograms allows the possibility rejecting the Gaussian model.

#### 2.2.4 Sequential simulation approach

The idea of this approach allows drawing the value of a variable  $Z(u)$  from its conditional distribution given the value of the most related covariance at the same location  $u$ . This means the conditioning is extended to include all data available within a neighborhood of  $u$ , including the original data and all previously simulated values.

Consider the joint distribution of  $N$  random variables  $Z_i$  with  $N$  very large. The  $N$  RV's  $Z_i$  may represent the same attribute at the  $N$  nodes of a dense grid discretizing the field  $A$ , or they can represent  $N$  different attributes measured at the same location, or they could represent a combination of  $K$  different attributes defined at the  $N'$  nodes of a grid with  $N = K N'$ . Next, consider the conditioning of these  $N$  RV's by a set of  $n$  data of any type symbolized by the notation  $| (n)$ . The corresponding  $N$ -variate ccdf is denoted:

$$F_{(N)}(z_1, \dots, z_N | (n)) = Pr ob \{ Z_i \leq z_i, i = 1, \dots, N | (n) \} \quad (2.18)$$

Eq. 2.18 is completely general with no limitations. Some or all variables  $Z_i$  could be categorical.

Successive application of the conditional probability relation shows that drawing an  $N$ -variate sample from the ccdf in Eq. 2.18 can be done in  $N$  successive steps, each involving a univariate ccdf with increasing levels of conditioning:



- draw a value  $z_1^{(l)}$  from the univariate cdf of  $Z_1$  given the original data  $(n)$ . The value  $z_1^{(l)}$  is now considered as a conditioning datum for all subsequent drawings; thus, the information set  $(n)$  is updated to  $(n+1) = (n) \cup \{Z_1 = z_1^{(l)}\}$ .
- draw a value  $z_2^{(l)}$  from the univariate cdf of  $Z_2$  given the updated data set  $(n+1)$ . Then updated the information set to  $(n+2) = (n+1) \cup \{Z_2 = z_2^{(l)}\}$ .
- sequentially consider all  $N$  RV's  $Z_i$ .

The set  $\{z_i^l, i=1, \dots, N\}$  represents a simulated joint realization of the  $N$  dependent RV's  $Z_i$ . If another realization is needed,  $\{z_i^r, i=1, \dots, N\}$ , the entire sequential drawing process is repeated. This sequential simulation procedure requires the determination of  $N$  univariate cdf's, more precisely:

$$\begin{aligned}
 &Pr ob \{ Z_1 \leq z_1 \mid (n) \} \\
 &Pr ob \{ Z_2 \leq z_2 \mid (n+1) \} \\
 &Pr ob \{ Z_3 \leq z_3 \mid (n+2) \} \\
 &\dots \\
 &Pr ob \{ Z_N \leq z_N \mid (n+N-1) \} \quad (2.19)
 \end{aligned}$$

The sequential simulation principle is independent of the algorithm or model used to establish the sequence in Eq.2.19 of univariate cdf's.

### 2.3 Sequential Gaussian Simulation (SGS)

Sequential Gaussian Simulation (SGS) is the most common and straightforward algorithm to generate realizations of a multivariate Gaussian field. By assuming Multivariate normal distribution and sequential simulation approach, SGS algorithm is simulated variable value one cell node after another in a sequential manner, subsequently using these values as the conditional data. To determine the mean and variance of cdf of RF  $Y(u)$  at location  $u$ , Ordinary Kriging is used. Ordinary Kriging (OK) is the best linear unbiased estimator (BLUE). The estimated is weighted which sum of weight is equal one and estimation variance is minimized.

$$Z_{OK}^*(u) = \sum_{\alpha=1}^n \nu_{\alpha}(u) Z(u_{\alpha}) \quad (2.20)$$

And stationary OK system:

$$\begin{cases} \sum_{\beta}^n \nu_{\beta}(u) C(u_{\beta} - u_{\alpha}) + \mu(u) = C(u - u_{\alpha}), & \alpha = 1, \dots, n \\ \sum_{\beta}^n \nu_{\beta}(u) = 1 \end{cases} \quad (2.21)$$

where  $Z(u)$  is the RV model at location  $u$ , the  $u_{\alpha}$ 's are the  $n$  data locations,  $Z_{OK}^*(u)$  is linear regression estimator, also called the Ordinary Kriging (OK) estimator,  $\nu_{\alpha}(u)$ 's are OK weight and  $\mu(u)$  is Lagrange parameter associated with the constraint  $\sum_{\beta}^n \nu_{\beta}(u) = 1$ .

Since defining a random path (sequence indicating the pattern, which all grid locations are visited at only once), random number is drawn. Simulated value at each node is generated from that ccdf following OK system with normal score variogram model at location  $u$ . According to idea of sequential simulation is to use previously simulated value as data for reproducing the covariance between all of simulated values. The number and structure of points included in the simulation is defined by the neighborhood search options. The ability to draw multiple realizations is achieved by setting a different random path for each realization. Under a multivariate Gaussian distribution, each ccdf is Gaussian. Therefore, the data are initially transformed into Normal space, and then simulated valued are finally transformed back into the original space.

The drawback of SGS is that each variable of interest simulated independently, which is deemed inadequate when the representation of the spatial dependence of several variables is needed.

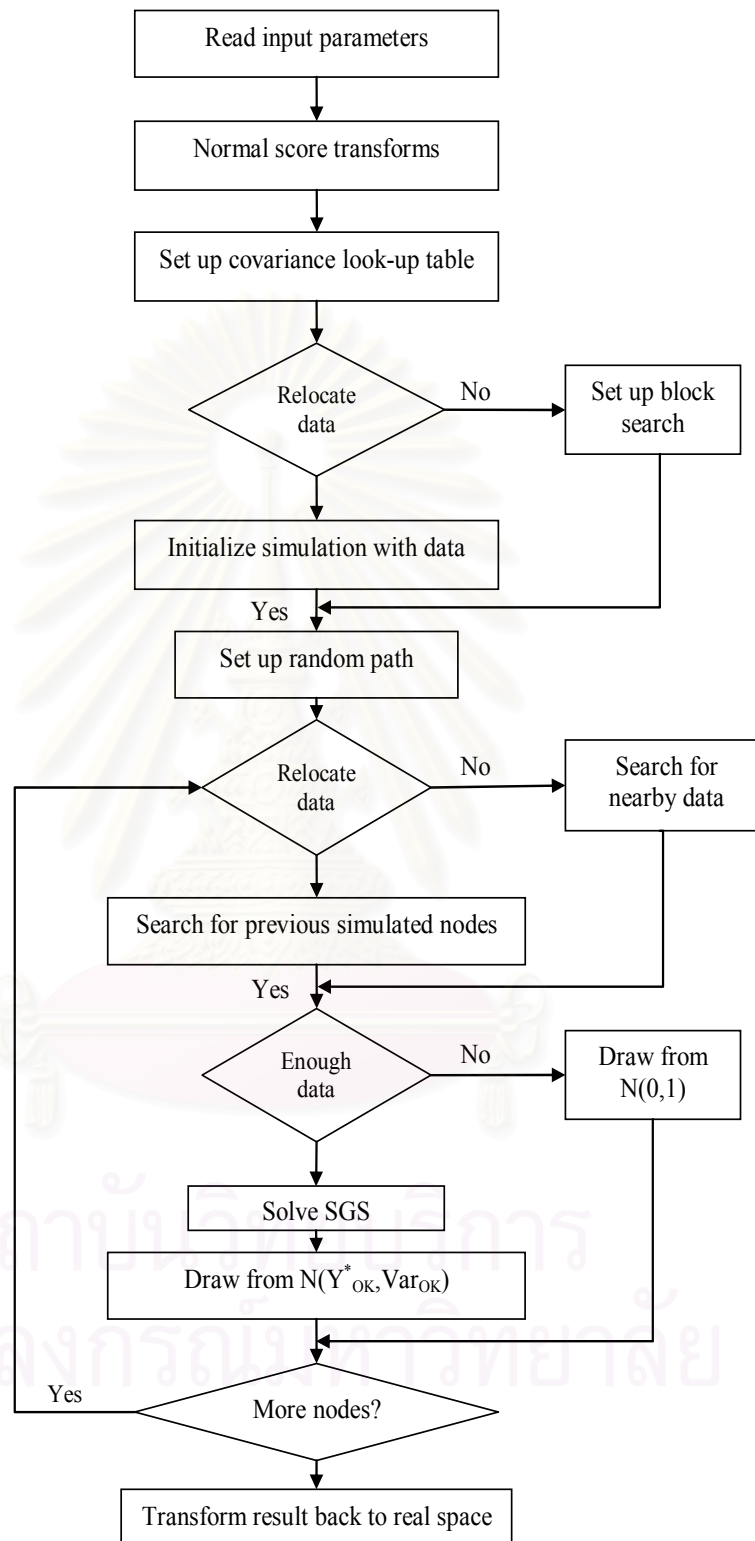


Figure 2.2: Sequential Gaussian Simulation (SGS) flow chart.

## 2.4 Sequential Gaussian Cosimulation (SGCOSIM)

### 2.4.1 The Bayesian framework

All algorithms for joint sequential simulation of several dependent variables are based on Bayes' conditional probability axiom.

Consider a set of  $K$  dependent random events  $A_1, \dots, A_K$  at any location  $u$ . The purpose is to derive alternative equiprobable joint realizations of these events:

$$\{a_j^{(l)}, j = 1, \dots, K\}, l = 1, \dots, L \text{ realizations} \quad (2.22)$$

The  $K$  random events  $A_j, j = 1, \dots, K$  are characterized by their joint  $K$ -variate probability distribution:

$$P\{A_j \leq a_j, j = 1, \dots, K\} = F_K(a_1, \dots, a_K) \quad (2.23)$$

Using Bayes' axiom for conditional probability,  $P(A \cap B) = P(A)P(B|A)$ , this  $K$ -variate cdf can be decomposed into the product of  $(K-1)$  univariate conditional cdf's (ccdf's) and a marginal cdf:

$$\begin{aligned} &P\{A_j \leq a_j, j = 1, \dots, K\} = \\ &P\{A_K \leq a_K | A_1 \leq a_1, \dots, A_{K-1} \leq a_{K-1}\} \cdot P\{A_j \leq a_j, j = 1, \dots, K-1\} = \\ &P\{A_K \leq a_K | A_1 \leq a_1, \dots, A_{K-1} \leq a_{K-1}\} \cdot P\{A_{K-1} \leq a_{K-1} | A_1 \leq a_1, \dots, A_{K-2} \leq a_{K-2}\} \\ &\cdot P\{A_j \leq a_j, j = 1, \dots, K-2\} = \dots = \\ &P\{A_K \leq a_K | A_1 \leq a_1, \dots, A_{K-1} \leq a_{K-1}\} \cdot P\{A_{K-1} \leq a_{K-1} | A_1 \leq a_1, \dots, A_{K-2} \leq a_{K-2}\} \\ &\dots P\{A_2 \leq a_2 | A_1 \leq a_1\} \cdot P\{A_1 \leq a_1\} = \\ &= F_K |_{(K-1)}(a_K | a_j, j = 1, \dots, K-1) \cdot F_{K-1} |_{(K-2)}(a_{K-1} | a_j, j = 1, \dots, K-2) \cdot F_{2|1}(a_2 | a_1) \cdot F_1(a_1) \end{aligned} \quad (2.24)$$

Based on this decomposition it is possible to construct a general sequential simulation algorithm to jointly simulate the  $K$  dependent events, by drawing from the sequence of univariate conditional cumulative distributions. This algorithm would consist of:

Step 1 – Draw the realization  $a_1$  from the marginal cdf:

$$F_1(a_1) = P\{A_1 \leq a_1\}$$

Step 2 – Determine the conditional cdf  $A_2$  given the previous realization  $A_1 = a_1$ :

$$P\{A_2 \leq a_2 \mid A_1 = a_1\} \text{ and then draw a realization } a_2 \text{ from that cdf.}$$

Step 3 – Determine the conditional cdf  $A_3$  given the joint realization  $A_1 = a_1$  and  $A_2 = a_2$ :

$$P\{A_3 \leq a_3 \mid A_1 = a_1, A_2 = a_2\} \text{ and draw a realization } a_3 \text{ from that cdf.}$$

Step  $K$  - Determine the conditional cdf  $A_K$  given  $A_j, j = 1, \dots, K-1$ :

$$P\{A_K \leq a_K \mid A_1 = a_1, \dots, A_{K-1} = a_{K-1}\} \text{ and draw a realization } a_K \text{ from it.}$$

To obtain another joint realization  $\{a_j^{(i)}, j = 1, \dots, K\}$  start all over again from the first step.

#### 2.4.2 Collocated Cokriging Model

Problem associated with a traditional full cokriging approach is matrix instability. In order to simplify the amount of model and calculation, the concept of collocated cokriging is proposed.

Consider the  $K$  primary variables  $Z_k, k = 1, \dots, K$  with normal scores  $Y_k, k = 1, \dots, K$ , and the secondary variables  $A_l, l = 1, \dots, L$  with normal scores  $B_l, l = 1, \dots, L$ . The idea of collocated cokriging amounts to retaining only the secondary  $B$ -data

closest to the location  $u$  where the primary variable  $Y(u)$  is to be estimated, e.g., the collocated secondary  $B(u)$ -datum. As it stands now, the procedure requires the secondary data be available at every node where the primary variable is being simulated. Theoretically, the closest secondary information could be considered if the distance between this information and the point being simulated is insignificant.

### ***Collocated Cokriging***

Given the primary variable  $Y(u)$ , sampled at  $n$  locations, and the secondary variable data  $B(u)$ , sampled at  $n'$  other locations, the collocated simple cokriging estimator is written

$$Y^*(u) - m_Y = \sum_{\alpha=1}^n \lambda_{\alpha} [Y(u_{\alpha}) - m_Y] + \nu [B(u) - m_B] \quad (2.25)$$

And the collocated simple cokriging system is

$$\left\{ \begin{array}{l} \sum_{\beta=1}^n \lambda_{\beta} C_Y(u_{\alpha} - u_{\beta}) + \nu C_{YB}(u_{\alpha} - u) = C_Y(u_{\alpha} - u), \quad \alpha = 1, \dots, n \\ \sum_{\beta} \lambda_{\beta} C_{BY}(u - u_{\beta}) + \nu C_B(0) = C_{BY}(0) \end{array} \right. \quad (2.26)$$

If the  $Y$ -data and the single  $B$ -datum are standardized to a unit variance, this system is written in terms correlogram.

$$\left\{ \begin{array}{l} \sum_{\beta=1}^n \lambda_{\beta} \rho_Y(u_{\alpha} - u_{\beta}) + \nu \rho_{YB}(u_{\alpha} - u) = \rho_Y(u_{\alpha} - u), \quad \alpha = 1, \dots, n \\ \sum_{\beta} \lambda_{\beta} \rho_{BY}(u - u_{\beta}) + \nu = \rho_{BY}(0) \end{array} \right. \quad (2.27)$$

where  $\rho_{BY}(h)$  is cross-correlogram between  $B$  and  $Y$ .



*Remarks*

- The number of equations in the system is  $(n+1)$ .
- If  $\rho_{YB}(0) = 1$ , i.e., if there is a perfect linear relation  $Y(u) = a + b B(u)$ , then  $\rho_{YB}(u_\alpha - u) = \rho_Y(u_\alpha - u)$ . The unique solution to Eq. 2.27 is  $\lambda_\beta = 0, \forall \beta$ , and  $\nu = 1$  as expected. This entails exactitude, i.e.,  $Y^*(u) = B(u)$ .
- If  $\rho_{BY}(h) = 0, \forall h$ , the unique solution is  $\nu = 0$ , and  $\lambda_\alpha$  identifies the SK weight considering only then  $Y(u_\alpha)$ -data.

$$\left\{ \begin{array}{l} \sum_{\beta=1}^n \lambda_\beta \rho_Y(u_\alpha - u_\beta) = \rho_Y(u_\alpha - u), \quad \alpha = 1, \dots, n \\ \nu = 0 \end{array} \right. \quad (2.28)$$

and  $Y^*(u) \equiv [Y(u)]_{SK}^*$  using only the  $n$   $Y(u_\alpha)$ -data. Thus, the estimator in Eq.2.25 is consistent at both limits  $\rho_{YB}(0) = 1$  and  $\rho_{BY}(h) = 0, \forall h$ .

- The cokriging Eq. 2.27 does not call for the  $B$ -covariance but still calls for inference and modeling of the cross-covariance  $C_{BY}(h)$ .

### 2.4.3 Markov Model

According to Eq.2.27 still calls for inference and modeling of primary co-variance  $C_Y(h)$  and the cross-covariance. The Markov model is developed to allow shortcutting inference of that cross-covariance under theorems. The Markov model allows the determination of the spatial structures of two variables, in this case the cross correlogram between the primary/hard or secondary/soft variable, by using the product relationship of their correlation coefficient and the spatial structure of primary/hard variable. It results in the following expression for the cross-covariance:

$$\rho_{YB}(h) = \rho_{YB}(0) \cdot \rho_Y(h), \forall h \quad (2.29)$$

#### 2.4.4 Collocated Cokriging with Markov Model

When account for both collocation idea and Markov model, the algorithm to jointly simulate multiple variables conditional to primary data and collocated secondary data proceeds as follows:

- Let the primary variables be  $Y_k(u)$ ,  $k = 1, \dots, K$
- The primary data are  $y_k(u_\alpha)$ ,  $\alpha = 1, \dots, n$
- Let the secondary variables be  $B_l(u)$ ,  $l = 1, \dots, L$
- The secondary data are  $b_l(u'_\beta)$ ,  $\beta = 1, \dots, N$  with, usually  $N \gg n$

The cokriging estimate and variance are

$$Y^*(u) = \sum_{\alpha=1}^n \lambda_\alpha Y(u_\alpha) + \sum_{l=1}^L \nu_l B_l(u) \quad (2.30)$$

With for COSK system

$$\left\{ \begin{array}{l} \sum_{\beta=1}^n \lambda_\beta \rho_Y(u_\beta - u_\alpha) + \sum_{l=1}^L \nu_l \rho_{YB_l}(u - u_\alpha) = \rho_Y(u - u_\alpha), \quad \alpha = 1, \dots, n \\ \sum_{\beta=1}^n \lambda_\beta \rho_{YB_l}(u - u_\beta) + \sum_{l'=1}^L \nu_{l'} \rho_{B_l B_{l'}}(0) = \rho_{YB_l}(0), \quad l = 1, \dots, L \end{array} \right.$$

$$\sigma_{COSK}^2(u) = 1 - \sum_{\alpha=1}^n \lambda_\alpha \rho_Y(u - u_\alpha) - \sum_{l=1}^L \nu_l \rho_{YB_l}(0) \quad (2.31)$$

The following covariance are called for

$\rho_Y(h)$ , to be inferred

$\rho_B(0) = Var\{B(u)\} = 1$

$\rho_{B_l B_{l'}}(0)$ , to be inferred,

Then  $\rho_{YB_l}(h) = E\{Y(u)B_l(u+h)\} = \rho_{YB_l}(0)\rho_Y(h), \forall l = 1, \dots, L$ , as given by Markov model.

Developing a joint conditional simulation is the necessity of having a practical tool for simulation simultaneously several spatially dependent variables. SGCOSIM consists of a generalization of the traditional sequential Gaussian simulation algorithm to deal with several primary and secondary variables. Each variable is simulated sequentially according to its normal cdf fully characterized through a cokriging system. Given hierarchy of primary variables, all previously simulated primary variables are considered as conditioning information for the simulation of next primary variable. The secondary must be known at all locations to be simulated. All data must be in Gaussian form, i.e. a normal score transform must be performed for all variables before applying the algorithm. The conditioning data used for the simulation of each primary variable consist of all original data and all previously simulated values of this primary variable found within a neighborhood of the point being simulated, plus the collocated values of the secondary variables, plus the collocated values of all previously simulated primary variables.

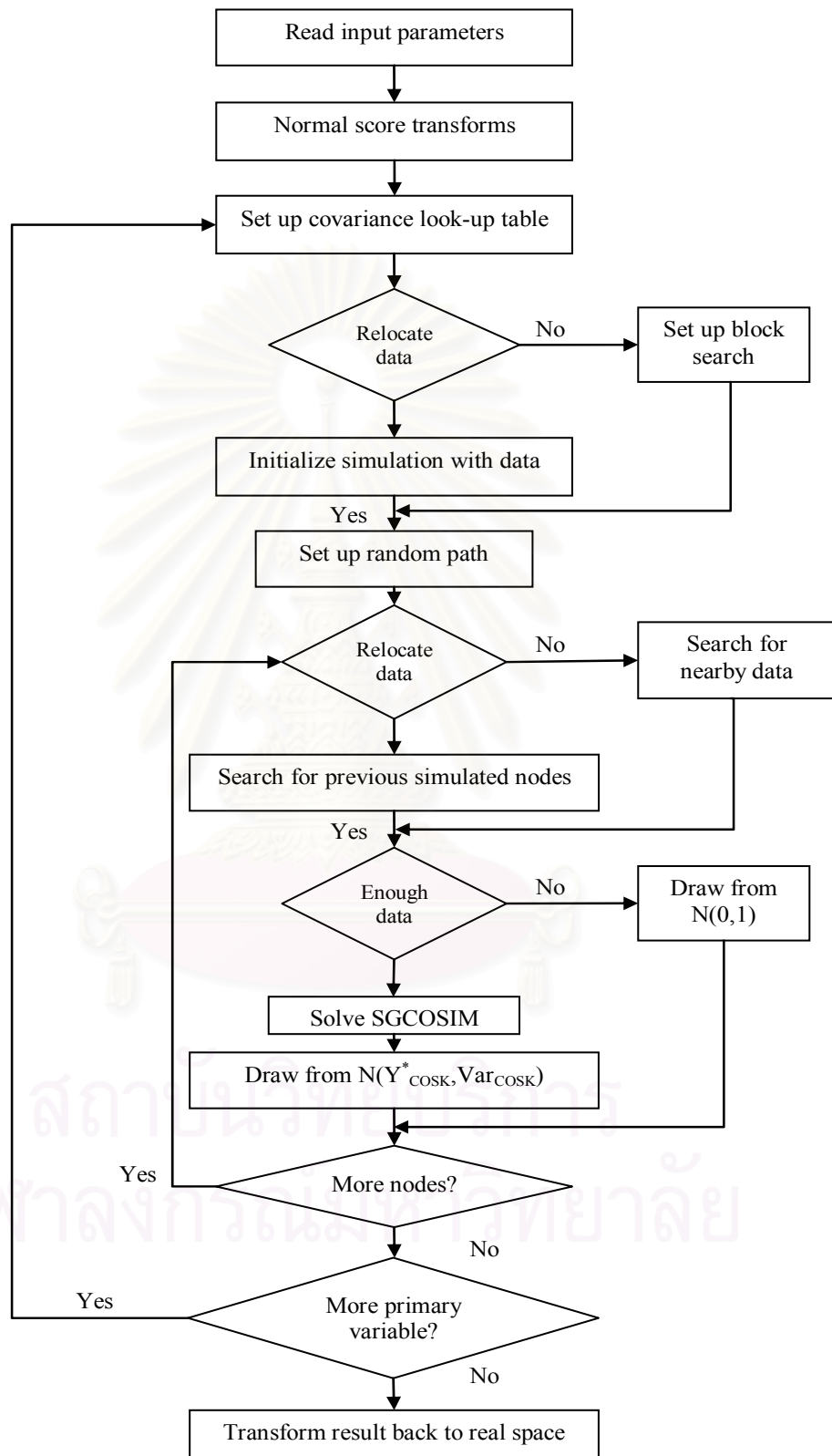


Figure 2.3: Sequential Gaussian Cosimulation (SGCOSIM) flow chart.

## CHAPTER III

### DATA PREPARATION

This chapter discusses data preparation in applying proposed stochastic simulation methods. In order to evaluate performance of the proposed methods to compute original hydrocarbon in place, the actual data set from a gas reservoir in the Gulf of Thailand was used. The data set consists of three directional wells. One formation from this reservoir was selected for this study. Since the wells are far apart from each other, distance adjustment was conducted to fulfill stochastic simulation method comparison objective. Finally, the last section presents other concerned parameters that were applied for all volumetric original hydrocarbon in place calculation throughout this study.

#### 3.1 General information of data set

The data set was obtained from one of the gas reservoirs in the Gulf of Thailand. They were collected from three directional wells, renamed “A”, “B”, and “C” throughout this study. Well A has been on production since 1997 whereas Well B and C have been producing since 2001. The schematic for these three wells is depicted in Figure 3.1. These wells were drilled through many formations. However, there is only one formation which all wells are connected. Therefore, this formation was selected for study and was renamed as Formation I.

The formation covers an area of 475 ft x 5,370 ft and has a thickness of 130 ft. In reality, the thickness of three wells is not equally. To model formation in rectangular, three wells were assumed to be the same thickness in this study. Due to a vast area but small number of wells, it is hard to see the relationship of reservoir properties among wells. On this account, wells were relocated to narrow space without changing direction of the wells. By doing this, the area of Formation I is reduced to 420 ft x 420 ft. From well log interpretation, there are four petrophysical properties, i.e., porosity, water saturation, permeability, and resistivity that are available. Logging was done for 0.5 ft interval along the measured depth (MD).

Well A is in the North-West (NW) direction while Well B and C are in the South-West (SW) direction. Since they are directional wells, the true vertical depth (TVD) corresponding to the Universal Transverse Mercator (UTM) coordinates of the log samples were calculated from MD and angle drilled well. Figure 3.2 shows location map of well log data in XY, XZ, and YZ coordinate.

Table 3.1: General information from well A, B, and C.

Well	A	B	C	Overall
Direction	North-West	South-West	South-West	-
Measure Depth (ft)	11,775-11,884	10,866-10,944	12,557-12,655	-
True Vertical Depth (ft)	8,686-8,733	8,605-8,662	8,645-8,718	8,605-8,733
Number of data	55	145	149	349

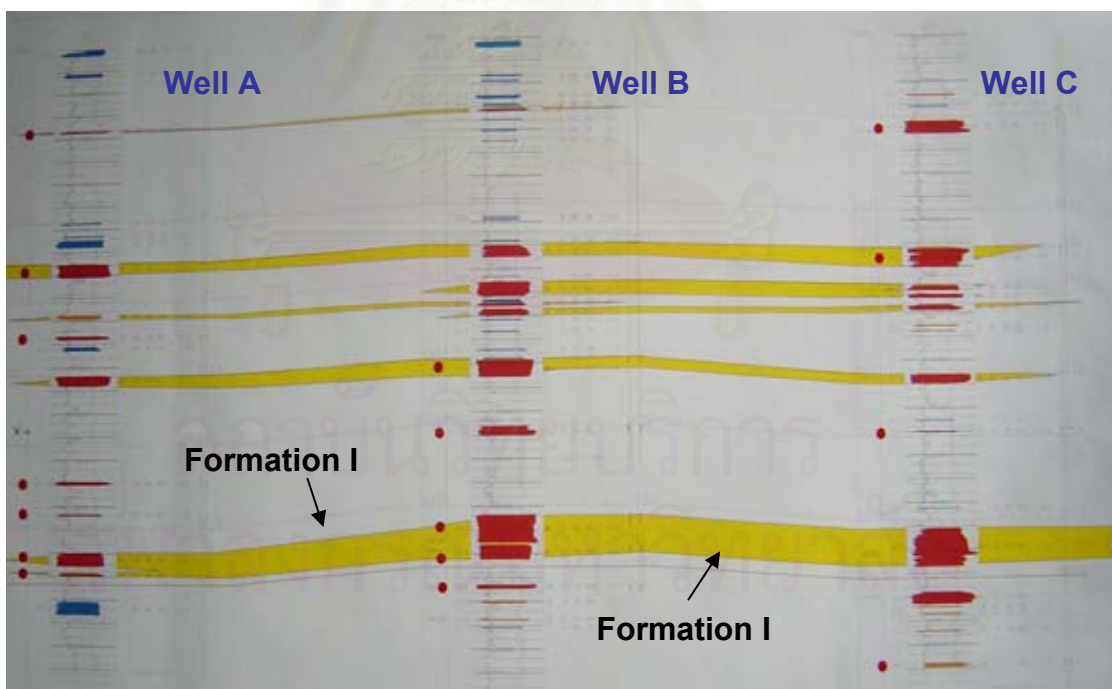


Figure 3.1: Schematic of Well A, B, and C.



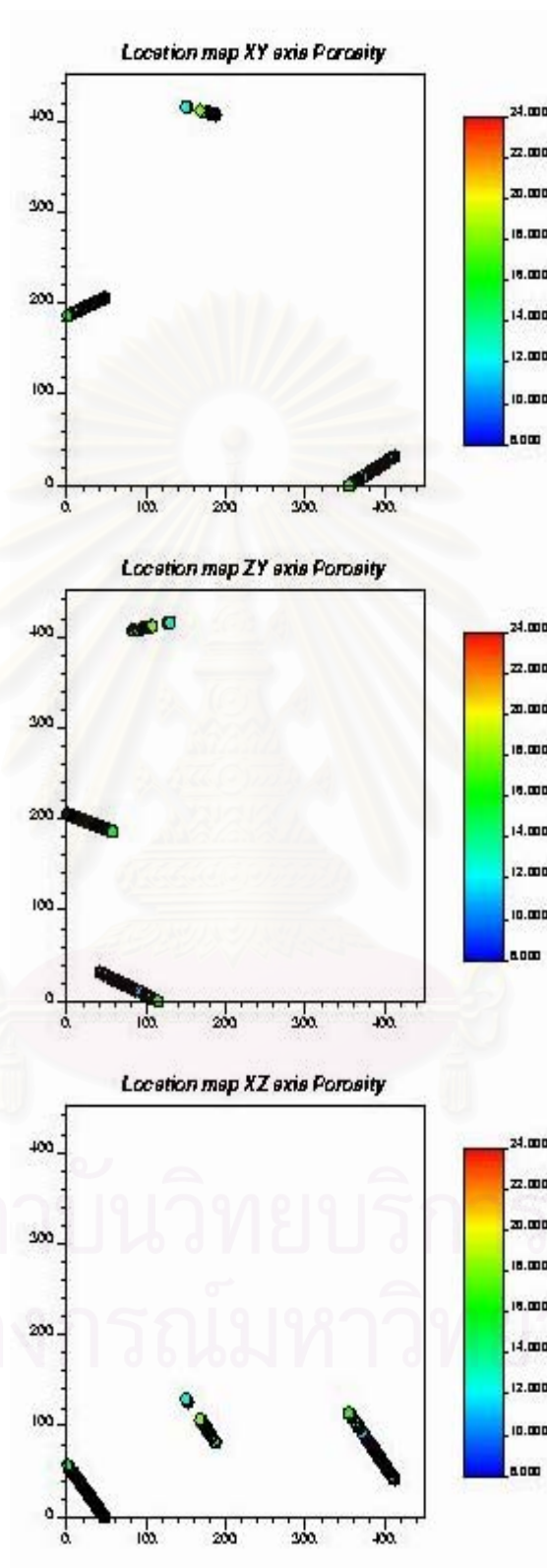


Figure 3.2: Location map of well log data in Formation I.

### 3.2 Statistical analysis of petrophysical variables

The statistical analysis of petrophysical variables, i.e., porosity, water saturation, permeability, and formation resistivity, was performed on 349 well log data taken from three wells in Formation I. All well log data and their locations (after relocation) are given in Table 3.2. Table 3.3 shows statistics of well log data in Formation I. Because porosity and water saturation are important variables in volumetric calculation of hydrocarbon in place, these parameters were set to be primary/hard variables. Permeability and formation resistivity were treated as secondary/soft variables (when simulated by Sequential Gaussian Cosimulation) due to there are strong correlation among variables and these information also are available from well log interpretation.

Figures 3.3 to 3.6 show histograms and cumulative distributions of porosity, water saturation, permeability, and formation resistivity. It can be seen that only the histogram and cumulative distribution of porosity shows Gaussian-like distribution with slightly positive skewness (+0.07) whereas histogram and cumulative distribution of water saturation, permeability, and formation resistivity show highly positive and negative skewness of -0.55, 3.29, and 2.93, respectively. The mean and median of porosity, water saturation, permeability, and formation resistivity are 16.63, 40.82, 13.32, and 27.84 and 16.40, 43.80, 11.80, and 28.16, respectively. The coefficients of variation of primary variables, porosity and water saturation, are lower than 1.0 (0.13 and 0.24) which indicate no presence of some erratic sample values that may have significant impact to the simulation process. The values of porosity are spread out in a narrow range from 10.00 to 22.62 which gives a low standard deviation of 2.21 and variance of 4.88. Narrow distribution is also observed in water saturation and formation resistivity. The water saturation and formation resistivity have standard deviation of 10.26 and 18.00 and variance of 105.18 and 324.09, respectively. A high variance is observed in permeability data with the variance of 1010.53. The permeability value ranges from 0.48 to 233.44.

Table 3.2: Porosity, water saturation, permeability, formation resistivity, and locations of Formation I.

Well	X	Y	Z	Po	Sw	k	Rt	Well	X	Y	Z	Po	Sw	k	Rt
A	187.28	406.93	82.16	15.44	51.00	7.97	14.29	B	45.47	204.97	1.83	20.12	52.90	67.82	33.48
A	186.96	407.00	82.56	15.60	39.50	10.22	13.82	B	45.18	204.85	2.20	20.46	52.60	80.37	32.74
A	186.64	407.07	82.96	15.41	42.80	9.08	13.12	B	44.88	204.73	2.57	20.83	51.30	97.53	32.64
A	186.32	407.14	83.36	14.66	53.10	5.43	12.60	B	44.58	204.60	2.93	20.72	46.10	94.81	35.13
A	186.00	407.21	83.76	13.89	48.10	3.82	12.43	B	44.28	204.48	3.30	20.43	42.50	84.65	36.51
A	185.68	407.29	84.16	13.02	20.00	3.60	12.60	B	43.98	204.35	3.67	20.00	41.70	68.87	37.21
A	182.81	407.93	87.76	15.88	54.10	9.01	17.01	B	43.68	204.23	4.03	19.68	42.10	58.47	37.35
A	182.49	408.00	88.16	16.20	47.70	11.44	17.01	B	43.38	204.11	4.40	19.64	43.20	56.89	37.23
A	182.17	408.07	88.56	16.27	47.40	11.96	16.93	B	43.08	203.98	4.76	19.87	44.90	62.86	37.09
A	181.85	408.14	88.96	16.23	50.70	11.30	16.89	B	42.78	203.86	5.13	20.24	45.90	74.80	36.98
A	181.53	408.21	89.36	16.12	54.50	10.19	16.93	B	42.48	203.73	5.50	20.36	45.40	79.67	36.71
A	181.21	408.28	89.76	16.10	59.00	9.65	16.97	B	42.18	203.61	5.86	20.25	44.40	76.39	36.41
A	178.97	408.78	92.56	15.74	59.00	7.93	16.96	B	41.88	203.49	6.23	20.05	45.40	68.78	36.23
A	178.65	408.85	92.96	14.94	57.70	5.20	16.95	B	41.58	203.36	6.59	19.65	47.50	55.65	36.07
A	178.33	408.92	93.36	14.25	57.20	3.56	16.96	B	41.28	203.24	6.96	19.39	49.90	47.98	35.90
A	178.01	408.99	93.76	14.08	58.10	3.21	16.93	B	40.98	203.12	7.33	19.32	51.30	45.79	35.72
A	177.37	409.14	94.56	15.18	58.70	5.86	16.99	B	40.68	202.99	7.69	19.48	49.70	50.34	35.62
A	177.05	409.21	94.97	15.78	51.00	8.78	17.02	B	40.38	202.87	8.06	19.87	46.20	62.77	35.41
A	176.73	409.28	95.37	16.40	41.50	13.71	17.01	B	40.08	202.74	8.43	20.35	42.90	81.58	35.03
A	176.41	409.35	95.77	16.84	37.80	18.15	17.06	B	39.78	202.62	8.79	20.79	41.60	101.91	34.80
A	176.09	409.42	96.17	16.82	43.70	16.61	17.12	B	39.48	202.50	9.16	20.94	40.90	110.35	34.73
A	175.77	409.49	96.57	16.58	50.70	13.54	17.12	B	39.18	202.37	9.52	20.62	40.40	95.07	34.87
A	175.45	409.56	96.97	16.41	51.40	12.30	17.13	B	38.88	202.25	9.89	19.92	40.20	67.79	35.67
A	175.13	409.63	97.37	16.18	48.90	11.12	17.15	B	38.58	202.12	10.26	19.22	39.60	47.77	36.43
A	174.80	409.71	97.77	15.99	47.60	10.22	17.19	B	38.28	202.00	10.62	18.64	38.70	36.00	36.57
A	174.48	409.78	98.18	16.05	48.10	10.43	17.26	B	37.98	201.88	10.99	18.08	38.30	27.01	36.65
A	174.16	409.85	98.58	16.19	49.70	11.05	17.34	B	37.68	201.75	11.35	17.86	40.40	23.52	36.76
A	173.84	409.92	98.98	16.50	53.50	12.53	17.38	B	37.38	201.63	11.72	18.17	43.70	26.87	36.81
A	173.52	409.99	99.38	16.85	58.70	14.31	17.40	B	37.09	201.50	12.09	18.65	46.80	33.56	36.87
A	172.56	410.21	100.58	16.74	59.40	13.38	17.62	B	36.79	201.38	12.45	18.89	47.80	37.68	36.81
A	172.24	410.28	100.99	16.44	55.70	11.75	17.73	B	36.49	201.26	12.82	18.89	46.10	38.29	36.68
A	171.92	410.35	101.39	15.93	54.20	9.04	17.81	B	36.18	201.13	13.19	18.68	44.10	34.90	36.58
A	171.60	410.42	101.79	15.94	53.20	9.17	17.88	B	35.88	201.01	13.56	18.38	43.20	30.16	36.41
A	171.28	410.49	102.19	16.62	50.60	13.57	17.89	B	35.58	200.88	13.92	18.27	43.70	28.53	36.05
A	170.96	410.56	102.59	17.40	48.60	20.97	17.88	B	35.28	200.76	14.29	18.26	44.30	28.29	35.62
A	170.64	410.63	102.99	17.92	50.10	27.01	17.91	B	34.98	200.64	14.66	18.14	44.50	26.49	35.34
A	170.31	410.71	103.40	17.89	53.00	25.71	17.98	B	34.68	200.51	15.02	17.96	43.90	24.24	35.22
A	169.99	410.78	103.80	17.13	53.60	17.22	18.07	B	34.38	200.39	15.39	17.92	41.80	24.29	35.17
A	169.67	410.85	104.20	16.53	51.40	12.77	18.15	B	34.08	200.26	15.76	18.02	40.20	25.99	35.11
A	169.35	410.92	104.60	16.76	50.60	14.59	18.21	B	33.78	200.14	16.13	18.17	40.70	27.93	35.05
A	169.03	410.99	105.00	17.04	53.00	16.49	18.24	B	33.48	200.01	16.49	18.23	41.20	28.66	34.93
A	168.71	411.06	105.41	16.95	53.20	15.60	18.34	B	33.18	199.89	16.86	17.78	39.80	22.96	34.79
A	168.39	411.13	105.81	17.21	48.10	18.71	18.65	B	32.88	199.77	17.23	17.32	37.90	18.36	34.68
A	168.07	411.21	106.21	17.89	46.30	27.03	19.15	B	32.58	199.64	17.59	16.96	38.90	15.07	34.45
A	167.74	411.28	106.61	18.37	49.60	33.05	19.54	B	32.28	199.52	17.96	16.70	41.10	12.87	33.91
A	167.42	411.35	107.02	18.53	53.40	34.79	19.24	B	31.98	199.39	18.33	16.61	42.20	12.17	32.96
A	167.10	411.42	107.42	18.04	59.90	26.35	17.60	B	31.68	199.27	18.69	16.68	42.70	12.72	31.85
A	151.98	414.78	126.35	12.26	48.00	1.33	15.67	B	31.38	199.14	19.06	16.77	44.70	13.29	30.82
A	151.66	414.86	126.76	12.50	39.10	1.64	16.77	B	31.08	199.02	19.43	16.79	47.30	13.19	29.74
A	151.33	414.93	127.16	12.73	39.30	1.82	17.58	B	30.78	198.90	19.80	16.68	49.10	12.42	28.67
A	151.01	415.00	127.56	13.35	39.00	2.55	17.92	B	30.48	198.77	20.16	16.62	51.60	11.83	28.05
A	150.69	415.07	127.97	14.20	33.00	4.53	17.51	B	30.18	198.65	20.53	16.63	53.50	11.72	27.94
A	150.37	415.14	128.37	14.67	29.50	6.48	16.37	B	29.88	198.52	20.90	16.55	53.40	11.19	27.92
A	150.05	415.21	128.77	14.16	34.00	4.81	15.00	B	29.58	198.40	21.27	16.29	51.30	9.92	27.89
A	149.72	415.29	129.18	12.33	45.70	1.56	13.55	B	29.28	198.28	21.63	15.92	48.30	8.30	27.89
B	46.97	205.59	0.00	18.71	34.40	38.55	37.60	B	28.97	198.15	22.00	15.52	47.10	6.72	27.90
B	46.67	205.47	0.37	19.83	39.10	64.33	37.98	B	28.67	198.03	22.37	15.27	47.90	5.82	27.96
B	46.37	205.35	0.74	20.17	45.80	72.39	36.63	B	28.37	197.90	22.73	15.35	48.90	6.02	27.95
B	46.07	205.22	1.10	20.23	51.60	72.30	34.56	B	28.07	197.78	23.10	15.56	47.30	6.85	27.92
B	45.77	205.10	1.47	20.18	52.70	69.82	33.48	B	27.77	197.65	23.47	15.60	43.40	7.30	28.00

Table 3.2: Porosity, water saturation, permeability, formation resistivity, and locations of Formation I (continued).

Well	X	Y	Z	Po	Sw	k	Rt	Well	X	Y	Z	Po	Sw	k	Rt
B	27.47	197.53	23.84	15.32	39.20	6.51	28.08	B	6.07	188.68	50.00	18.69	28.70	39.85	40.31
B	27.17	197.41	24.20	14.68	36.40	4.70	28.11	B	5.76	188.55	50.37	19.00	29.20	46.20	41.33
B	26.87	197.28	24.57	14.20	35.90	3.61	28.11	B	5.46	188.43	50.74	19.36	30.70	54.01	41.91
B	26.57	197.16	24.94	14.44	38.10	4.03	28.12	B	5.16	188.30	51.10	19.62	31.00	61.21	42.46
B	26.27	197.03	25.31	15.11	39.20	5.80	28.17	B	4.86	188.18	51.48	19.55	29.10	59.98	43.09
B	25.97	196.91	25.67	15.67	37.80	8.03	28.20	B	4.56	188.05	51.84	19.25	26.20	53.18	43.81
B	25.67	196.78	26.04	15.89	36.00	9.28	28.16	B	4.25	187.93	52.21	19.04	24.50	48.73	44.66
B	25.37	196.66	26.41	15.78	35.00	8.81	28.11	B	3.95	187.80	52.58	19.00	25.20	47.18	45.45
B	25.07	196.54	26.77	15.30	36.10	6.68	28.08	B	3.65	187.68	52.95	18.96	28.00	44.60	46.04
B	24.77	196.41	27.14	14.67	39.70	4.51	28.04	B	3.35	187.55	53.32	18.92	29.90	42.62	46.34
B	24.46	196.29	27.51	14.49	44.10	3.90	27.98	B	3.04	187.43	53.69	19.04	30.20	45.32	46.47
B	24.16	196.16	27.88	14.73	46.30	4.36	27.90	B	2.74	187.30	54.06	19.29	29.40	51.64	46.74
B	23.86	196.04	28.25	14.80	45.10	4.61	27.65	B	2.44	187.18	54.43	19.46	26.80	57.67	47.07
B	23.56	195.91	28.62	14.63	43.40	4.27	27.32	B	2.14	187.05	54.80	19.56	23.60	62.78	47.29
B	23.26	195.79	28.98	14.14	43.60	3.24	27.31	B	1.83	186.93	55.17	19.52	19.50	65.16	47.24
B	22.96	195.66	29.35	13.47	45.10	2.15	27.79	B	1.53	186.80	55.54	19.38	16.20	63.94	47.07
B	22.66	195.54	29.72	13.36	44.10	2.02	28.49	B	1.23	186.68	55.91	19.19	14.90	59.16	47.12
B	22.36	195.41	30.09	13.99	38.00	3.09	29.08	B	0.92	186.55	56.28	18.76	16.60	46.50	47.38
B	20.55	194.67	32.30	14.72	37.20	4.65	30.12	B	0.62	186.43	56.65	17.73	23.70	24.55	47.36
B	20.25	194.54	32.67	14.54	41.10	4.01	30.15	B	0.32	186.30	57.02	15.67	34.90	7.06	46.30
B	19.95	194.42	33.03	15.12	41.00	5.58	30.18	C	411.97	31.58	41.42	13.82	52.00	4.32	12.50
B	19.65	194.29	33.40	16.01	38.70	9.39	30.18	C	411.38	31.25	42.17	11.89	59.80	1.36	12.51
B	19.34	194.17	33.77	16.86	35.50	15.42	30.14	C	411.09	31.09	42.55	11.79	54.30	1.40	12.46
B	19.04	194.04	34.14	17.79	32.90	26.03	30.06	C	410.79	30.93	42.92	12.41	54.40	1.95	12.52
B	18.74	193.92	34.51	18.28	33.80	33.16	30.00	C	409.32	30.12	44.80	10.00	47.70	0.57	13.00
B	18.44	193.80	34.88	18.28	37.50	31.97	29.98	C	408.14	29.48	46.30	10.65	59.10	0.76	11.54
B	18.14	193.67	35.24	18.26	41.30	30.40	29.97	C	406.08	28.34	48.92	13.13	42.40	3.19	13.93
B	17.84	193.55	35.61	17.96	44.10	25.37	29.86	C	405.79	28.18	49.30	13.94	43.70	4.60	14.88
B	17.54	193.42	35.98	17.35	46.40	17.97	29.61	C	405.49	28.02	49.67	13.90	33.60	5.17	15.70
B	17.24	193.30	36.35	16.55	48.10	11.55	29.32	C	405.20	27.86	50.05	13.33	26.10	4.27	16.32
B	16.93	193.17	36.72	16.12	45.70	9.40	29.03	C	404.90	27.70	50.42	13.55	25.50	4.77	16.77
B	16.63	193.05	37.08	15.83	41.10	8.40	28.71	C	404.61	27.54	50.80	15.04	28.30	9.92	17.14
B	16.33	192.92	37.45	16.13	36.90	10.44	28.33	C	404.31	27.37	51.17	16.21	32.60	16.63	17.45
B	16.03	192.80	37.82	16.86	33.20	16.25	27.93	C	404.02	27.21	51.55	16.24	39.30	14.91	17.62
B	14.83	192.30	39.29	16.08	33.10	10.85	26.85	C	403.72	27.05	51.92	15.67	46.30	9.86	17.62
B	13.62	191.80	40.77	14.67	43.30	4.44	26.41	C	403.43	26.89	52.30	14.98	46.70	6.85	17.41
B	13.32	191.68	41.14	15.71	50.20	7.40	26.58	C	403.14	26.73	52.67	14.37	41.40	5.48	16.91
B	13.01	191.55	41.51	16.59	51.20	11.80	26.93	C	402.84	26.57	53.05	14.06	40.50	4.80	16.46
B	12.71	191.43	41.88	16.92	48.90	14.31	27.37	C	402.55	26.41	53.42	14.23	48.40	4.61	16.52
B	12.41	191.30	42.25	16.80	46.30	13.72	27.76	C	401.66	25.92	54.55	12.94	55.60	1.98	17.44
B	12.11	191.18	42.61	17.06	43.90	16.06	28.03	C	401.37	25.76	54.92	11.93	35.60	1.53	17.65
B	11.81	191.05	42.98	17.49	43.80	20.17	28.31	C	401.07	25.60	55.30	11.78	25.50	1.66	18.14
B	11.50	190.93	43.35	17.37	46.20	18.41	28.55	C	400.78	25.44	55.67	13.94	32.60	4.61	19.27
B	11.20	190.80	43.72	16.77	47.00	13.28	28.65	C	400.49	25.27	56.05	15.87	40.70	10.88	20.64
B	10.90	190.68	44.09	15.86	43.50	8.35	28.78	C	400.19	25.11	56.42	16.47	44.20	13.76	21.70
B	10.60	190.55	44.46	14.80	38.40	4.85	29.05	C	399.90	24.95	56.80	16.32	49.00	11.74	22.39
B	10.30	190.43	44.83	14.28	34.30	3.78	29.37	C	399.60	24.79	57.17	15.56	57.60	6.94	22.75
B	9.99	190.30	45.20	14.60	30.70	4.71	29.74	C	397.83	23.82	59.42	15.15	59.80	5.37	23.28
B	9.69	190.18	45.57	16.04	27.30	10.95	30.31	C	397.54	23.66	59.80	15.27	58.40	5.82	23.43
B	9.39	190.05	45.94	17.01	27.00	18.39	31.22	C	396.66	23.17	60.92	15.41	57.00	6.27	24.25
B	9.09	189.93	46.31	17.96	28.40	29.27	32.44	C	396.36	23.01	61.30	15.47	53.80	6.66	24.71
B	8.78	189.80	46.68	18.50	29.60	37.53	33.94	C	396.07	22.85	61.67	15.22	51.90	5.94	25.01
B	8.48	189.68	47.05	18.70	31.10	40.40	35.55	C	395.77	22.69	62.05	14.93	45.60	5.49	25.18
B	8.18	189.55	47.41	18.77	33.00	40.64	36.77	C	395.48	22.53	62.42	14.58	37.50	5.09	25.35
B	7.88	189.43	47.78	18.65	34.40	37.44	37.38	C	395.18	22.37	62.80	14.36	35.80	4.58	25.56
B	7.58	189.30	48.15	18.48	36.40	33.50	37.70	C	394.89	22.20	63.17	14.62	41.30	4.85	25.75
B	7.28	189.18	48.52	18.52	38.90	33.45	37.93	C	394.60	22.04	63.54	15.17	44.30	6.25	25.94
B	6.97	189.05	48.89	18.66	38.80	35.86	38.18	C	394.30	21.88	63.92	15.63	44.30	8.01	26.23
B	6.67	188.93	49.26	18.57	35.30	35.36	38.45	C	394.01	21.72	64.29	15.85	45.50	8.82	26.55
B	6.37	188.80	49.63	18.50	30.90	35.47	39.10	C	393.72	21.56	64.67	15.94	48.70	8.85	26.70





Table 3.3: Statistics of well log data in Formation I.

Statistical Data	Porosity (P)	Water Saturation (Sw)	Permeability (k)	Formation Resistivity (Rt)
Mean	16.63	40.82	13.32	27.84
Variance	4.88	105.18	1010.53	324.09
Standard Deviation	2.21	10.26	31.79	18.00
Median (P50)	16.40	43.80	11.80	28.16
Minimum	10.00	14.90	0.48	11.54
Maximum	22.62	60.00	233.44	113.07
Skewness	0.07	-0.55	3.29	2.93
Kurtosis	0.07	-0.36	14.64	9.92
Coeff. of variation	0.13	0.24	1.32	0.58

It was found that there are significant correlations among primary and secondary variables. Correlations among variables are shown in Table 3.4. Between primary variables, porosity and water saturation are negatively correlated with the correlation value of -0.3415. The correlations of water saturation-permeability and water saturation-resistivity also show negative correlation with correlation value of -0.4243 and -0.6250, respectively. On the other hand, porosity-permeability and porosity-resistivity are positively correlated with correlation value of 0.8108 and 0.6043, respectively. In addition, secondary variables which are permeability and resistivity, are highly correlated with correlation value of 0.7456. Either positively or negatively correlation implies that the variables are interdependent.

Table 3.4: Correlation among variables in Formation I.

Correlation	Porosity (P)	Water Saturation (Sw)	Permeability (k)	Formation Resistivity (Rt)
Porosity	1.0000	-0.3415	0.8108	0.6043
Water Saturation		1.0000	-0.4243	-0.6250
Permeability			1.0000	0.7456
Formation Resistivity				1.0000



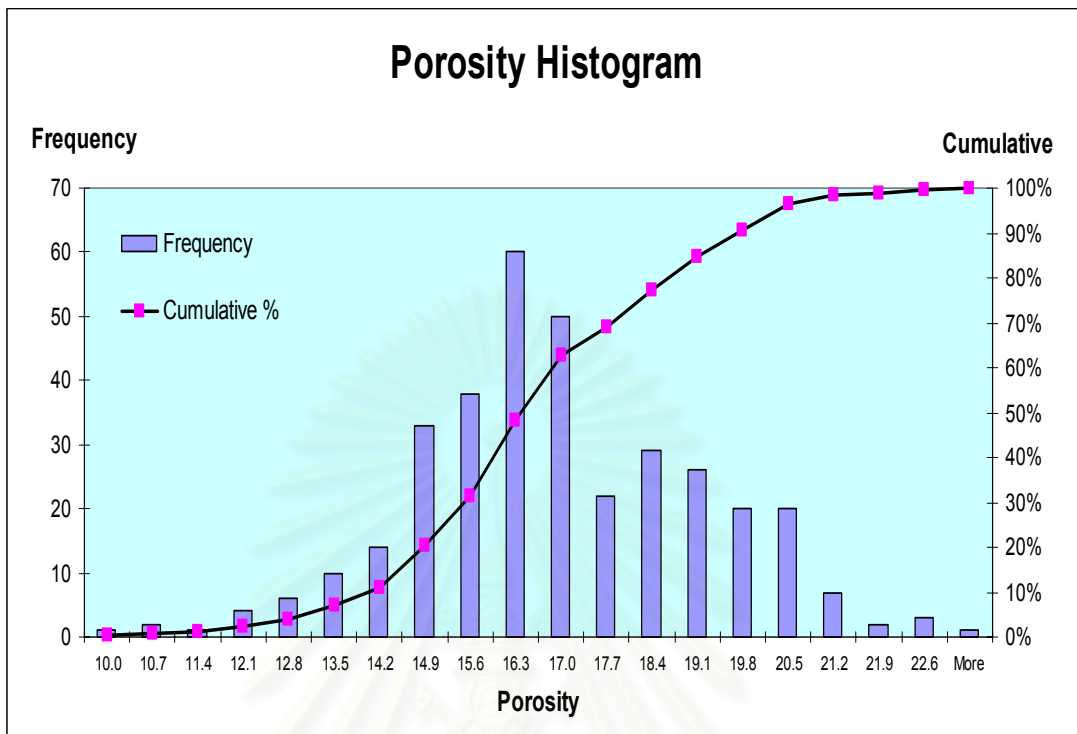


Figure 3.3: Porosity histogram and cumulative distribution.

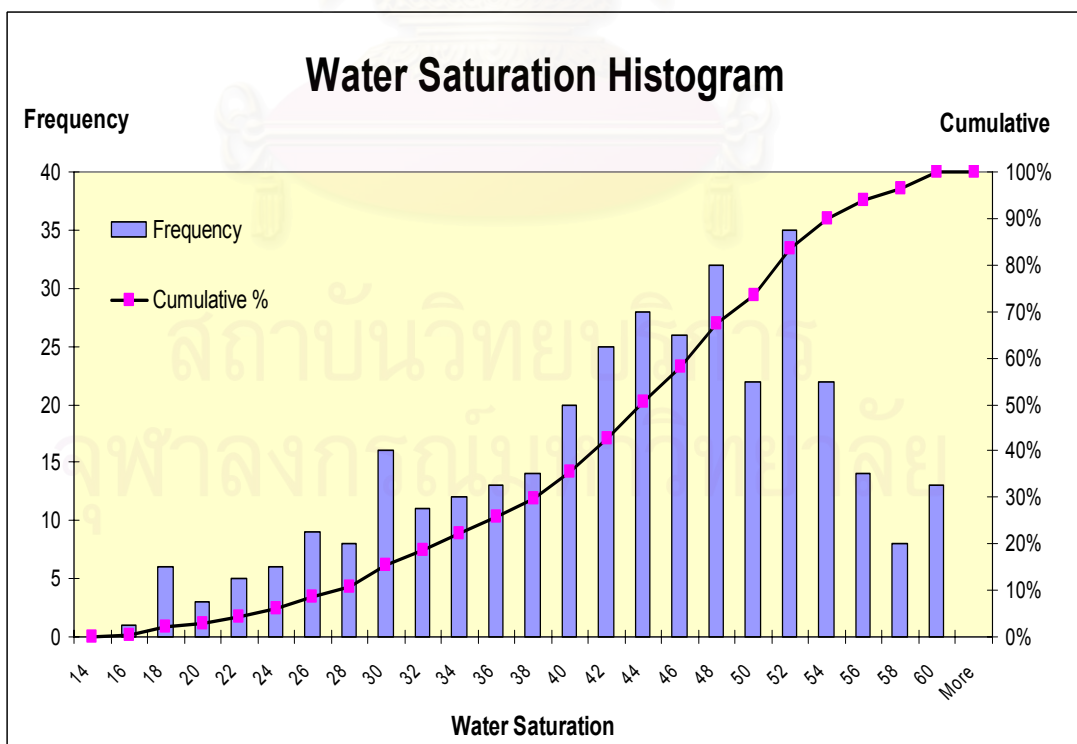


Figure 3.4: Water saturation histogram and cumulative distribution.

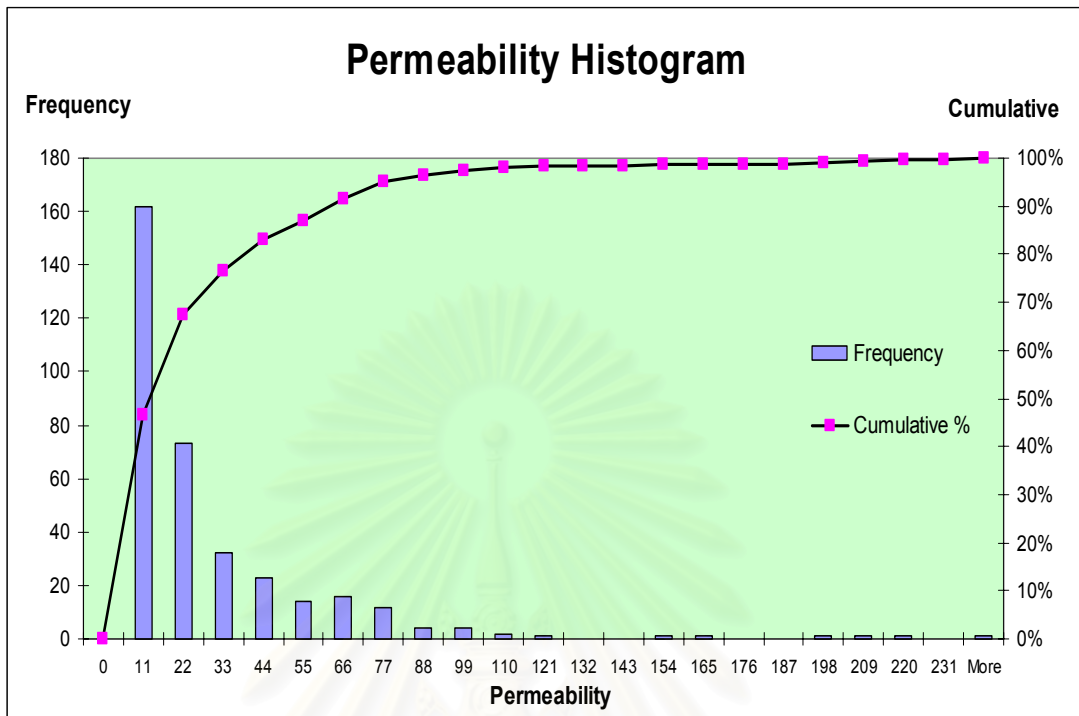


Figure 3.5: Permeability histogram and cumulative distribution.

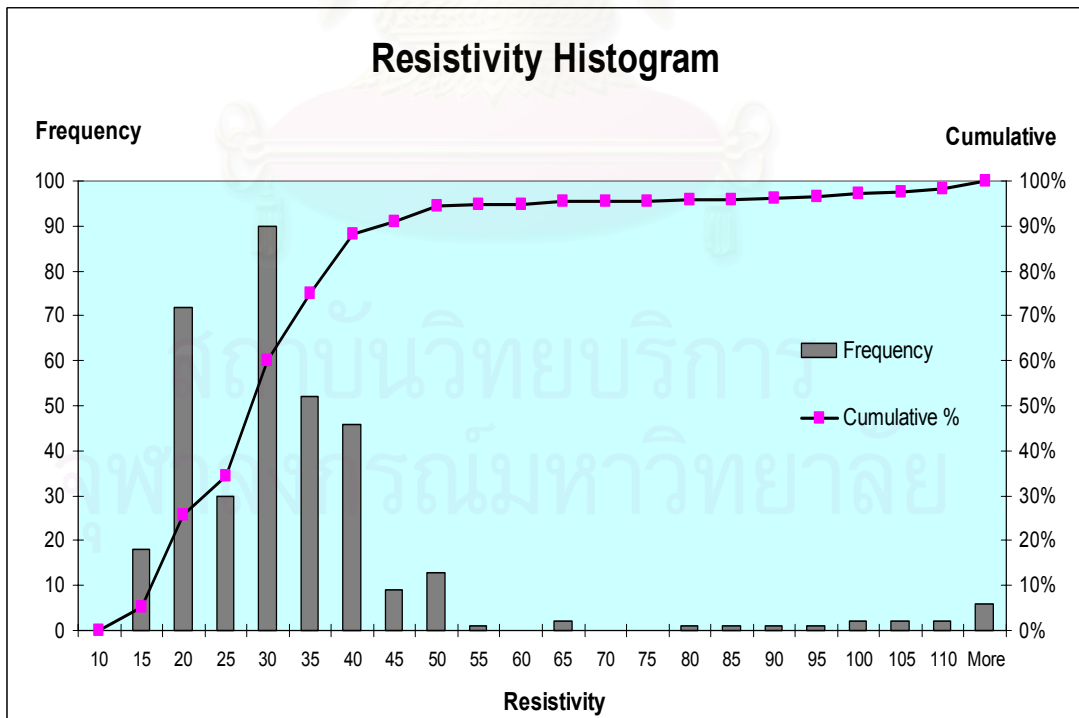


Figure 3.6: Resistivity histogram and cumulative distribution.

### 3.3 Related parameters for volumetric OGIP calculation

In volumetric OGIP estimation, apart from porosity and water saturation variables which in this study were generated by stochastic simulation methods, volume of reservoir and gas formation volume factor are also needed. These parameters were treated as constant throughout the entire OGIP calculation under various stochastic methods.

#### *Volume*

Formation I covers an area of 420 ft x 420 ft and has a thickness of 130 ft. The total volume of Formation I is then 22,932,000 cu.ft. or 526.45 acre-ft. Since the available data are dense at locations along directional wells, the refined grid block in the z-axis was divided to a fine resolution of 1 ft in height while the length along the x and y axes were set to be 20 ft . With this division, the grid block was constructed with the size of 20 ft x 20 ft x1 ft. Thus, the volume per block is 400 cu.ft, and the total number of grid blocks in Formation I is 57,330.

#### *Gas Formation Volume Factor*

Gas formation volume factor is defined as the actual volume occupied by a given quantity of gas at some pressure and temperature divided by the volume which gas would occupy at standard conditions. It is calculated from the equation.

$$B_g = \frac{p_{sc} Z T}{T_{sc} p} \quad (3.1)$$

where pressure is in psia and temperature is in R,  $p_{sc} = 14.7$  psia and  $T_{sc} = 520$  R. The calculated gas formation volume factor for Formation I is shown in Table 3.5. The average gas formation volume factor is  $1.4753 \times 10^{-4}$  res. cu.ft./scf which is used throughout the study.

Table 3.5: Gas formation volume factor for three wells located in Formation I.

Well	Reservoir Pressure (psia)	Reservoir Temperature (R)	Gas Compressibility factor (Z)	Gas Formation Volume Factor ( $B_g$ )
Well A	3,947	785	0.93	1.4799E-04
Well B	4,027	780	0.96	1.4877E-04
Well C	4,108	780	0.96	1.4584E-04
Formation I				1.4753E-04

Substituting the reservoir and block volume and gas formation volume factor values, volumetric OGIP equation can be rewritten as follows:

For Formation I,

$$OGIP = \frac{Ah \phi (1 - S_w)}{B_g} = \frac{22,932,000 \text{ ft}^3 \phi (1 - S_w)}{1.4753 * 10^{-4}} = 155.44 \phi (1 - S_w) \text{ Bcf} \quad (3.2)$$

For a block in Formation I,

$$OGIP = \frac{Ah \phi (1 - S_w)}{B_g} = \frac{400 \text{ ft}^3 \phi (1 - S_w)}{1.4753 * 10^{-4}} = 2.7113 \times 10^{-3} \phi (1 - S_w) \text{ Bcf} \quad (3.3)$$

สถาบันวิทยบริการ  
จุฬาลงกรณ์มหาวิทยาลัย

## CHAPTER IV

### APPLICATION OF STOCHASTIC SIMULATION IN ESTIMATION OF HYDROCARBON IN PLACE

Porosity and water saturation play an important role when estimating original hydrocarbon in place using the volumetric method. Three stochastic simulation methods: Monte Carlo Simulation, Sequential Gaussian Simulation, and Sequential Gaussian Cosimulation, were used to simulate the distributions of porosity and water saturation which are defined as primary variables. Permeability and resistivity which are secondary variables were incorporated in the Sequential Gaussian Cosimulation. Then, hydrocarbon in place was estimated based on the input of these properties. In this chapter, each section discusses a generation of primary and secondary (if requires) variables according to each simulation method and then estimate of OGIP. Once OGIPs had been estimated, the results from different methods were compared.

#### 4.1 Monte Carlo Simulation (MCS)

In the first method, porosity and water saturation which are input variables were estimated by Monte Carlo Simulation (MCS). To perform MCS, first, the probability distributions of input variables were defined; then, random samples of each probability distribution were drawn to produce a number of input realizations. Each set of input realizations was then used to compute output distribution (OGIP). Since porosity and water saturation are correlated, sensitivity analysis by Second Moment method was conducted in order to quantify the effect of input variables on OGIP output.

##### 4.1.1 Probability distribution of input variables

According to data preparation in Chapter III, the number of samples is 349. Referring to Figure 3.3, the probability distribution of porosity can be fairly defined as normal distribution with a mean value of 0.1663 and standard deviation of 0.0221.

On the other hand, water saturation is best fit with lognormal distribution with mean value of 0.4229 and standard deviation of 0.1026 as referred from Figure 3.4.

#### 4.1.2 OGIP calculation

As stated in the chapter II, the accuracy of MCS depends on the number of realizations. Hence, percent error in variance was used to define the required number of realizations. At 95% confidence level, this can be approximated as

$$\text{Percent error in variance} = 196 \left[ \frac{2}{(N-1)} \right]^{0.5} \quad (4.1)$$

The percent errors in variance for different numbers of realization are shown in Table 4.1. The number of realization of 15,000 was selected in this study because of justification to achieve a good degree of accuracy with a manageable number of runs.

Table 4.1: Percentage error in variance for various numbers of realization.

Number of Realizations	% Error in Variance
100's	27.86
1,000's	8.77
10,000's	2.77
15,000's	2.26
30,000's	1.60
75,000's	1.01
100,000's	0.88
150,000's	0.72

Fifteen thousand realizations of porosity and water saturation were generated as input variables, OGIPs were computed by substituting the value from each input realizations into Eq. 3.2. When input variables were generated at random based on their distributions, it is observed that statistics of the random data show a good agreement with statistics of the original data as shown in Table 4.2. The mean



value of porosity is close to the original data while the mean value of water saturation is much higher than the original data. The median values of variables show the same result as found in the mean values of variables with original data. The standard deviation and variance values of porosity and water saturation are slightly less than the original data. It also can be seen that porosity and water saturation are no longer correlated. This is because each variable was separately generated in a random fashion.

Table 4.2: Comparison between statistics of original and random data.

Statistics	Porosity		Water Saturation	
	Original Data	Random Data	Original Data	Random Data
Mean	16.63	16.90	42.29	44.66
Std. Deviation	2.21	2.19	10.26	9.19
Variance	4.88	4.80	105.18	84.41
Minimum	10.00	10.00	14.90	14.90
Maximum	22.62	22.62	60.00	60.00
Median (P50)	16.40	16.62	43.80	46.10
Skewness	0.072	0.093	-0.555	-0.721
Kurtosis	0.074	-0.079	-0.358	0.172
Coeff. of variability	0.133	0.130	0.243	0.206
Mean Standard Error	0.118	0.018	0.549	0.075
Correlation			Original Data	Random Data
Porosity VS Water Saturation			-0.3415	0.0135

The OGIP values obtained from Monte Carlo Simulation are depicted in Figures 4.1 and 4.2 and Table 4.3 displays the statistics of OGIP values. The OGIP value ranges from 6.516 to 29.169 Bcf with a mean and variance of 14.534, 9.320, respectively. The values corresponding to various percentiles are shown in Table 4.4. The result of OGIP distribution is obviously lognormal distribution and positive skewness. Lognormal distribution of OGIP results from the fact that MCS concurs with the Central Limit Theorem that when variables of any distributions are multiplied, the output distribution is approximately lognormal.

Table 4.3: The OGIP statistics from MCS.

Statistics	OGIP obtained from MCS (Bcf)
No. of realizations	15,000
Mean	14.534
Standard Deviation	3.053
Variance	9.320
Minimum	6.516
Maximum	29.169
Median (P50)	14.139
Skewness	0.667
Kurtosis	0.572
Coefficient of variability	0.210
Mean Standard Error	0.025

Table 4.4: OGIP at various percentiles from MCS.

Percentile	OGIP obtained from MCS (Bcf)
0%	6.516
10%	10.993
20%	11.962
25%	12.333
30%	12.713
40%	13.441
50%	14.139
60%	14.908
70%	15.829
75%	16.351
80%	16.967
90%	18.668
100%	29.169

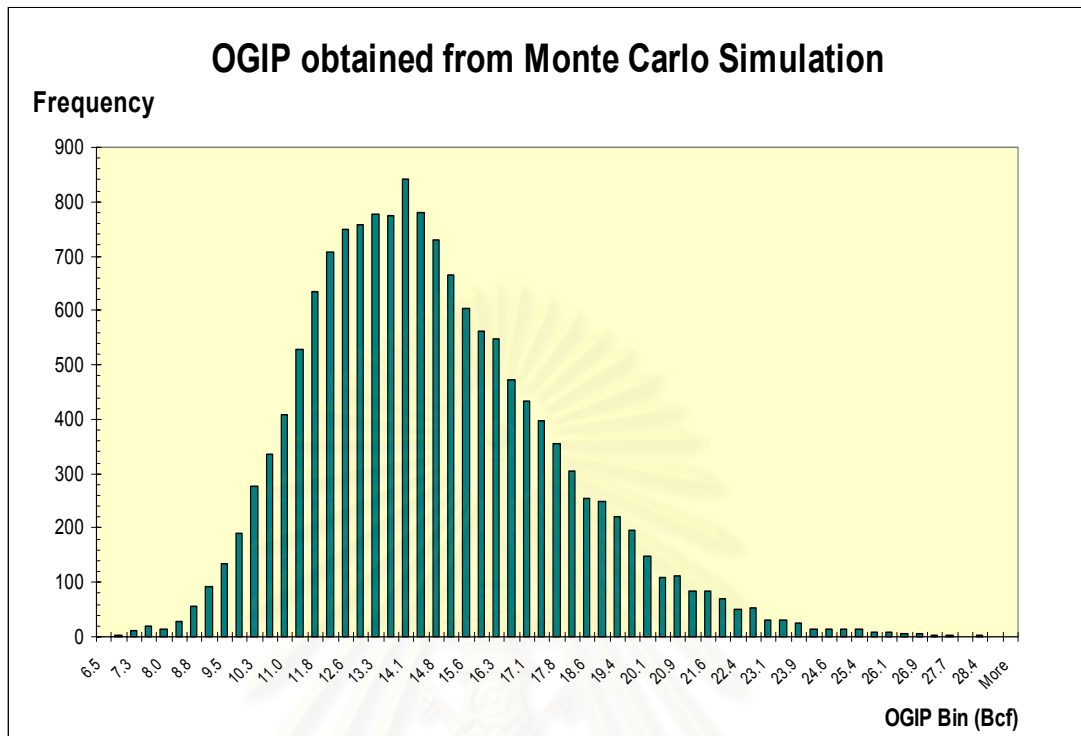


Figure 4.1: OGIP probability distribution function from MCS.

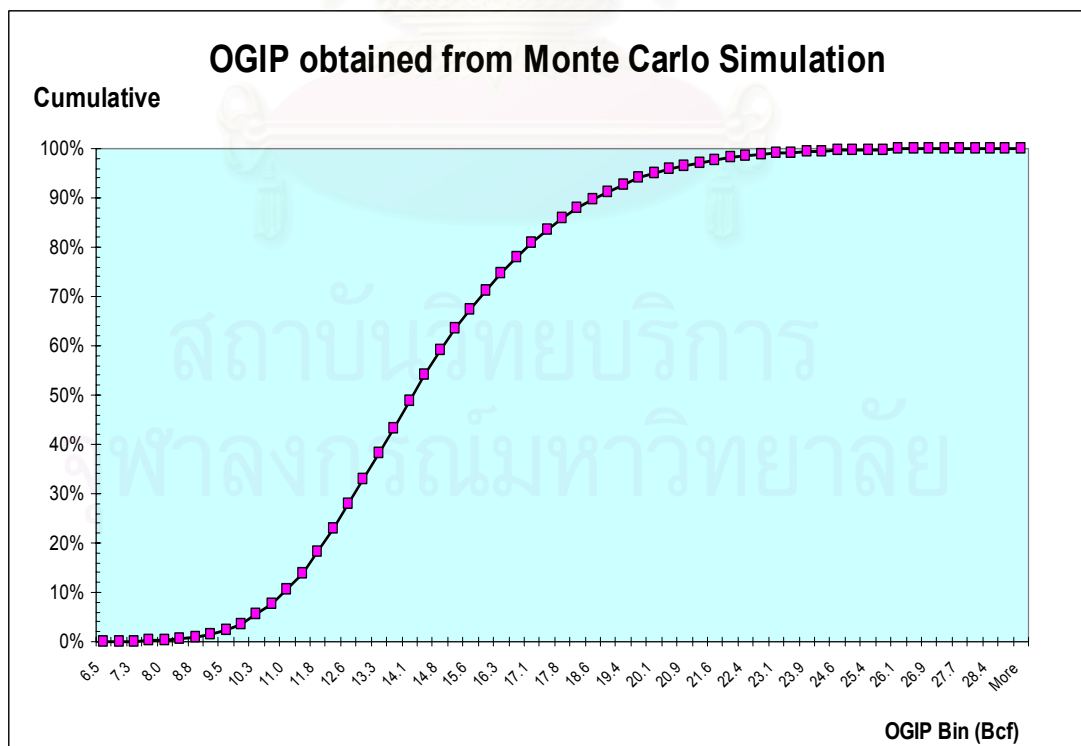


Figure 4.2: OGIP cumulative distribution function from MCS.

### 4.1.3 Sensitivity analysis

The important assumption of MCS is input variables are independent. However, porosity and water saturation are interdependent. When correlation between variables is taken into account, this would have some effect on the output. To describe sensitivity of input to output, the Second-Moment method was applied in this case. The variance of  $F$  is defined as:

$$V[F] = \sigma^2_F = E[(F - E[F])^2] \quad (4.2)$$

where  $F$  is an uncertainty quantity which depends on the parameter vector,  $x$ , and  $E[F]$  denotes the expected value. Consider a first-order Taylor series expansion around the mean point,  $\hat{x}$ :

$$F(x) \cong F(\hat{x}) + \sum_i \frac{\partial F}{\partial x_i} (x_i - \hat{x}_i) \quad (4.3)$$

with  $\hat{x}$  being the vector of mean values of the uncertain parameters. Taking the expected value of both sides of this expression, we obtain

$$E(F) \cong F(\hat{x}) + \sum_i \frac{\partial F}{\partial x_i} E[x_i - \hat{x}_i] \quad (4.4)$$

Assuming small and uniformly distributed parameter perturbations around the mean value such that the expectation term in the right hand side of Eq. 4.4 can be dropped and all higher-order terms neglected, we obtain

$$E[F] \cong F(\hat{x}) \quad (4.5)$$

Substituting Eq. 4.3 and Eq. 4.5 in Eq. 4.2, we have

$$V(F) \cong \sum_i \sum_j \frac{\partial F}{\partial x_i} \frac{\partial F}{\partial x_j} E[(x_i - \hat{x}_i)(x_j - \hat{x}_j)] \cong \sum_i \sum_j \frac{\partial F}{\partial x_i} \frac{\partial F}{\partial x_j} C[x_i x_j] \quad (4.6)$$

where the covariance,  $C[x_i x_j] = \rho_{ij} \sigma[x_i] \sigma[x_j]$ , is expressed in terms of the parameter correlation coefficient,  $\rho_{ij}$ , and the individual parameter standard

deviation,  $\sigma$ . The variance of  $F$  is thus seen to depend on the variance-covariance relation of the input parameters as well as its sensitivity to the uncertain inputs.

The total variance of OGIP when applying the Second-Moment method is the summation of derivative of OGIP taken with respect to porosity and water saturation. Referring to Eq. 3.2, the total variance of OGIP is as follows:

$$Var(OGIP) = \sum_{\phi} \sum_{S_w} \left. \frac{\partial(OGIP)}{\partial \phi} \right|_{\bar{\phi}} \left. \frac{\partial(OGIP)}{\partial S_w} \right|_{\bar{S}_w} C(\phi, S_w)$$

where  $\frac{\partial(OGIP)}{\partial \phi} = 155.44 (1 - S_w)$ ,  $\frac{\partial(OGIP)}{\partial S_w} = -155.44 \phi$ , and

$C(\phi, S_w) = \rho_{\phi S_w} \sigma_{\phi} \sigma_{S_w}$ . Therefore, the total variance of OGIP is

$$Var(OGIP) = \left[ \frac{\partial(OGIP)}{\partial \phi} \right]^2 Var(\phi) + 2 \frac{\partial(OGIP)}{\partial \phi} \frac{\partial(OGIP)}{\partial S_w} C(\phi, S_w) + \left[ \frac{\partial(OGIP)}{\partial S_w} \right]^2 Var(S_w)$$

when considering correlation between porosity and water saturation and

$$Var(OGIP) = \left[ \frac{\partial(OGIP)}{\partial \phi} \right]^2 Var(\phi) + \left[ \frac{\partial(OGIP)}{\partial S_w} \right]^2 Var(S_w)$$

when considering no correlation between porosity and water saturation.

Table 4.5: Sensitivity analysis of input variables to OGIP output.

Input variables	Variance contribution to mean OGIP			
	Considering correlation	Considering no correlation		
		Sensitivity coeff.	Variability	Total variance
Porosity	5.717	8,046.022	0.0005	3.924
Water Saturation	8.819	667.990	0.0105	7.026
Variance of OGIP	14.537	-	-	10.951

Substituting original statistics of porosity and water saturation, the total variance of OGIP is 14.537 when considering correlation between variables. It can be seen that water saturation has a higher variance contribution to OGIP than

porosity as the values are 8.819 and 5.717, respectively. Assuming no correlation, the result still behaves in the same manner, i.e., there is higher variance contribution from water saturation than from porosity.

Also shown in Table 4.5 are sensitivity coefficient and variability of porosity and water saturation which contribute to the total variance of OGIP output when considering no correlation. The sensitivity coefficient is a measure of how much the output will be changed when the input is changed. On the other hand, variability is uncertainty of input variable. Even porosity's sensitivity value of 8046.02 is higher than the value for water saturation which is 667.99, porosity variation of 0.005 is too small compared to value of 0.0105 for water saturation. Therefore, the effect of porosity on variance of OGIP is significantly reduced. It is obvious that either including or excluding correlation, water saturation contributes much effect on variance of OGIP. Moreover, there is significant increase of variance (by 33%) when considering the correlation. With a substantial impact on output variance, the correlation should be taken into account to avoid underestimation of the inherent uncertainty of input variables. In summary, the dispersion of output depends on the degree of correlation of input parameters.

## **4.2 Sequential Gaussian Simulation (SGS)**

The second method employed in this study to determine the distribution of porosity and water saturation is Sequential Gaussian Simulation (SGS). Built on geostatistical simulation framework, SGS is able to produce equally probable maps (realizations) of input variables. Practically, SGS is conducted in 2 steps which are structural analysis and conditional simulation. Structural analysis aims at determining spatial continuity which is known as variogram model. As required by Gaussian algorithm, transforming original data to normal score space and bivariate normality checking have to be performed to ensure multiGaussian random function agreement. Then, Sequential Gaussian Simulation can be performed. In this study, GSLIB program was used to construct variogram model of porosity and water saturation and to simulate their spatial distributions. Porosity and water saturation



values were simulated in three dimensions (3-D). When realizations of all input variables were generated, OGIPs were then estimated.

#### **4.2.1 Structure analysis (Variogram model)**

SGS is built on multivariate normal distribution which means that its univariate statistic has to be normal as well. Therefore, input variables have to be transformed to normal score data before doing anything further. SGS was performed on porosity and water saturation independently. Normal score transformed data for porosity and water saturation using GSLIB program are shown in Table 4.6. The first three columns in the table are X, Y, and Z coordinate. The next two columns are porosity and water saturation and the last two columns are normal score transform of porosity and water saturation, respectively. Histogram of normal score porosity and water saturation are illustrated in Figure 4.3.

As mentioned before, structural analysis or variogram model can be used to quantify the spatial variability of spatial phenomena, in this case, porosity and water saturation. The variogram is a measure of geological variability in terms of distance and direction. The geological variability is quite different in vertical and horizontal directions. In general, there is typically much greater spatial correlation in the horizontal plane. In the field selected for this study, a total of 349 log data are available. They were obtained from three wells at location along directional well paths that intersect the 130 ft-thick formation called Formation I. Petrophysical data were evaluated at every 0.5 ft interval. With this setting, the data set is representative of properties in the vertical direction while it is hard to find the correlation among data in the horizontal direction due to larger separation distance. Owing to this limitation, the omni-direction variogram calculation was applied to the data set. However, an attempt has been made to calculate directional variogram defined in the south-east (SE) direction in order to capture the spatial structure in three directional wells.

Table 4.6: Porosity and water saturation normal score transform.

X	Y	Z	P	S	NS:P	NS:S	X	Y	Z	P	S	NS:P	NS:S
411.97	31.58	41.42	13.82	52.00	-1.433	0.964	387.55	18.18	72.52	15.45	46.30	-0.568	0.247
411.38	31.25	42.17	11.89	59.80	-2.083	2.325	387.25	18.01	72.90	15.18	49.30	-0.690	0.576
411.09	31.09	42.55	11.79	54.30	-2.150	1.322	386.96	17.85	73.27	14.76	50.70	-0.865	0.709
410.79	30.93	42.92	12.41	54.40	-1.880	1.357	386.66	17.69	73.64	14.36	48.70	-1.152	0.518
409.32	30.12	44.80	10.00	47.70	-2.982	0.414	386.37	17.53	74.02	14.32	43.80	-1.166	0.000
408.14	29.48	46.30	10.65	59.10	-2.449	2.083	386.08	17.37	74.39	14.77	40.10	-0.855	-0.367
406.08	28.34	48.92	13.13	42.40	-1.643	-0.166	385.78	17.21	74.76	15.52	37.30	-0.543	-0.585
405.79	28.18	49.30	13.94	43.70	-1.375	-0.043	385.49	17.05	75.14	16.33	34.40	-0.022	-0.756
405.49	28.02	49.67	13.90	33.60	-1.394	-0.794	385.20	16.89	75.51	16.96	30.10	0.314	-1.010
405.20	27.86	50.05	13.33	26.10	-1.565	-1.357	384.90	16.73	75.89	17.43	25.80	0.453	-1.394
404.90	27.70	50.42	13.55	25.50	-1.474	-1.413	384.61	16.56	76.26	17.63	25.40	0.493	-1.453
404.61	27.54	50.80	15.04	28.30	-0.775	-1.166	384.31	16.40	76.64	17.54	28.10	0.485	-1.225
404.31	27.37	51.17	16.21	32.60	-0.101	-0.886	384.02	16.24	77.01	17.37	30.50	0.437	-0.987
404.02	27.21	51.55	16.24	39.30	-0.065	-0.422	383.73	16.08	77.38	17.27	29.90	0.406	-1.035
403.72	27.05	51.92	15.67	46.30	-0.445	0.269	383.43	15.92	77.76	17.07	28.10	0.367	-1.195
403.43	26.89	52.30	14.98	46.70	-0.794	0.306	383.14	15.76	78.13	16.85	29.50	0.262	-1.072
403.14	26.73	52.67	14.37	41.40	-1.125	-0.239	382.85	15.60	78.50	16.57	31.70	0.101	-0.897
402.84	26.57	53.05	14.06	40.50	-1.305	-0.329	382.55	15.44	78.88	16.38	32.70	-0.007	-0.865
402.55	26.41	53.42	14.23	48.40	-1.210	0.501	382.26	15.27	79.25	16.45	33.50	0.036	-0.804
401.66	25.92	54.55	12.94	55.60	-1.733	1.496	381.96	15.11	79.63	16.69	34.60	0.173	-0.727
401.37	25.76	54.92	11.93	35.60	-2.024	-0.681	381.67	14.95	80.00	17.01	36.80	0.329	-0.610
401.07	25.60	55.30	11.78	25.50	-2.229	-1.433	381.38	14.79	80.38	17.15	39.90	0.390	-0.375
400.78	25.44	55.67	13.94	32.60	-1.357	-0.876	381.08	14.63	80.75	17.08	43.00	0.375	-0.122
400.49	25.27	56.05	15.87	40.70	-0.329	-0.321	380.79	14.47	81.12	17.03	45.80	0.344	0.188
400.19	25.11	56.42	16.47	44.20	0.050	0.050	380.50	14.31	81.50	16.84	47.70	0.247	0.422
399.90	24.95	56.80	16.32	49.00	-0.029	0.559	380.20	14.15	81.87	16.53	47.40	0.072	0.383
399.60	24.79	57.17	15.56	57.60	-0.501	1.733	379.91	13.99	82.25	16.30	46.60	-0.036	0.299
397.83	23.82	59.42	15.15	59.80	-0.737	2.449	379.61	13.82	82.62	16.29	46.70	-0.043	0.314
397.54	23.66	59.80	15.27	58.40	-0.654	1.839	379.32	13.66	82.99	16.18	44.20	-0.130	0.057
396.66	23.17	60.92	15.41	57.00	-0.593	1.590	379.03	13.50	83.37	16.07	36.30	-0.195	-0.637
396.36	23.01	61.30	15.47	53.80	-0.559	1.240	378.73	13.34	83.74	16.18	29.10	-0.137	-1.125
396.07	22.85	61.67	15.22	51.90	-0.672	0.941	378.44	13.18	84.11	16.03	28.20	-0.225	-1.180
395.77	22.69	62.05	14.93	45.60	-0.814	0.159	378.15	13.02	84.49	15.63	28.10	-0.477	-1.210
395.48	22.53	62.42	14.58	37.50	-1.059	-0.576	377.85	12.86	84.86	15.37	24.40	-0.602	-1.541
395.18	22.37	62.80	14.36	35.80	-1.138	-0.672	377.56	12.70	85.24	15.73	22.70	-0.390	-1.702
394.89	22.20	63.17	14.62	41.30	-1.035	-0.254	377.26	12.54	85.61	16.80	27.50	0.225	-1.256
394.60	22.04	63.54	15.17	44.30	-0.718	0.065	376.97	12.37	85.99	18.17	31.70	0.637	-0.908
394.30	21.88	63.92	15.63	44.30	-0.469	0.079	376.68	12.21	86.36	19.42	31.20	1.138	-0.919
394.01	21.72	64.29	15.85	45.50	-0.344	0.151	376.38	12.05	86.73	20.09	27.50	1.474	-1.272
393.72	21.56	64.67	15.94	48.70	-0.276	0.526	376.09	11.89	87.11	20.17	23.70	1.518	-1.590
393.42	21.40	65.04	16.00	53.10	-0.247	1.085	375.80	11.73	87.48	19.88	23.60	1.375	-1.672
393.13	21.24	65.41	16.15	54.50	-0.144	1.394	375.50	11.57	87.85	19.74	24.80	1.305	-1.496
392.83	21.08	65.79	16.41	52.40	0.014	0.987	375.21	11.41	88.23	20.03	23.90	1.433	-1.565
392.54	20.92	66.16	16.36	50.40	-0.014	0.672	374.91	11.25	88.60	20.66	21.50	1.839	-1.733
392.25	20.75	66.54	16.05	50.20	-0.210	0.645	374.62	11.08	88.98	21.57	20.00	2.150	-1.971
391.95	20.59	66.91	15.72	51.40	-0.406	0.834	374.33	10.92	89.35	22.34	20.60	2.449	-1.801
391.66	20.43	67.28	15.24	51.60	-0.663	0.919	374.03	10.76	89.73	22.62	21.20	2.982	-1.766
391.37	20.27	67.66	14.91	51.60	-0.824	0.865	373.74	10.60	90.10	22.42	20.10	2.628	-1.880
391.07	20.11	68.03	15.13	51.60	-0.746	0.886	373.45	10.44	90.47	22.10	17.90	2.325	-2.150
390.78	19.95	68.41	15.52	51.60	-0.534	0.897	373.15	10.28	90.85	21.60	16.30	2.229	-2.449
390.48	19.79	68.78	15.55	51.20	-0.518	0.785	372.86	10.12	91.22	20.71	16.50	1.880	-2.325
390.19	19.63	69.15	15.20	50.80	-0.681	0.727	372.56	9.96	91.60	19.47	18.00	1.166	-2.083
389.90	19.47	69.53	14.68	51.60	-0.941	0.908	372.27	9.80	91.97	17.43	20.30	0.461	-1.839
389.60	19.30	69.90	14.01	51.10	-1.322	0.775	371.98	9.63	92.34	14.52	26.00	-1.085	-1.375
389.31	19.14	70.28	13.27	50.90	-1.590	0.746	371.68	9.47	92.72	11.23	40.80	-2.325	-0.306
389.02	18.98	70.65	12.98	53.80	-1.702	1.256	367.86	7.38	97.58	13.17	41.70	-1.616	-0.217
388.72	18.82	71.02	13.59	53.10	-1.453	1.098	367.57	7.22	97.95	15.71	42.80	-0.429	-0.137
388.43	18.66	71.40	14.67	47.30	-0.975	0.360	367.28	7.06	98.33	17.52	43.50	0.477	-0.065
388.13	18.50	71.77	15.36	42.00	-0.610	-0.188	366.98	6.89	98.70	18.32	43.50	0.727	-0.072
387.84	18.34	72.15	15.51	42.00	-0.551	-0.195	366.69	6.73	99.08	18.42	44.30	0.765	0.072

Table 4.6: Porosity and water saturation normal score transform (continued).

X	Y	Z	P	S	NS:P	NS:S	X	Y	Z	P	S	NS:P	NS:S
366.40	6.57	99.45	18.41	46.60	0.756	0.291	37.68	201.75	11.35	17.86	40.40	0.534	-0.344
366.10	6.41	99.82	18.28	50.00	0.718	0.628	37.38	201.63	11.72	18.17	43.70	0.645	-0.029
365.81	6.25	100.20	17.72	51.90	0.501	0.952	37.09	201.50	12.09	18.65	46.80	0.855	0.321
365.51	6.09	100.57	16.89	49.70	0.291	0.602	36.79	201.38	12.45	18.89	47.80	0.952	0.429
365.22	5.93	100.95	16.10	45.70	-0.181	0.173	36.49	201.26	12.82	18.89	46.10	0.941	0.210
364.93	5.77	101.32	15.72	43.20	-0.414	-0.115	36.18	201.13	13.19	18.68	44.10	0.876	0.029
364.63	5.61	101.69	15.78	43.70	-0.360	-0.036	35.88	201.01	13.56	18.38	43.20	0.746	-0.108
364.34	5.44	102.07	15.95	46.30	-0.262	0.262	35.58	200.88	13.92	18.27	43.70	0.690	-0.022
364.05	5.28	102.44	16.22	50.30	-0.086	0.663	35.28	200.76	14.29	18.26	44.30	0.672	0.086
363.75	5.12	102.82	16.44	54.40	0.029	1.339	34.98	200.64	14.66	18.14	44.50	0.628	0.101
363.46	4.96	103.19	16.22	57.10	-0.094	1.616	34.68	200.51	15.02	17.96	43.90	0.585	0.014
363.16	4.80	103.56	15.89	56.30	-0.314	1.565	34.38	200.39	15.39	17.92	41.80	0.559	-0.202
362.87	4.64	103.94	15.94	53.10	-0.284	1.111	34.08	200.26	15.76	18.02	40.20	0.602	-0.352
362.58	4.48	104.31	16.02	53.00	-0.232	1.047	33.78	200.14	16.13	18.17	40.70	0.654	-0.314
362.28	4.32	104.69	15.72	55.70	-0.398	1.541	33.48	200.01	16.49	18.23	41.20	0.663	-0.262
361.99	4.15	105.06	15.17	57.10	-0.727	1.643	33.18	199.89	16.86	17.78	39.80	0.518	-0.383
361.69	3.99	105.43	14.76	54.90	-0.876	1.433	32.88	199.77	17.23	17.32	37.90	0.414	-0.543
361.40	3.83	105.81	14.69	52.00	-0.908	0.975	32.58	199.64	17.59	16.96	38.90	0.321	-0.469
361.11	3.67	106.18	14.69	54.70	-0.919	1.413	32.28	199.52	17.96	16.70	41.10	0.181	-0.269
358.76	2.38	109.17	10.15	50.80	-2.628	0.737	31.98	199.39	18.33	16.61	42.20	0.122	-0.173
358.46	2.22	109.55	12.79	47.30	-1.766	0.367	31.68	199.27	18.69	16.68	42.70	0.159	-0.151
358.17	2.06	109.92	15.01	48.20	-0.785	0.485	31.38	199.14	19.06	16.77	44.70	0.202	0.108
357.88	1.90	110.30	16.23	52.90	-0.079	1.035	31.08	199.02	19.43	16.79	47.30	0.217	0.352
357.58	1.74	110.67	16.62	57.30	0.137	1.702	30.78	198.90	19.80	16.68	49.10	0.166	0.568
357.29	1.58	111.05	16.46	59.30	0.043	2.150	30.48	198.77	20.16	16.62	51.60	0.130	0.876
355.53	0.61	113.29	14.63	60.00	-1.010	2.982	30.18	198.65	20.53	16.63	53.50	0.151	1.195
355.23	0.45	113.66	15.18	55.40	-0.700	1.453	29.88	198.52	20.90	16.55	53.40	0.086	1.166
354.94	0.29	114.04	15.71	53.90	-0.422	1.272	29.58	198.40	21.27	16.29	51.30	-0.050	0.814
354.64	0.13	114.41	16.56	55.50	0.094	1.474	29.28	198.28	21.63	15.92	48.30	-0.299	0.493
46.97	205.59	0.00	18.71	34.40	0.908	-0.737	28.97	198.15	22.00	15.52	47.10	-0.526	0.337
46.67	205.47	0.37	19.83	39.10	1.322	-0.445	28.67	198.03	22.37	15.27	47.90	-0.645	0.437
46.37	205.35	0.74	20.17	45.80	1.541	0.195	28.37	197.90	22.73	15.35	48.90	-0.619	0.543
46.07	205.22	1.10	20.23	51.60	1.590	0.930	28.07	197.78	23.10	15.56	47.30	-0.510	0.344
45.77	205.10	1.47	20.18	52.70	1.565	1.010	27.77	197.65	23.47	15.60	43.40	-0.485	-0.079
45.47	204.97	1.83	20.12	52.90	1.496	1.022	27.47	197.53	23.84	15.32	39.20	-0.628	-0.437
45.18	204.85	2.20	20.46	52.60	1.766	0.998	27.17	197.41	24.20	14.68	36.40	-0.930	-0.619
44.88	204.73	2.57	20.83	51.30	2.024	0.824	26.87	197.28	24.57	14.20	35.90	-1.240	-0.663
44.58	204.60	2.93	20.72	46.10	1.923	0.217	26.57	197.16	24.94	14.44	38.10	-1.111	-0.526
44.28	204.48	3.30	20.43	42.50	1.733	-0.159	26.27	197.03	25.31	15.11	39.20	-0.765	-0.429
43.98	204.35	3.67	20.00	41.70	1.413	-0.210	25.97	196.91	25.67	15.67	37.80	-0.461	-0.559
43.68	204.23	4.03	19.68	42.10	1.288	-0.181	25.67	196.78	26.04	15.89	36.00	-0.306	-0.654
43.38	204.11	4.40	19.64	43.20	1.256	-0.101	25.37	196.66	26.41	15.78	35.00	-0.367	-0.709
43.08	203.98	4.76	19.87	44.90	1.357	0.115	25.07	196.54	26.77	15.30	36.10	-0.637	-0.645
42.78	203.86	5.13	20.24	45.90	1.616	0.202	24.77	196.41	27.14	14.67	39.70	-0.987	-0.390
42.48	203.73	5.50	20.36	45.40	1.702	0.137	24.46	196.29	27.51	14.49	44.10	-1.098	0.022
42.18	203.61	5.86	20.25	44.40	1.643	0.094	24.16	196.16	27.88	14.73	46.30	-0.886	0.254
41.88	203.49	6.23	20.05	45.40	1.453	0.144	23.86	196.04	28.25	14.80	45.10	-0.845	0.130
41.58	203.36	6.59	19.65	47.50	1.272	0.390	23.56	195.91	28.62	14.63	43.40	-1.022	-0.086
41.28	203.24	6.96	19.39	49.90	1.125	0.619	23.26	195.79	28.98	14.14	43.60	-1.272	-0.050
40.98	203.12	7.33	19.32	51.30	1.085	0.804	22.96	195.66	29.35	13.47	45.10	-1.496	0.122
40.68	202.99	7.69	19.48	49.70	1.180	0.610	22.66	195.54	29.72	13.36	44.10	-1.518	0.043
40.38	202.87	8.06	19.87	46.20	1.339	0.225	22.36	195.41	30.09	13.99	38.00	-1.339	-0.534
40.08	202.74	8.43	20.35	42.90	1.672	-0.130	20.55	194.67	32.30	14.72	37.20	-0.897	-0.593
39.78	202.62	8.79	20.79	41.60	1.971	-0.225	20.25	194.54	32.67	14.54	41.10	-1.072	-0.276
39.48	202.50	9.16	20.94	40.90	2.083	-0.299	19.95	194.42	33.03	15.12	41.00	-0.756	-0.291
39.18	202.37	9.52	20.62	40.40	1.801	-0.337	19.65	194.29	33.40	16.01	38.70	-0.239	-0.493
38.88	202.25	9.89	19.92	40.20	1.394	-0.360	19.34	194.17	33.77	16.86	35.50	0.284	-0.690
38.58	202.12	10.26	19.22	39.60	1.047	-0.398	19.04	194.04	34.14	17.79	32.90	0.526	-0.855
38.28	202.00	10.62	18.64	38.70	0.834	-0.501	18.74	193.92	34.51	18.28	33.80	0.700	-0.785
37.98	201.88	10.99	18.08	38.30	0.619	-0.518	18.44	193.80	34.88	18.28	37.50	0.709	-0.568

Table 4.6: Porosity and water saturation normal score transform (continued).

X	Y	Z	P	S	NS:P	NS:S	X	Y	Z	P	S	NS:P	NS:S
18.14	193.67	35.24	18.26	41.30	0.681	-0.247	182.81	407.93	87.76	15.88	54.10	-0.321	1.288
17.84	193.55	35.61	17.96	44.10	0.576	0.036	182.49	408.00	88.16	16.20	47.70	-0.108	0.406
17.54	193.42	35.98	17.35	46.40	0.422	0.284	182.17	408.07	88.56	16.27	47.40	-0.057	0.375
17.24	193.30	36.35	16.55	48.10	0.079	0.453	181.85	408.14	88.96	16.23	50.70	-0.072	0.718
16.93	193.17	36.72	16.12	45.70	-0.166	0.166	181.53	408.21	89.36	16.12	54.50	-0.159	1.375
16.63	193.05	37.08	15.83	41.10	-0.352	-0.284	181.21	408.28	89.76	16.10	59.00	-0.173	2.024
16.33	192.92	37.45	16.13	36.90	-0.151	-0.602	178.97	408.78	92.56	15.74	59.00	-0.383	1.971
16.03	192.80	37.82	16.86	33.20	0.276	-0.814	178.65	408.85	92.96	14.94	57.70	-0.804	1.766
14.83	192.30	39.29	16.08	33.10	-0.188	-0.824	178.33	408.92	93.36	14.25	57.20	-1.195	1.672
13.62	191.80	40.77	14.67	43.30	-0.964	-0.094	178.01	408.99	93.76	14.08	58.10	-1.288	1.801
13.32	191.68	41.14	15.71	50.20	-0.437	0.654	177.37	409.14	94.56	15.18	58.70	-0.709	1.923
13.01	191.55	41.51	16.59	51.20	0.115	0.794	177.05	409.21	94.97	15.78	51.00	-0.375	0.756
12.71	191.43	41.88	16.92	48.90	0.299	0.534	176.73	409.28	95.37	16.40	41.50	0.000	-0.232
12.41	191.30	42.25	16.80	46.30	0.232	0.276	176.41	409.35	95.77	16.84	37.80	0.254	-0.551
12.11	191.18	42.61	17.06	43.90	0.360	0.007	176.09	409.42	96.17	16.82	43.70	0.239	-0.014
11.81	191.05	42.98	17.49	43.80	0.469	-0.007	175.77	409.49	96.57	16.58	50.70	0.108	0.700
11.50	190.93	43.35	17.37	46.20	0.429	0.232	175.45	409.56	96.97	16.41	51.40	0.007	0.855
11.20	190.80	43.72	16.77	47.00	0.210	0.329	175.13	409.63	97.37	16.18	48.90	-0.122	0.551
10.90	190.68	44.09	15.86	43.50	-0.337	-0.057	174.80	409.71	97.77	15.99	47.60	-0.254	0.398
10.60	190.55	44.46	14.80	38.40	-0.834	-0.510	174.48	409.78	98.18	16.05	48.10	-0.202	0.469
10.30	190.43	44.83	14.28	34.30	-1.180	-0.765	174.16	409.85	98.58	16.19	49.70	-0.115	0.593
9.99	190.30	45.20	14.60	30.70	-1.047	-0.975	173.84	409.92	98.98	16.50	53.50	0.057	1.210
9.69	190.18	45.57	16.04	27.30	-0.217	-1.288	173.52	409.99	99.38	16.85	58.70	0.269	1.880
9.39	190.05	45.94	17.01	27.00	0.337	-1.305	172.56	410.21	100.58	16.74	59.40	0.188	2.229
9.09	189.93	46.31	17.96	28.40	0.593	-1.152	172.24	410.28	100.99	16.44	55.70	0.022	1.518
8.78	189.80	46.68	18.50	29.60	0.785	-1.047	171.92	410.35	101.39	15.93	54.20	-0.291	1.305
8.48	189.68	47.05	18.70	31.10	0.897	-0.930	171.60	410.42	101.79	15.94	53.20	-0.269	1.152
8.18	189.55	47.41	18.77	33.00	0.930	-0.845	171.28	410.49	102.19	16.62	50.60	0.144	0.681
7.88	189.43	47.78	18.65	34.40	0.845	-0.746	170.96	410.56	102.59	17.40	48.60	0.445	0.510
7.58	189.30	48.15	18.48	36.40	0.775	-0.628	170.64	410.63	102.99	17.92	50.10	0.568	0.637
7.28	189.18	48.52	18.52	38.90	0.804	-0.477	170.31	410.71	103.40	17.89	53.00	0.551	1.059
6.97	189.05	48.89	18.66	38.80	0.865	-0.485	169.99	410.78	103.80	17.13	53.60	0.383	1.225
6.67	188.93	49.26	18.57	35.30	0.824	-0.700	169.67	410.85	104.20	16.53	51.40	0.065	0.845
6.37	188.80	49.63	18.50	30.90	0.794	-0.952	169.35	410.92	104.60	16.76	50.60	0.195	0.690
6.07	188.68	50.00	18.69	28.70	0.886	-1.138	169.03	410.99	105.00	17.04	53.00	0.352	1.072
5.76	188.55	50.37	19.00	29.20	0.998	-1.098	168.71	411.06	105.41	16.95	53.20	0.306	1.138
5.46	188.43	50.74	19.36	30.70	1.098	-0.964	168.39	411.13	105.81	17.21	48.10	0.398	0.477
5.16	188.30	51.10	19.62	31.00	1.240	-0.941	168.07	411.21	106.21	17.89	46.30	0.543	0.239
4.86	188.18	51.48	19.55	29.10	1.210	-1.111	167.74	411.28	106.61	18.37	49.60	0.737	0.585
4.56	188.05	51.84	19.25	26.20	1.059	-1.339	167.42	411.35	107.02	18.53	53.40	0.814	1.180
4.25	187.93	52.21	19.04	24.50	1.022	-1.518	167.10	411.42	107.42	18.04	59.90	0.610	2.628
3.95	187.80	52.58	19.00	25.20	0.987	-1.474	151.98	414.78	126.35	12.26	48.00	-1.971	0.445
3.65	187.68	52.95	18.96	28.00	0.975	-1.240	151.66	414.86	126.76	12.50	39.10	-1.839	-0.453
3.35	187.55	53.32	18.92	29.90	0.964	-1.022	151.33	414.93	127.16	12.73	39.30	-1.801	-0.414
3.04	187.43	53.69	19.04	30.20	1.010	-0.998	151.01	415.00	127.56	13.35	39.00	-1.541	-0.461
2.74	187.30	54.06	19.29	29.40	1.072	-1.085	150.69	415.07	127.97	14.20	33.00	-1.225	-0.834
2.44	187.18	54.43	19.46	26.80	1.152	-1.322	150.37	415.14	128.37	14.67	29.50	-0.952	-1.059
2.14	187.05	54.80	19.56	23.60	1.225	-1.643	150.05	415.21	128.77	14.16	34.00	-1.256	-0.775
1.83	186.93	55.17	19.52	19.50	1.195	-2.024	149.72	415.29	129.18	12.33	45.70	-1.923	0.181
1.53	186.80	55.54	19.38	16.20	1.111	-2.628							
1.23	186.68	55.91	19.19	14.90	1.035	-2.982							
0.92	186.55	56.28	18.76	16.60	0.919	-2.229							
0.62	186.43	56.65	17.73	23.70	0.510	-1.616							
0.32	186.30	57.02	15.67	34.90	-0.453	-0.718							
187.28	406.93	82.16	15.44	51.00	-0.576	0.765							
186.96	407.00	82.56	15.60	39.50	-0.493	-0.406							
186.64	407.07	82.96	15.41	42.80	-0.585	-0.144							
186.32	407.14	83.36	14.66	53.10	-0.998	1.125							
186.00	407.21	83.76	13.89	48.10	-1.413	0.461							
185.68	407.29	84.16	13.02	20.00	-1.672	-1.923							



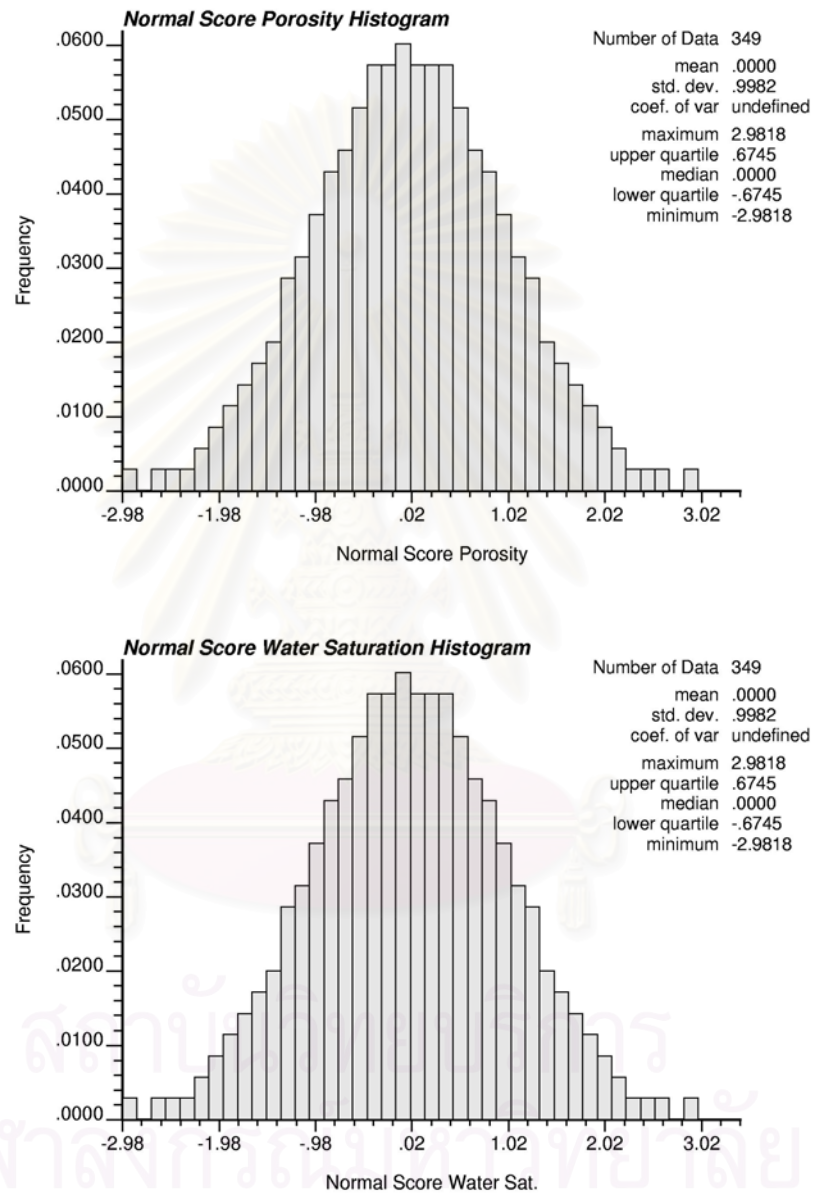


Figure 4.3: Histogram of normal score transform for porosity and water saturation.

Figures 4.4 and 4.5 exhibit omni-directional variograms of the original data and normal score transform of porosity and water saturation. Both are modeled by spherical model with 10%-30% nugget and a range of 100-120 ft using normal score transform. Figures 4.6 and 4.7 show the variograms in the SE direction of the original data and normal score transform of porosity and water saturation. The variogram parameters in omni and SE directions for original and normal score transform of porosity and water saturation are summarized in Table 4.7.

Table 4.7: Variogram parameters in omni and south-east (SE) directions of porosity and water saturation.

Variable	Directional Variogram	Model	Original Data			Normal Score Data		
			Sill	Nugget	Range (ft)	Sill	Nugget	Range (ft)
Porosity	Omni	Spherical	4.9	1.5	100	1.0	0.3	100
Water Saturation	Omni	Spherical	110.0	30.0	120	1.0	0.3	120
Porosity	South-East	Spherical	4.4	0.8	100	1.0	0.1	100
Water Saturation	South-East	Spherical	105.0	30.0	120	1.0	0.3	120

In an effort to maximize number of data in the search area, dip angle was set at 30 degree, and dip tolerance was at 22.5 degree. Similar to omni-directional model, spherical models were used in the SE direction for both variables. In normal score space, the nugget effect of porosity variogram in the SE direction is slightly lower than that in the omni-direction while those of water saturation are identical. For all search directions, water saturation seems to have more spatial continuity than porosity by 20 ft in distance. However, a lower nugget effect of porosity variogram at 0.1 compared to that of water saturation at 0.3 implies higher local variation in water saturation. And this is justified when compared to the original statistics or the variance of porosity and water saturation which are 4.88 and 105.18, respectively.

After constructing variogram model, there is a need to check for bivariate normal distribution before conducting simulation.



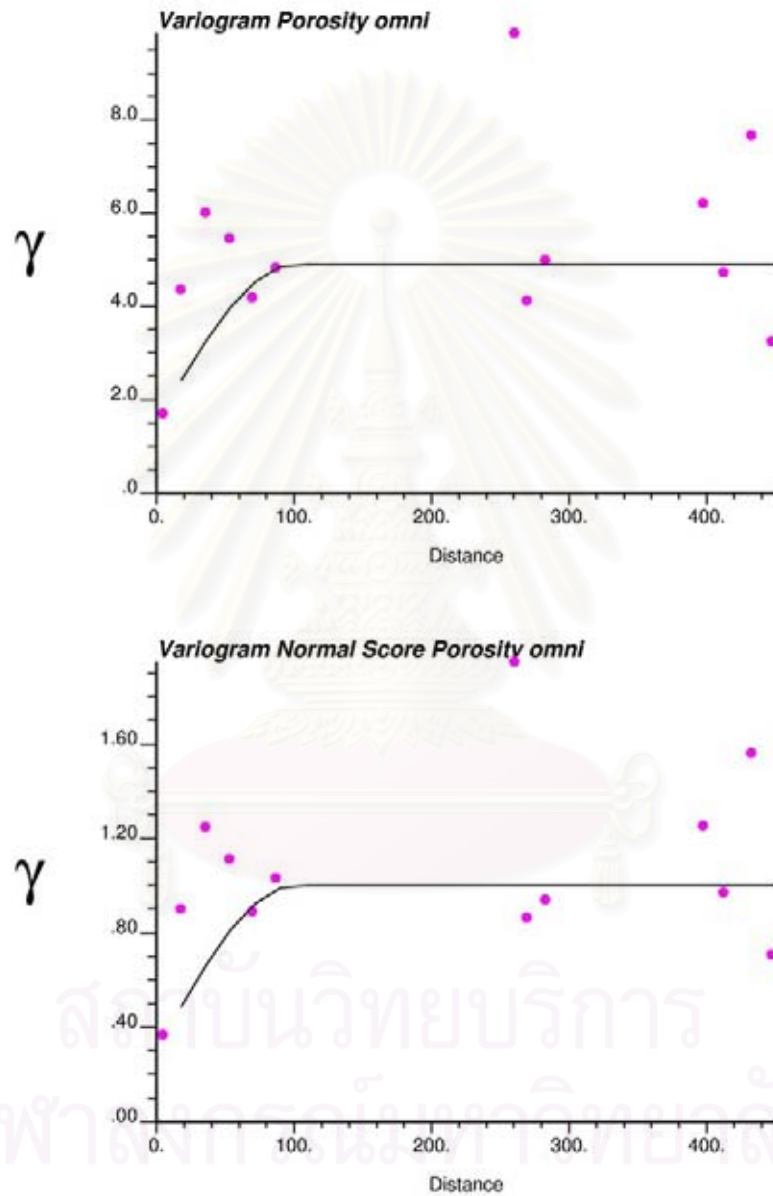


Figure 4.4: Omni-directional variograms of the original data and normal score transform of porosity.

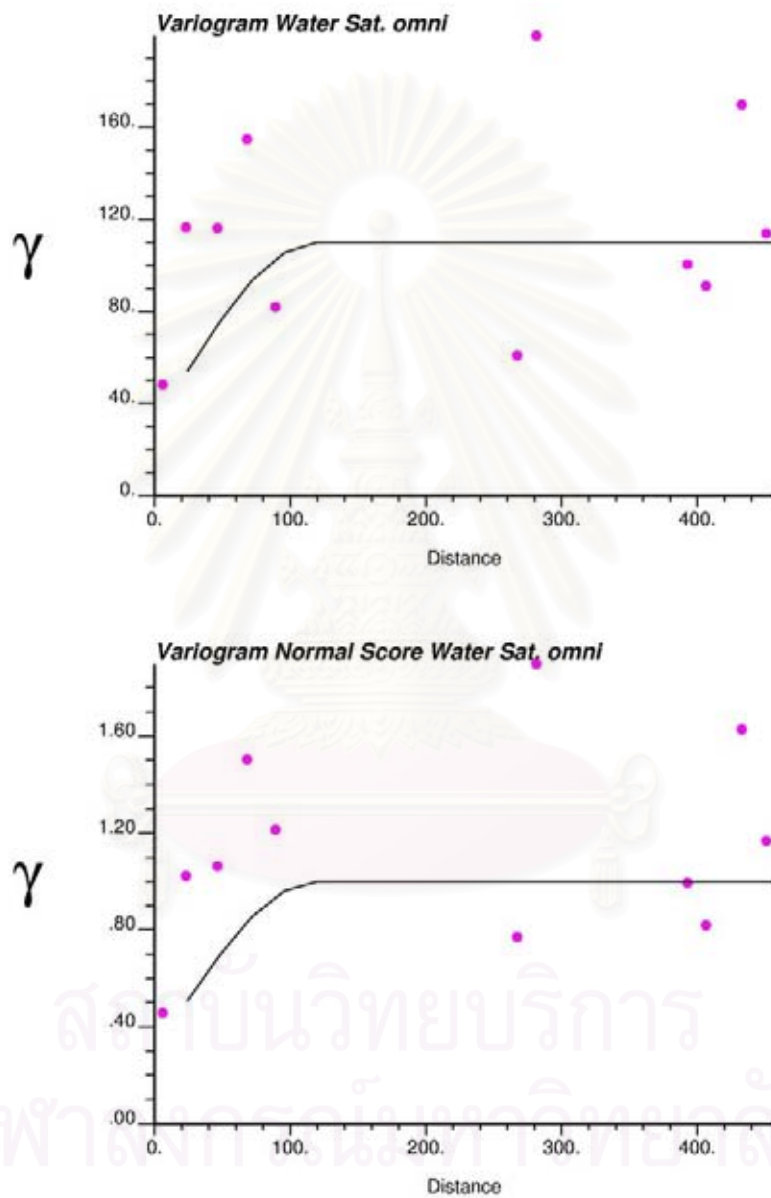


Figure 4.5: Omni-directional variograms of the original data and normal score transform of water saturation.

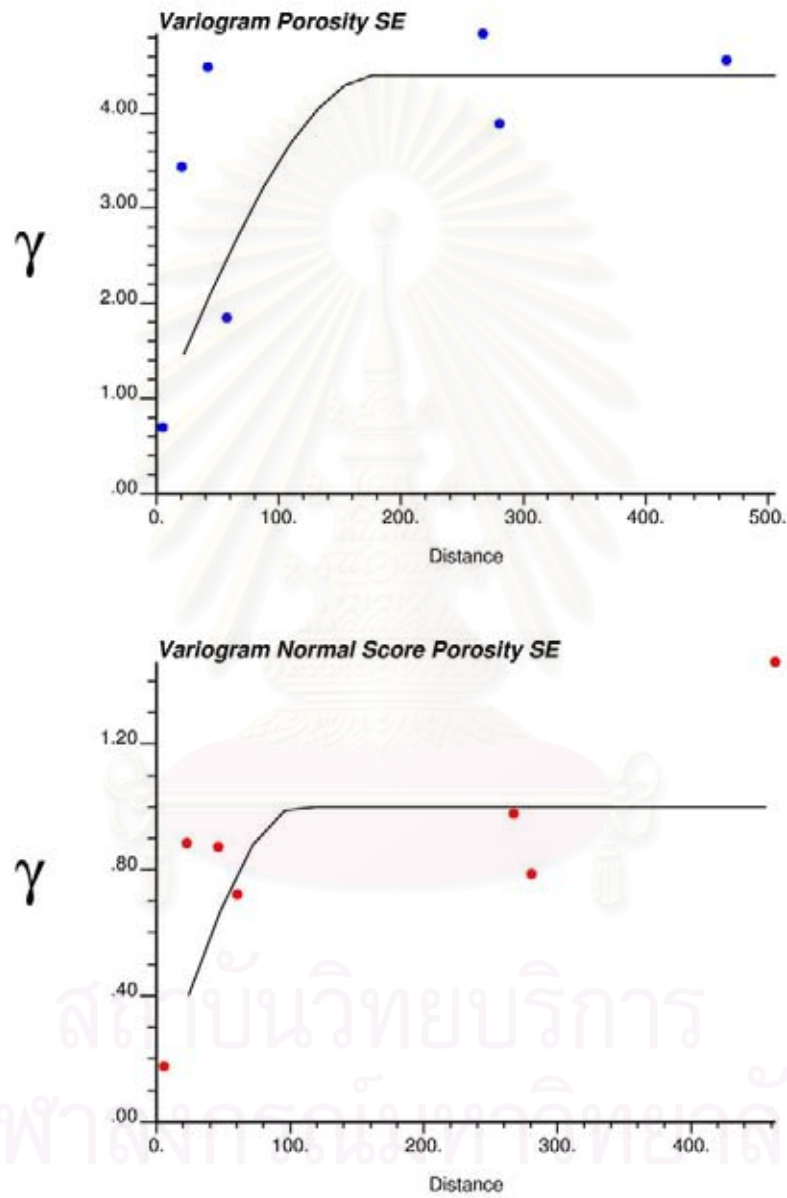


Figure 4.6: Variograms in the south-east (SE) direction of the original data and normal score transform of porosity.

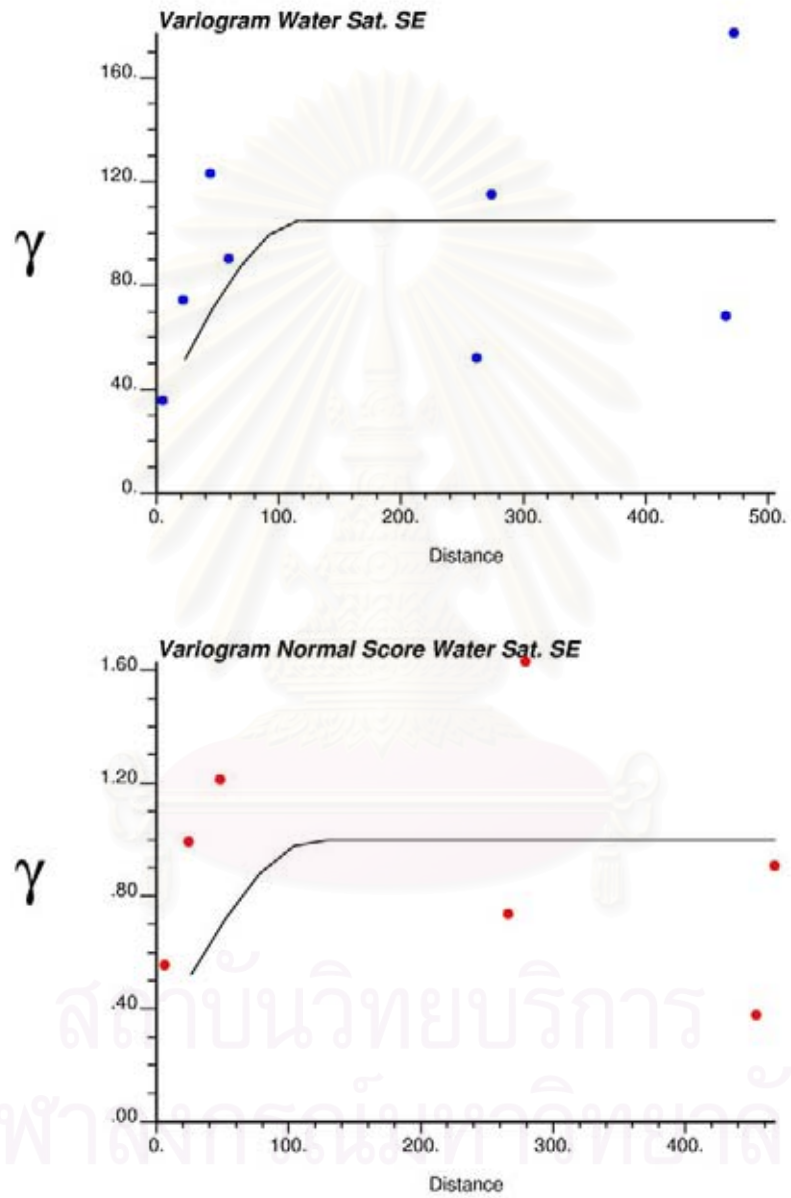


Figure 4.7: Variograms in the south-east (SE) direction of the original data and normal score transform of water saturation.

### ***Checking for Bivariate Normality***

When applying a Gaussian technique, the first step is to perform the normal score transform of the data. This transform defines new variable which is, by construction, (univariate) standard normal distribution. However, the transform does not guarantee that the variables are multivariate normally distributed as required by multiGaussian model. Thus, before applying Gaussian simulation, it is necessary to check whether the variables agree with the hypothesis.

In practice, checking for bivariate normality is implemented by comparing the experimental indicator variogram calculated at different cutoffs to the theoretical indicator variogram (Almeida, 1993). In this study, the experimental indicator variograms of porosity and water saturation at median cutoff (0.5 cdf value) were calculated and then compared to the theoretical indicator variogram. Figures 4.8 and 4.9 show the experimental and theoretical indicator variograms corresponding to the median for porosity and water saturation. As shown in the figures, these variogram models show a generally good agreement for median cutoff for porosity and water saturation. Thus, the results imply no rejection of the hypothesis of bi-Gaussian model. Hence, the multiGaussian model is deemed appropriate for this study.

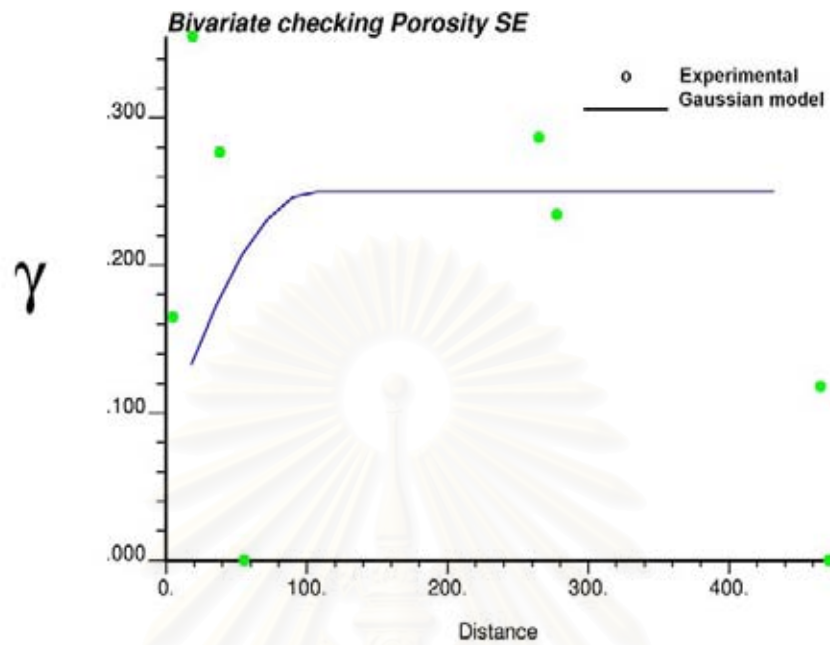


Figure 4.8: Experimental and Gaussian model-derived indicator variograms for porosity at median cutoff (0.5 cdf value).

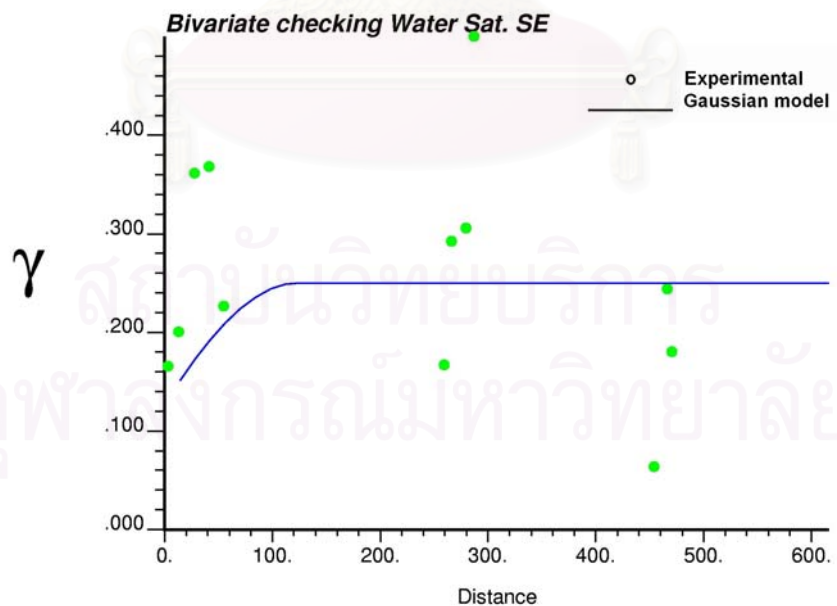


Figure 4.9: Experimental and Gaussian model-derived indicator variograms for water saturation at median cutoff (0.5 cdf value).



#### 4.2.2 Sequential Gaussian Simulation

SGS algorithm is performed with the conditional cumulative distribution function characterized through the simple Kriging system. At each step in the process, a node is selected, original data and previously simulated data are used to estimate the mean and variance of local distribution of variable and then a simulated value is sampled from the distribution. The number and structure of points included in the simulation is defined by the neighborhood search options. The ability to draw multiple realizations is achieved by setting a different random path for each realization. A random path is a sequence indicating the patterns which all the grid locations are visited at only once. Hence, the resulting multiple image maps of property of interest look differently while statistics are similar.

In this study, 100 realizations of porosity and water saturation were generated and used as inputs to calculate OGIP. This number of realization is large enough to justify the result when compared to other stochastic methods. The reservoir of the size 420 ft x 420 ft x 130 ft was divided into 21 x 21 x 130 grids/node for simulation corresponding to a grid block size of 20 ft x 20 ft x 1 ft. GSLIB program was used to run SGS to generate 100 realizations of porosity and water saturation.

Practically, only blocks located within the search distance are simulated using the constructed probability density function; therefore, the simulated blocks are clustered around well locations. About 30-40% of blocks were simulated using this procedure whereas the values for the rest of the blocks were inferred from the original statistics. In this analysis, the simulated blocks that draw the simulated values from the constructed probability distribution function are called local distribution blocks while blocks that draw simulated values from the original data statistics are called global distribution blocks. In Kriging matrix construction, the local distribution blocks are located within the search volume, and the global distribution blocks are located outside the search volume. The SGS parameter files are given in Appendix A.1 and A.2, respectively.

Statistics of simulated porosity and water saturation of each realization are given in Appendix B.1. An example of porosity and water saturation realizations obtained from SGS-local and global distribution are shown in Figures 4.10 and 4.11. To check whether SGS preserves the original statistics, particular simulated porosity and water saturation realizations were selected to compare with the original. Table 4.8 compares the statistics of the 50<sup>th</sup> realization of simulated porosity and water saturation with those of the original data. It can be seen that distributions of the 50<sup>th</sup> simulated porosity and water saturation realization generally reveal a similar pattern to the original data distributions, indicating the reliability of the results. Only correlation between porosity and water saturation is noted to be much deviated from the original value. Furthermore, porosity and water saturation in some realizations are no longer correlated. This is because each variable was separately generated.

Table 4.8: Statistics of the 50<sup>th</sup> realization of porosity and water saturation generated by SGS-local and global distribution.

Statistics	Porosity		Water Saturation	
	Original Data	SGS	Original Data	SGS
Mean	16.63	16.59	42.29	43.87
Standard Deviation	2.21	2.05	10.26	9.29
Variance	4.88	4.21	105.18	86.35
Minimum	10.00	10.00	14.90	14.90
Maximum	22.62	22.69	60.00	60.00
Median	16.40	16.33	43.80	45.40
Skewness	0.072	0.154	-0.555	-0.664
Kurtosis	0.074	0.061	-0.358	-0.020
Coefficient of variability	0.133	0.124	0.243	0.212
Mean Standard Error	0.890	0.069	2.264	0.183
Correlation	Original Data		Simulated data	
Porosity VS. Water Sat.	-0.3415		-0.0339	

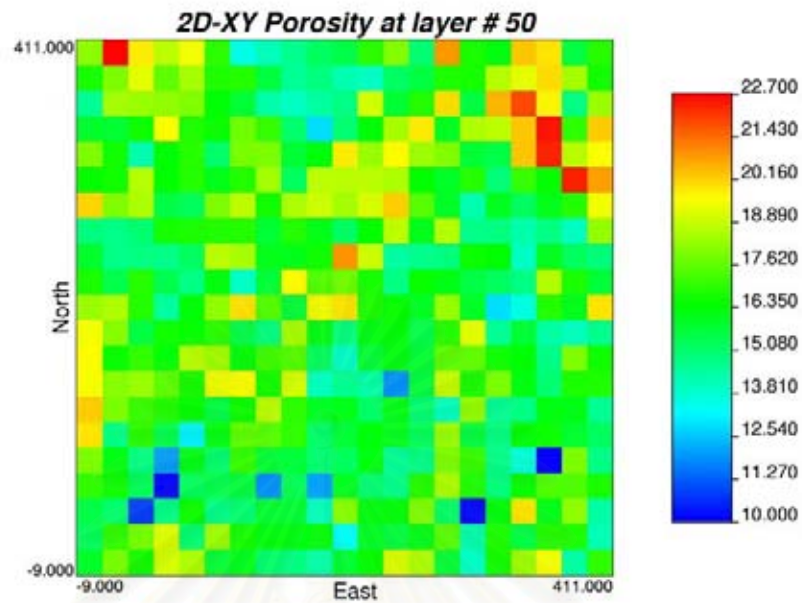


Figure 4.10: Example of porosity realization generated by SGS-local and global distribution at layer # 50.

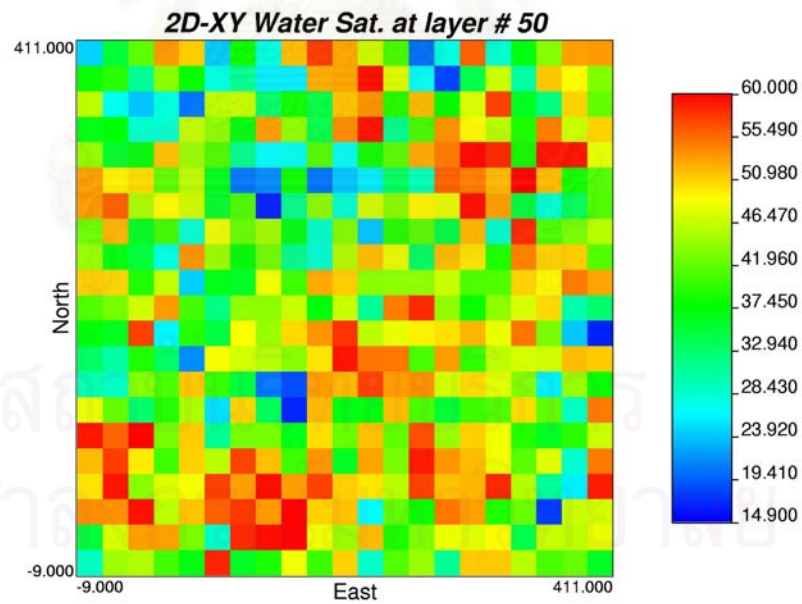


Figure 4.11: Example of water saturation realization generated by SGS-local and global distribution at layer # 50.

For each set of realizations of variables, OGIP thus was calculated based on simulated values at local grid blocks (substituting simulated variables in Eq. 3.3). OGIP values for 100 realizations of variables generated with SGS-local and global distribution are given in Appendix C.1. Histogram of simulated data is illustrated in Figure 4.12. Table 4.9 shows summary statistics of OGIP distribution obtained from SGS-local and global distribution. The distribution of OGIP value calculated from 100 realizations ranges from 14.26 to 15.56 Bcf with a mean and variance of 14.840 and 0.079, respectively. A small positive skewness of the OGIP distribution indicates that the distribution is slightly skewed to the left. The dispersion of distribution which is measured by coefficient of variation is less than one (0.019). It indicates a small degree of variation of OGIP values. OGIP at various percentiles is illustrated in Table 4.10.

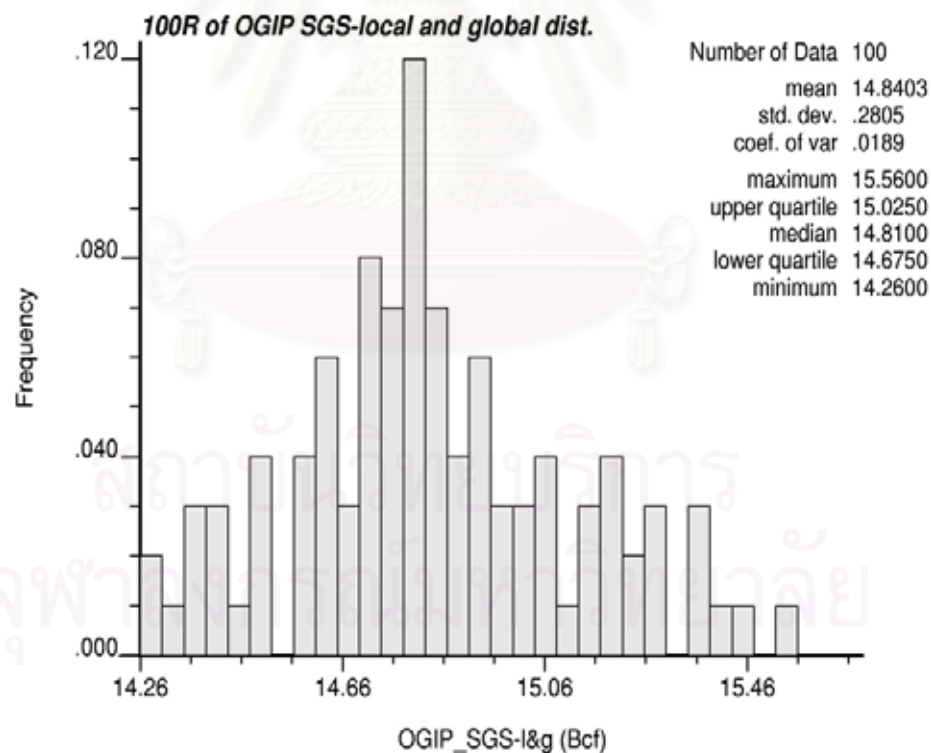


Figure 4.12: Histogram of OGIP obtained from SGS-local and global distribution variables.

Table 4.9: The OGIP statistics from SGS-local and global distribution

<b>Statistics</b>	<b>OGIP obtained from SGS-local and global distribution (Bcf)</b>
<b>No. of realizations</b>	<b>100</b>
<b>Mean</b>	<b>14.840</b>
<b>Standard Deviation</b>	<b>0.281</b>
<b>Variance</b>	<b>0.079</b>
<b>Minimum</b>	<b>14.260</b>
<b>Maximum</b>	<b>15.560</b>
<b>Skewness</b>	<b>0.279</b>
<b>Kurtosis</b>	<b>-0.229</b>
<b>Coefficient of variability</b>	<b>0.019</b>
<b>Mean Standard Error</b>	<b>0.028</b>

Table 4.10: OGIP at various percentiles from SGS-local and global distribution.

<b>Percentile</b>	<b>OGIP obtained from SGS-local and global distribution (Bcf)</b>
<b>0%</b>	<b>14.263</b>
<b>10%</b>	<b>14.478</b>
<b>20%</b>	<b>14.619</b>
<b>25%</b>	<b>14.683</b>
<b>30%</b>	<b>14.707</b>
<b>40%</b>	<b>14.767</b>
<b>50%</b>	<b>14.811</b>
<b>60%</b>	<b>14.857</b>
<b>70%</b>	<b>14.934</b>
<b>75%</b>	<b>15.017</b>
<b>80%</b>	<b>15.076</b>
<b>90%</b>	<b>15.219</b>
<b>100%</b>	<b>15.562</b>



### **4.3 Sequential Gaussian Cosimulation (SGCOSIM)**

The third method to determine spatial distributions of porosity and water saturation is to use SGCOSIM. SGCOSIM is conducted in the same manner as SGS which is to perform structural analysis and conditional simulation. Moreover, SGCOSIM allows incorporation of secondary variables in addition to primary variable. This method relies on secondary variable that should be sampled more densely than the primary variable. Furthermore, primary and secondary variables have to be interdependent. The dependency between variables can be expressed as the correlation coefficient. In this study, GSLIB program was used to construct variogram model of primary variables, i.e., porosity and water saturation and secondary variable, i.e., permeability and resistivity. The program was also used to run simulation for primary variables. Then, 100 realizations of primary variables were simulated. OGIP were then estimated.

#### **4.3.1 Structure analysis (Variogram model)**

Variogram of porosity and water saturation which are constructed using SGS can be applied for SGCOSIM. The additional steps are to establish the variogram for secondary variables, i.e., permeability and resistivity. As required by Gaussian assumption, all variables were transformed to normal score data. The structural analysis was performed on transformed data. Normal score transform for permeability and resistivity using GSLIB program are illustrated in Table 4.11. The first three columns in the table are X, Y, and Z coordinate. The next two columns are permeability and resistivity and the last two columns are normal score transform of permeability and resistivity, respectively. The statistical analysis of secondary variables is given in section 3.2. Histogram of original and normal score permeability and resistivity are illustrated in Figures 4.13 and 4.14.



Table 4.11: Permeability and resistivity normal score transform.

X	Y	Z	K	Rt	NS:K	NS:Rt	X	Y	Z	K	Rt	NS:K	NS:Rt
411.97	31.58	41.42	4.32	12.50	-1.180	-2.325	387.55	18.18	72.52	6.92	27.52	-0.576	-0.225
411.38	31.25	42.17	1.36	12.51	-2.150	-2.229	387.25	18.01	72.90	5.73	27.68	-0.765	-0.195
411.09	31.09	42.55	1.40	12.46	-2.083	-2.449	386.96	17.85	73.27	4.44	28.07	-1.125	-0.050
410.79	30.93	42.92	1.95	12.52	-1.733	-2.150	386.66	17.69	73.64	3.61	28.52	-1.357	0.057
409.32	30.12	44.80	0.57	13.00	-2.449	-1.971	386.37	17.53	74.02	3.75	28.97	-1.322	0.130
408.14	29.48	46.30	0.76	11.54	-2.325	-2.982	386.08	17.37	74.39	5.01	29.48	-0.876	0.195
406.08	28.34	48.92	3.19	13.93	-1.474	-1.801	385.78	17.21	74.76	7.83	29.94	-0.501	0.232
405.79	28.18	49.30	4.60	14.88	-1.072	-1.672	385.49	17.05	75.14	12.57	30.33	0.072	0.329
405.49	28.02	49.67	5.17	15.70	-0.855	-1.565	385.20	16.89	75.51	18.74	30.76	0.414	0.360
405.20	27.86	50.05	4.27	16.32	-1.195	-1.541	384.90	16.73	75.89	25.60	31.12	0.534	0.429
404.90	27.70	50.42	4.77	16.77	-0.975	-1.413	384.61	16.56	76.26	28.61	31.28	0.663	0.461
404.61	27.54	50.80	9.92	17.14	-0.217	-1.085	384.31	16.40	76.64	26.03	31.32	0.559	0.469
404.31	27.37	51.17	16.63	17.45	0.329	-0.941	384.02	16.24	77.01	22.89	31.24	0.461	0.453
404.02	27.21	51.55	14.91	17.62	0.232	-0.897	383.73	16.08	77.38	22.06	30.95	0.453	0.390
403.72	27.05	51.92	9.86	17.62	-0.232	-0.876	383.43	15.92	77.76	20.60	30.65	0.437	0.352
403.43	26.89	52.30	6.85	17.41	-0.585	-0.964	383.14	15.76	78.13	17.91	30.60	0.360	0.344
403.14	26.73	52.67	5.48	16.91	-0.804	-1.375	382.85	15.60	78.50	14.88	30.78	0.225	0.367
402.84	26.57	53.05	4.80	16.46	-0.941	-1.474	382.55	15.44	78.88	13.16	30.97	0.101	0.398
402.55	26.41	53.42	4.61	16.52	-1.047	-1.453	382.26	15.27	79.25	13.47	31.02	0.137	0.406
401.66	25.92	54.55	1.98	17.44	-1.702	-0.952	381.96	15.11	79.63	15.07	31.03	0.239	0.414
401.37	25.76	54.92	1.53	17.65	-2.024	-0.865	381.67	14.95	80.00	17.25	31.16	0.344	0.437
401.07	25.60	55.30	1.66	18.14	-1.839	-0.756	381.38	14.79	80.38	17.71	31.41	0.352	0.477
400.78	25.44	55.67	4.61	19.27	-1.035	-0.672	381.08	14.63	80.75	16.32	31.64	0.306	0.493
400.49	25.27	56.05	10.88	20.64	-0.108	-0.637	380.79	14.47	81.12	15.36	31.79	0.254	0.510
400.19	25.11	56.42	13.76	21.70	0.181	-0.602	380.50	14.31	81.50	13.54	31.76	0.151	0.501
399.90	24.95	56.80	11.74	22.39	-0.014	-0.568	380.20	14.15	81.87	11.55	31.42	-0.029	0.485
399.60	24.79	57.17	6.94	22.75	-0.568	-0.526	379.91	13.99	82.25	10.42	30.87	-0.166	0.383
397.83	23.82	59.42	5.37	23.28	-0.834	-0.429	379.61	13.82	82.62	10.40	30.34	-0.173	0.337
397.54	23.66	59.80	5.82	23.43	-0.727	-0.422	379.32	13.66	82.99	10.14	30.09	-0.202	0.269
396.66	23.17	60.92	6.27	24.25	-0.672	-0.414	379.03	13.50	83.37	10.65	30.28	-0.144	0.314
396.36	23.01	61.30	6.66	24.71	-0.637	-0.406	378.73	13.34	83.74	12.52	31.06	0.050	0.422
396.07	22.85	61.67	5.94	25.01	-0.700	-0.398	378.44	13.18	84.11	11.47	32.59	-0.050	0.534
395.77	22.69	62.05	5.49	25.18	-0.794	-0.390	378.15	13.02	84.49	8.94	34.82	-0.375	0.654
395.48	22.53	62.42	5.09	25.35	-0.865	-0.383	377.85	12.86	84.86	8.00	37.54	-0.469	1.085
395.18	22.37	62.80	4.58	25.56	-1.085	-0.375	377.56	12.70	85.24	9.70	40.49	-0.247	1.210
394.89	22.20	63.17	4.85	25.75	-0.919	-0.367	377.26	12.54	85.61	15.40	44.61	0.262	1.305
394.60	22.04	63.54	6.25	25.94	-0.681	-0.360	376.97	12.37	85.99	28.35	52.25	0.645	1.616
394.30	21.88	63.92	8.01	26.23	-0.461	-0.352	376.68	12.21	86.36	51.22	63.55	1.085	1.643
394.01	21.72	64.29	8.82	26.55	-0.390	-0.337	376.38	12.05	86.73	72.06	75.51	1.518	1.702
393.72	21.56	64.67	8.85	26.70	-0.383	-0.314	376.09	11.89	87.11	76.43	85.83	1.643	1.766
393.42	21.40	65.04	8.65	26.71	-0.414	-0.306	375.80	11.73	87.48	65.23	93.41	1.375	1.801
393.13	21.24	65.41	9.26	26.69	-0.306	-0.321	375.50	11.57	87.85	59.62	98.20	1.225	1.880
392.83	21.08	65.79	10.90	26.78	-0.101	-0.299	375.21	11.41	88.23	68.80	102.16	1.453	1.923
392.54	20.92	66.16	10.79	27.06	-0.130	-0.276	374.91	11.25	88.60	95.82	106.74	1.880	2.024
392.25	20.75	66.54	9.12	27.30	-0.329	-0.269	374.62	11.08	88.98	148.22	110.15	2.150	2.150
391.95	20.59	66.91	7.54	27.33	-0.518	-0.247	374.33	10.92	89.35	207.47	111.31	2.449	2.229
391.66	20.43	67.28	5.77	27.38	-0.756	-0.232	374.03	10.76	89.73	233.44	112.18	2.982	2.449
391.37	20.27	67.66	4.80	27.66	-0.964	-0.202	373.74	10.60	90.10	216.20	113.07	2.628	2.982
391.07	20.11	68.03	5.38	28.20	-0.824	0.022	373.45	10.44	90.47	193.11	113.02	2.325	2.628
390.78	19.95	68.41	6.58	28.76	-0.645	0.101	373.15	10.28	90.85	157.22	111.93	2.229	2.325
390.48	19.79	68.78	6.71	29.04	-0.619	0.144	372.86	10.12	91.22	104.46	109.23	2.024	2.083
390.19	19.63	69.15	5.57	29.10	-0.785	0.173	372.56	9.96	91.60	56.05	104.63	1.152	1.971
389.90	19.47	69.53	4.13	29.05	-1.225	0.159	372.27	9.80	91.97	19.10	96.84	0.422	1.839
389.60	19.30	69.90	2.87	28.92	-1.518	0.122	371.98	9.63	92.34	3.61	82.90	-1.339	1.733
389.31	19.14	70.28	1.90	28.79	-1.766	0.115	371.68	9.47	92.72	0.48	63.64	-2.982	1.672
389.02	18.98	70.65	1.57	28.61	-1.923	0.072	367.86	7.38	97.58	2.54	19.72	-1.565	-0.654
388.72	18.82	71.02	2.24	28.33	-1.616	0.043	367.57	7.22	97.95	9.64	20.81	-0.262	-0.628
388.43	18.66	71.40	4.41	28.05	-1.152	-0.057	367.28	7.06	98.33	24.06	21.59	0.493	-0.610
388.13	18.50	71.77	6.96	27.80	-0.559	-0.173	366.98	6.89	98.70	35.66	22.19	0.824	-0.576
387.84	18.34	72.15	7.57	27.59	-0.510	-0.217	366.69	6.73	99.08	36.62	22.65	0.855	-0.551

Table 4.11: Permeability and resistivity normal score transform (continued).

X	Y	Z	K	Rt	NS:K	NS:Rt	X	Y	Z	K	Rt	NS:K	NS:Rt
366.40	6.57	99.45	35.15	23.01	0.794	-0.493	37.68	201.75	11.35	23.52	36.76	0.485	0.952
366.10	6.41	99.82	31.47	23.17	0.709	-0.461	37.38	201.63	11.72	26.87	36.81	0.593	0.975
365.81	6.25	100.20	23.03	23.17	0.477	-0.453	37.09	201.50	12.09	33.56	36.87	0.765	0.998
365.51	6.09	100.57	15.43	23.16	0.276	-0.469	36.79	201.38	12.45	37.68	36.81	0.886	0.987
365.22	5.93	100.95	10.77	23.09	-0.137	-0.477	36.49	201.26	12.82	38.29	36.68	0.897	0.930
364.93	5.77	101.32	9.15	22.88	-0.321	-0.510	36.18	201.13	13.19	34.90	36.58	0.785	0.897
364.63	5.61	101.69	9.41	22.69	-0.276	-0.534	35.88	201.01	13.56	30.16	36.41	0.690	0.855
364.34	5.44	102.07	9.95	22.65	-0.210	-0.543	35.58	200.88	13.92	28.53	36.05	0.654	0.814
364.05	5.28	102.44	10.84	22.81	-0.122	-0.518	35.28	200.76	14.29	28.29	35.62	0.637	0.765
363.75	5.12	102.82	11.50	23.08	-0.043	-0.485	34.98	200.64	14.66	26.49	35.34	0.585	0.737
363.46	4.96	103.19	9.85	23.25	-0.239	-0.437	34.68	200.51	15.02	24.24	35.22	0.501	0.727
363.16	4.80	103.56	8.38	23.22	-0.429	-0.445	34.38	200.39	15.39	24.29	35.17	0.510	0.718
362.87	4.64	103.94	8.98	22.91	-0.367	-0.501	34.08	200.26	15.76	25.99	35.11	0.551	0.700
362.58	4.48	104.31	9.48	22.44	-0.269	-0.559	33.78	200.14	16.13	27.93	35.05	0.628	0.690
362.28	4.32	104.69	7.86	22.07	-0.493	-0.585	33.48	200.01	16.49	28.66	34.93	0.672	0.672
361.99	4.15	105.06	5.78	21.81	-0.746	-0.593	33.18	199.89	16.86	22.96	34.79	0.469	0.637
361.69	3.99	105.43	4.80	21.33	-0.952	-0.619	32.88	199.77	17.23	18.36	34.68	0.383	0.619
361.40	3.83	105.81	4.92	20.37	-0.886	-0.645	32.58	199.64	17.59	15.07	34.45	0.247	0.602
361.11	3.67	106.18	4.92	19.15	-0.897	-0.690	32.28	199.52	17.96	12.87	33.91	0.094	0.585
358.76	2.38	109.17	0.54	14.26	-2.628	-1.766	31.98	199.39	18.33	12.17	32.96	0.022	0.559
358.46	2.22	109.55	2.35	14.61	-1.590	-1.702	31.68	199.27	18.69	12.72	31.85	0.079	0.518
358.17	2.06	109.92	7.33	15.49	-0.534	-1.616	31.38	199.14	19.06	13.29	30.82	0.122	0.375
357.88	1.90	110.30	12.54	16.40	0.065	-1.496	31.08	199.02	19.43	13.19	29.74	0.108	0.210
357.58	1.74	110.67	14.10	17.16	0.195	-1.059	30.78	198.90	19.80	12.42	28.67	0.043	0.086
357.29	1.58	111.05	12.40	17.68	0.036	-0.855	30.48	198.77	20.16	11.83	28.05	0.007	-0.065
355.53	0.61	113.29	4.75	17.07	-0.987	-1.138	30.18	198.65	20.53	11.72	27.94	-0.022	-0.115
355.23	0.45	113.66	6.74	17.26	-0.602	-1.035	29.88	198.52	20.90	11.19	27.92	-0.072	-0.130
354.94	0.29	114.04	9.10	17.33	-0.337	-1.010	29.58	198.40	21.27	9.92	27.89	-0.225	-0.166
354.64	0.13	114.41	14.08	16.93	0.188	-1.305	29.28	198.28	21.63	8.30	27.89	-0.445	-0.159
46.97	205.59	0.00	38.55	37.60	0.908	1.098	28.97	198.15	22.00	6.72	27.90	-0.610	-0.151
46.67	205.47	0.37	64.33	37.98	1.339	1.138	28.67	198.03	22.37	5.82	27.96	-0.718	-0.101
46.37	205.35	0.74	72.39	36.63	1.565	0.908	28.37	197.90	22.73	6.02	27.95	-0.690	-0.108
46.07	205.22	1.10	72.30	34.56	1.541	0.610	28.07	197.78	23.10	6.85	27.92	-0.593	-0.137
45.77	205.10	1.47	69.82	33.48	1.496	0.576	27.77	197.65	23.47	7.30	28.00	-0.543	-0.086
45.47	204.97	1.83	67.82	33.48	1.413	0.568	27.47	197.53	23.84	6.51	28.08	-0.654	-0.043
45.18	204.85	2.20	80.37	32.74	1.702	0.551	27.17	197.41	24.20	4.70	28.11	-1.010	-0.014
44.88	204.73	2.57	97.53	32.64	1.923	0.543	26.87	197.28	24.57	3.61	28.11	-1.375	-0.029
44.58	204.60	2.93	94.81	35.13	1.801	0.709	26.57	197.16	24.94	4.03	28.12	-1.240	-0.007
44.28	204.48	3.30	84.65	36.51	1.766	0.876	26.27	197.03	25.31	5.80	28.17	-0.737	0.007
43.98	204.35	3.67	68.87	37.21	1.474	1.035	25.97	196.91	25.67	8.03	28.20	-0.453	0.014
43.68	204.23	4.03	58.47	37.35	1.195	1.059	25.67	196.78	26.04	9.28	28.16	-0.299	0.000
43.38	204.11	4.40	56.89	37.23	1.166	1.047	25.37	196.66	26.41	8.81	28.11	-0.398	-0.022
43.08	203.98	4.76	62.86	37.09	1.305	1.022	25.07	196.54	26.77	6.68	28.08	-0.628	-0.036
42.78	203.86	5.13	74.80	36.98	1.590	1.010	24.77	196.41	27.14	4.51	28.04	-1.111	-0.072
42.48	203.73	5.50	79.67	36.71	1.672	0.941	24.46	196.29	27.51	3.90	27.98	-1.272	-0.094
42.18	203.61	5.86	76.39	36.41	1.616	0.845	24.16	196.16	27.88	4.36	27.90	-1.166	-0.144
41.88	203.49	6.23	68.78	36.23	1.433	0.834	23.86	196.04	28.25	4.61	27.65	-1.059	-0.210
41.58	203.36	6.59	55.65	36.07	1.138	0.824	23.56	195.91	28.62	4.27	27.32	-1.210	-0.254
41.28	203.24	6.96	47.98	35.90	1.047	0.804	23.26	195.79	28.98	3.24	27.31	-1.433	-0.262
40.98	203.12	7.33	45.79	35.72	0.987	0.794	22.96	195.66	29.35	2.15	27.79	-1.643	-0.181
40.68	202.99	7.69	50.34	35.62	1.072	0.775	22.66	195.54	29.72	2.02	28.49	-1.672	0.050
40.38	202.87	8.06	62.77	35.41	1.272	0.746	22.36	195.41	30.09	3.09	29.08	-1.496	0.166
40.08	202.74	8.43	81.58	35.03	1.733	0.681	20.55	194.67	32.30	4.65	30.12	-1.022	0.276
39.78	202.62	8.79	101.91	34.80	1.971	0.645	20.25	194.54	32.67	4.01	30.15	-1.256	0.291
39.48	202.50	9.16	110.35	34.73	2.083	0.628	19.95	194.42	33.03	5.58	30.18	-0.775	0.299
39.18	202.37	9.52	95.07	34.87	1.839	0.663	19.65	194.29	33.40	9.39	30.18	-0.291	0.306
38.88	202.25	9.89	67.79	35.67	1.394	0.785	19.34	194.17	33.77	15.42	30.14	0.269	0.284
38.58	202.12	10.26	47.77	36.43	1.035	0.865	19.04	194.04	34.14	26.03	30.06	0.568	0.262
38.28	202.00	10.62	36.00	36.57	0.845	0.886	18.74	193.92	34.51	33.16	30.00	0.737	0.254
37.98	201.88	10.99	27.01	36.65	0.610	0.919	18.44	193.80	34.88	31.97	29.98	0.718	0.247

Table 4.11: Permeability and Resistivity normal score transform (continued).

X	Y	Z	K	Rt	NS:K	NS:Rt	X	Y	Z	K	Rt	NS:K	NS:Rt
18.14	193.67	35.24	30.40	29.97	0.700	0.239	182.81	407.93	87.76	9.01	17.01	-0.360	-1.180
17.84	193.55	35.61	25.37	29.86	0.526	0.225	182.49	408.00	88.16	11.44	17.01	-0.057	-1.210
17.54	193.42	35.98	17.97	29.61	0.367	0.202	182.17	408.07	88.56	11.96	16.93	0.014	-1.339
17.24	193.30	36.35	11.55	29.32	-0.036	0.181	181.85	408.14	88.96	11.30	16.89	-0.065	-1.394
16.93	193.17	36.72	9.40	29.03	-0.284	0.137	181.53	408.21	89.36	10.19	16.93	-0.195	-1.322
16.63	193.05	37.08	8.40	28.71	-0.422	0.094	181.21	408.28	89.76	9.65	16.97	-0.254	-1.240
16.33	192.92	37.45	10.44	28.33	-0.151	0.036	178.97	408.78	92.56	7.93	16.96	-0.485	-1.256
16.03	192.80	37.82	16.25	27.93	0.299	-0.122	178.65	408.85	92.96	5.20	16.95	-0.845	-1.288
14.83	192.30	39.29	10.85	26.85	-0.115	-0.291	178.33	408.92	93.36	3.56	16.96	-1.413	-1.272
13.62	191.80	40.77	4.44	26.41	-1.138	-0.344	178.01	408.99	93.76	3.21	16.93	-1.453	-1.357
13.32	191.68	41.14	7.40	26.58	-0.526	-0.329	177.37	409.14	94.56	5.86	16.99	-0.709	-1.225
13.01	191.55	41.51	11.80	26.93	0.000	-0.284	177.05	409.21	94.97	8.78	17.02	-0.406	-1.166
12.71	191.43	41.88	14.31	27.37	0.210	-0.239	176.73	409.28	95.37	13.71	17.01	0.166	-1.195
12.41	191.30	42.25	13.72	27.76	0.173	-0.188	176.41	409.35	95.77	18.15	17.06	0.375	-1.152
12.11	191.18	42.61	16.06	28.03	0.291	-0.079	176.09	409.42	96.17	16.61	17.12	0.321	-1.111
11.81	191.05	42.98	20.17	28.31	0.429	0.029	175.77	409.49	96.57	13.54	17.12	0.144	-1.125
11.50	190.93	43.35	18.41	28.55	0.398	0.065	175.45	409.56	96.97	12.30	17.13	0.029	-1.098
11.20	190.80	43.72	13.28	28.65	0.115	0.079	175.13	409.63	97.37	11.12	17.15	-0.079	-1.072
10.90	190.68	44.09	8.35	28.78	-0.437	0.108	174.80	409.71	97.77	10.22	17.19	-0.181	-1.047
10.60	190.55	44.46	4.85	29.05	-0.908	0.151	174.48	409.78	98.18	10.43	17.26	-0.159	-1.022
10.30	190.43	44.83	3.78	29.37	-1.305	0.188	174.16	409.85	98.58	11.05	17.34	-0.086	-0.998
9.99	190.30	45.20	4.71	29.74	-0.998	0.217	173.84	409.92	98.98	12.53	17.38	0.057	-0.987
9.69	190.18	45.57	10.95	30.31	-0.094	0.321	173.52	409.99	99.38	14.31	17.40	0.202	-0.975
9.39	190.05	45.94	18.39	31.22	0.390	0.445	172.56	410.21	100.58	13.38	17.62	0.130	-0.886
9.09	189.93	46.31	29.27	32.44	0.681	0.526	172.24	410.28	100.99	11.75	17.73	-0.007	-0.845
8.78	189.80	46.68	37.53	33.94	0.876	0.593	171.92	410.35	101.39	9.04	17.81	-0.352	-0.834
8.48	189.68	47.05	40.40	35.55	0.930	0.756	171.60	410.42	101.79	9.17	17.88	-0.314	-0.814
8.18	189.55	47.41	40.64	36.77	0.941	0.964	171.28	410.49	102.19	13.57	17.89	0.159	-0.804
7.88	189.43	47.78	37.44	37.38	0.865	1.072	170.96	410.56	102.59	20.97	17.88	0.445	-0.824
7.58	189.30	48.15	33.50	37.70	0.756	1.111	170.64	410.63	102.99	27.01	17.91	0.602	-0.794
7.28	189.18	48.52	33.45	37.93	0.746	1.125	170.31	410.71	103.40	25.71	17.98	0.543	-0.775
6.97	189.05	48.89	35.86	38.18	0.834	1.152	169.99	410.78	103.80	17.22	18.07	0.337	-0.765
6.67	188.93	49.26	35.36	38.45	0.804	1.166	169.67	410.85	104.20	12.77	18.15	0.086	-0.746
6.37	188.80	49.63	35.47	39.10	0.814	1.180	169.35	410.92	104.60	14.59	18.21	0.217	-0.737
6.07	188.68	50.00	39.85	40.31	0.919	1.195	169.03	410.99	105.00	16.49	18.24	0.314	-0.727
5.76	188.55	50.37	46.20	41.33	0.998	1.225	168.71	411.06	105.41	15.60	18.34	0.284	-0.718
5.46	188.43	50.74	54.01	41.91	1.125	1.240	168.39	411.13	105.81	18.71	18.65	0.406	-0.709
5.16	188.30	51.10	61.21	42.46	1.256	1.256	168.07	411.21	106.21	27.03	19.15	0.619	-0.700
4.86	188.18	51.48	59.98	43.09	1.240	1.272	167.74	411.28	106.61	33.05	19.54	0.727	-0.663
4.56	188.05	51.84	53.18	43.81	1.111	1.288	167.42	411.35	107.02	34.79	19.24	0.775	-0.681
4.25	187.93	52.21	48.73	44.66	1.059	1.322	167.10	411.42	107.42	26.35	17.60	0.576	-0.908
3.95	187.80	52.58	47.18	45.45	1.022	1.339	151.98	414.78	126.35	1.33	15.67	-2.229	-1.590
3.65	187.68	52.95	44.60	46.04	0.964	1.357	151.66	414.86	126.76	1.64	16.77	-1.880	-1.433
3.35	187.55	53.32	42.62	46.34	0.952	1.394	151.33	414.93	127.16	1.82	17.58	-1.801	-0.919
3.04	187.43	53.69	45.32	46.47	0.975	1.413	151.01	415.00	127.56	2.55	17.92	-1.541	-0.785
2.74	187.30	54.06	51.64	46.74	1.098	1.433	150.69	415.07	127.97	4.53	17.51	-1.098	-0.930
2.44	187.18	54.43	57.67	47.07	1.180	1.474	150.37	415.14	128.37	6.48	16.37	-0.663	-1.518
2.14	187.05	54.80	62.78	47.29	1.288	1.541	150.05	415.21	128.77	4.81	15.00	-0.930	-1.643
1.83	186.93	55.17	65.16	47.24	1.357	1.518	149.72	415.29	129.18	1.56	13.55	-1.971	-1.880
1.53	186.80	55.54	63.94	47.07	1.322	1.453							
1.23	186.68	55.91	59.16	47.12	1.210	1.496							
0.92	186.55	56.28	46.50	47.38	1.010	1.590							
0.62	186.43	56.65	24.55	47.36	0.518	1.565							
0.32	186.30	57.02	7.06	46.30	-0.551	1.375							
187.28	406.93	82.16	7.97	14.29	-0.477	-1.733							
186.96	407.00	82.56	10.22	13.82	-0.188	-1.839							
186.64	407.07	82.96	9.08	13.12	-0.344	-1.923							
186.32	407.14	83.36	5.43	12.60	-0.814	-2.083							
186.00	407.21	83.76	3.82	12.43	-1.288	-2.628							
185.68	407.29	84.16	3.60	12.60	-1.394	-2.024							

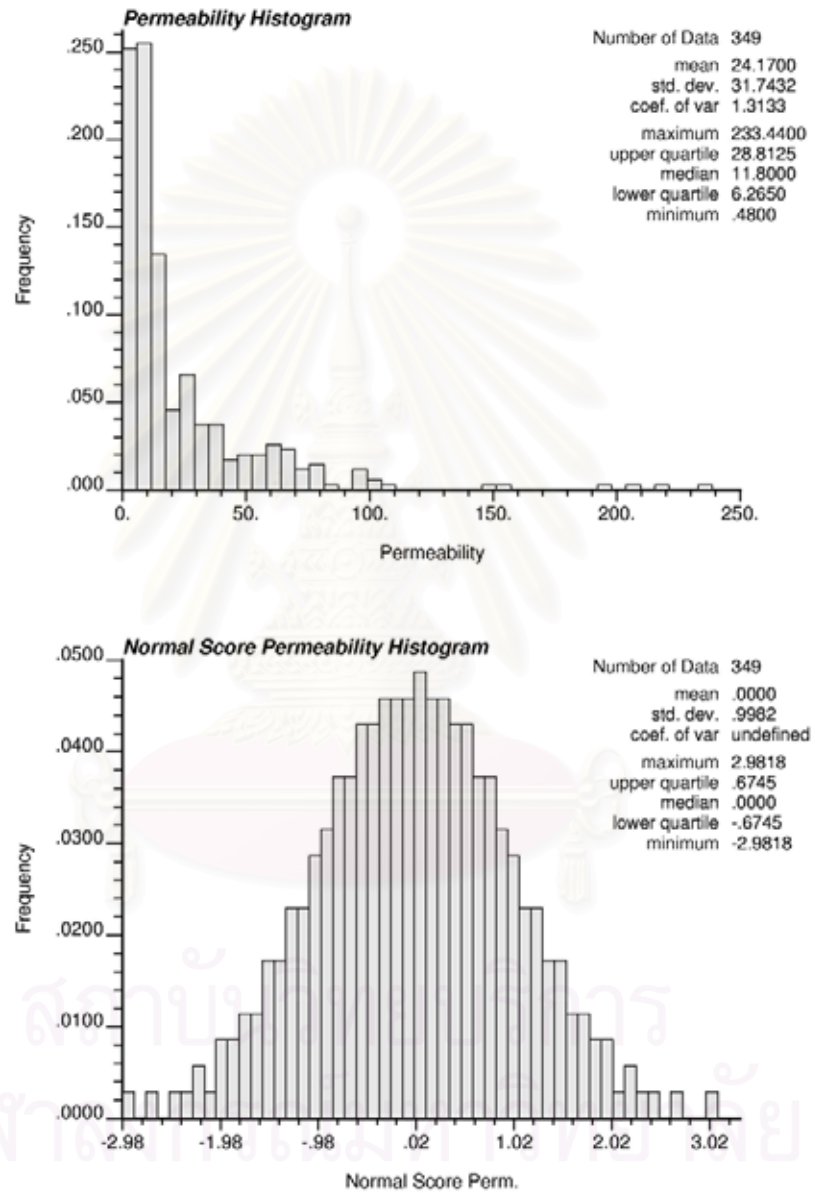


Figure 4.13: Histogram of original and normal score transform of permeability.

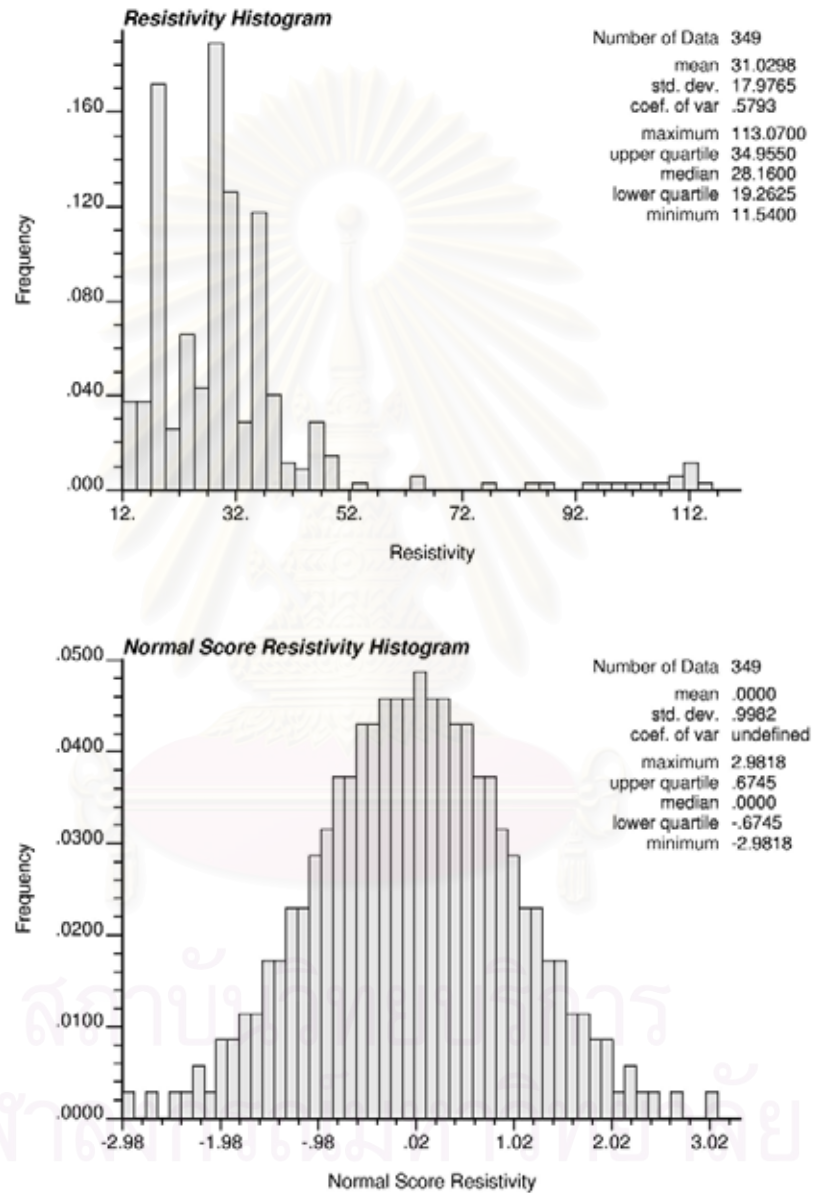


Figure 4.14: Histogram of original and normal score transform of resistivity.



To determine the spatial structure for permeability and resistivity, variogram calculations were performed. An omni-directional variogram calculation was carried out with an expectation that searching in all directions will increase possibility of finding pairs of data. It is noted that when omni-direction is applied, the spatial variability is assumed to be the same for all directions; hence, the variogram is an isotropic model. It is important to note that the contribution of secondary variables to the simulation of primary variables depends largely on two factors which are the degree of correlation among variables and their spatial structures. Large correlation values between primary and secondary variables (Table 3.4) justify the incorporation of secondary the variables in simulation of primary variables through the use of SGCOSIM method. Figures 4.15 and 4.16 illustrate the variograms in omni-direction for the original data and normal score transform of permeability and resistivity, respectively.

Permeability and resistivity are best fitted by spherical model with 10-30% nugget and a range of 110-130 ft for normal score. The parameters for the omni-directional variograms of the original and normal score transform of permeability and resistivity are given in Table 4.12.

Table 4.12: Parameters for omni-directional variograms of permeability and resistivity.

Variable	Directional Variogram	Model	Original Data			Normal Score Data		
			Sill	Nugget	Range (ft)	Sill	Nugget	Range (ft)
Permeability	Omni	Spherical	1010.0	300.0	140	1.0	0.3	130
Resistivity	Omni	Spherical	320.0	100.0	110	1.0	0.1	110

As mentioned before, there is a need to check for multivariate normal distribution on both primary and secondary variables. The check for bivariate normality of permeability and resistivity was performed in the next step.



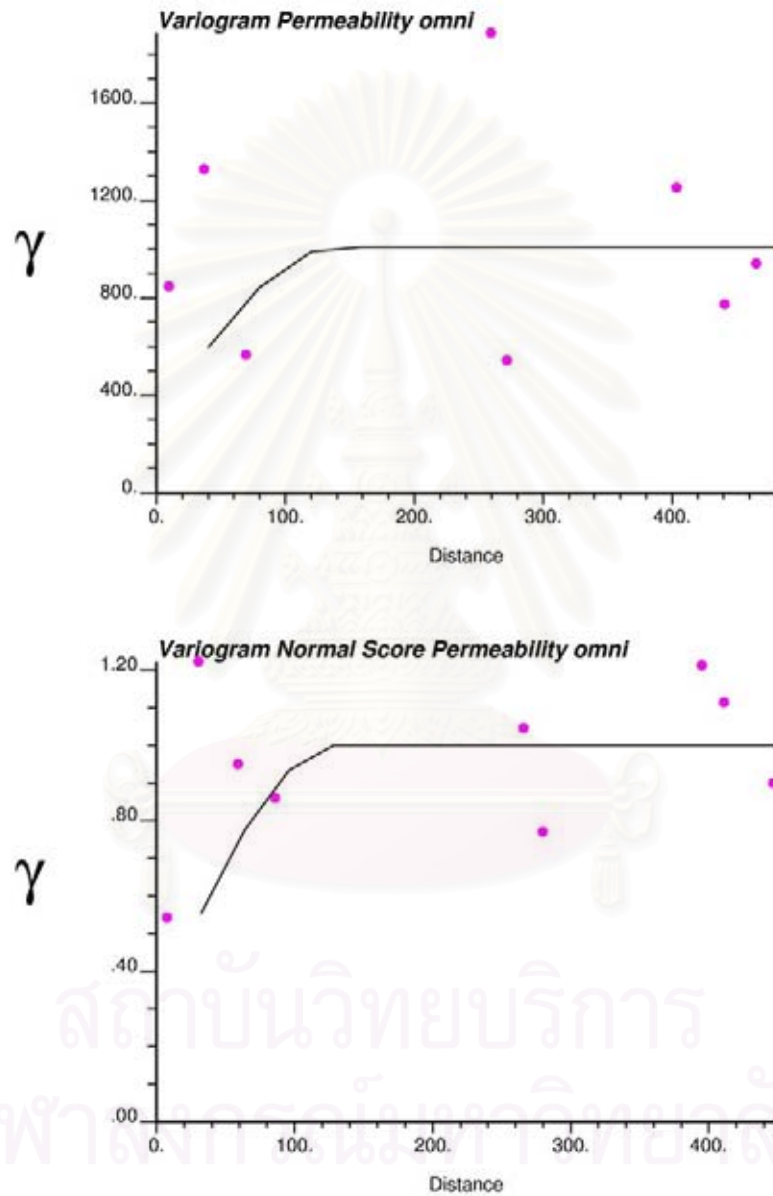


Figure 4.15: Omni-directional variogram of the original data and normal score transform of permeability.

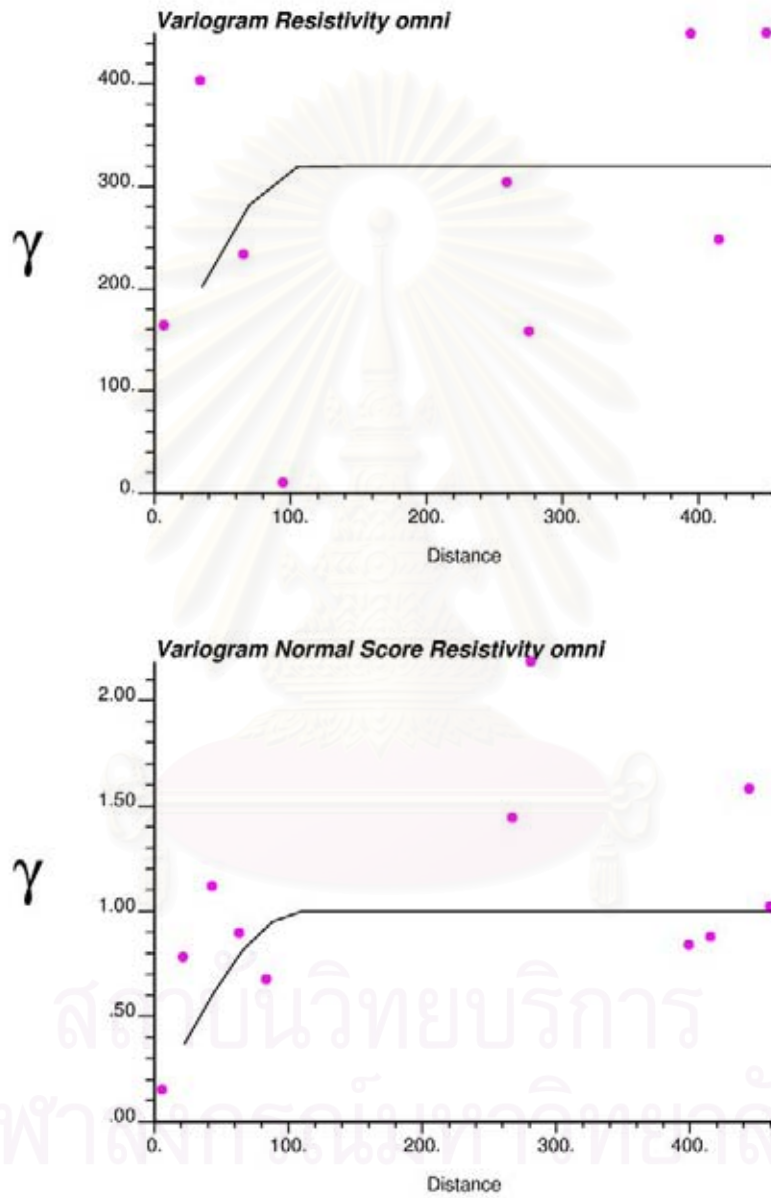


Figure 4.16: Omni-directional variogram of the original data and normal score transform of resistivity.

### Checking for Bivariate Normality

Similar to the checking of bivariate normality of primary variables, the experimental indicator variograms of permeability and resistivity at median cutoff (0.5 cdf value) were calculated and compared to the theoretical indicator variograms. Figures 4.17 and 4.18 show the experimental and theoretical indicator variograms corresponding to the median cutoff for permeability and resistivity, respectively. As seen in the figures, the experimental and theoretical indicator variograms show generally good correspondence, implying that the secondary variables follow multiGaussian assumption.

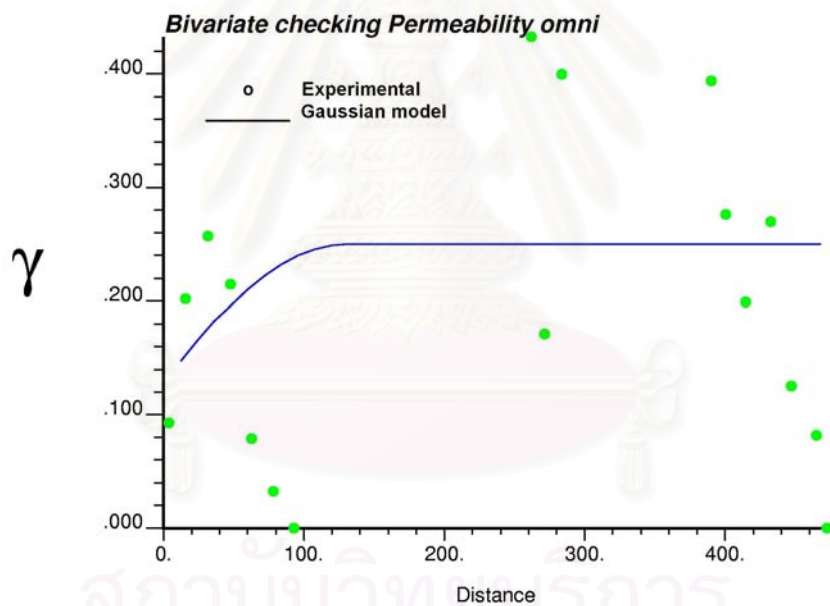


Figure 4.17: Experimental and Gaussian model-derived indicator variograms for permeability at median cutoff (0.5 cdf value).

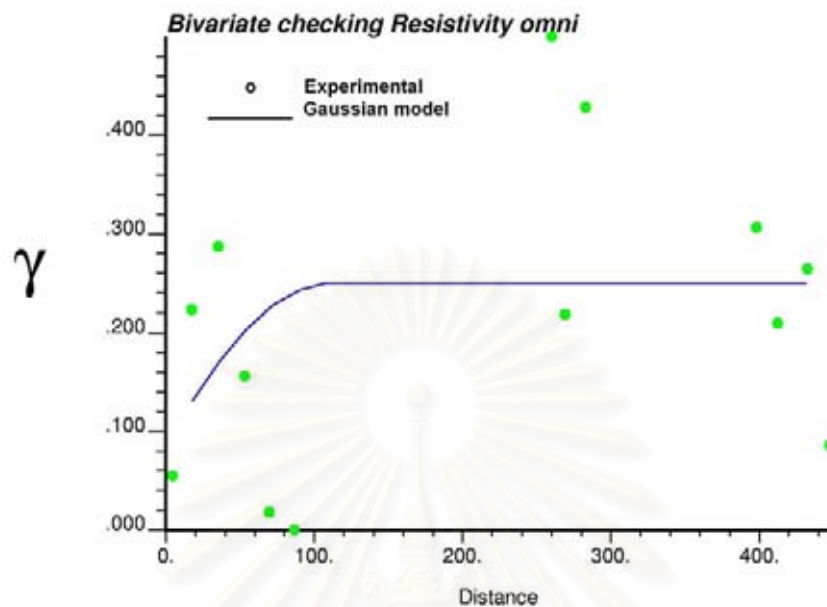


Figure 4.18: Experimental and Gaussian model-derived indicator variograms for resistivity at median cutoff (0.5 cdf value).

### 4.3.2 Sequential Gaussian Cosimulation

In order to perform SGCOSIM, the hierarchy of primary variables was defined. In this study, porosity was considered as the first primary variable to be simulated, and the other primary variable to be jointly simulated was water saturation. The permeability and resistivity were then considered to be secondary variables. In cosimulation, the secondary data must be available at all points to be simulated. Since the permeability and resistivity are available at the same locations as primary data, it is necessary to complete that information with a prior simulation. SGS and Collocated SGS were applied to simulate secondary variables for all blocks in the area of study.

The grid discretization is the same as in case of SGS, i.e., 21 x 21 x 130 grids/node corresponding to a block size of 20 ft x 20 ft x 1ft. The simulation for all variables was performed in three dimensions (3-D). GSLIB program was used to simulate the distribution of resistivity via SGS and permeability via Collocated SGS. The SGS and Collocated SGS parameter files are provided in Appendix A.3 and A.4,

respectively. Once the permeability and resistivity were available at all grid blocks, the SGCOSIM algorithm was applied. The variogram models used for all variables were prepared as discussed earlier. The cross-covariance between primary and secondary variables was inferred from the product of correlation coefficient between primary and secondary variables and the spatial structure of primary variable as defined in Markov assumption. Only linear correlation coefficients are required as described in Chapter II. Therefore, correlation coefficient matrix file (Appendix A.6) between primary and secondary variables, must be provided when performing SGCOSIM.

One hundred realizations of porosity and water saturation were simulated and are given in Appendix B.2. The SGCOSIM parameter file is given in Appendix A.5. An example of porosity and water saturation realizations obtained from SGCOSIM-local distribution are shown in Figures 4.19 and 4.20. To check whether SGCOSIM preserves the original statistics, particular simulated porosity and water saturation realizations were selected to compare with the original data. Table 4.13 compares the statistics of the 50<sup>th</sup> realization of simulated porosity and water saturation with those of the original data. It is observed that distributions of the 50<sup>th</sup> simulated porosity and water saturation realization are close to original statistics. It can be said that the original statistics still preserve in cosimulation process.

Table 4.13: Statistics of the 50<sup>th</sup> realization of porosity and water saturation generated by SGCOSIM-local and global distribution.

Statistics	Porosity		Water Saturation	
	Original Data	SGCOSIM	Original Data	SGCOSIM
Mean	16.63	16.64	42.29	42.39
Standard Deviation	2.21	2.18	10.26	10.78
Variance	4.88	4.74	105.18	116.11
Minimum	10.00	10.00	14.90	14.90
Maximum	22.62	22.70	60.00	60.00
Median	16.40	16.41	43.80	44.10
Skewness	0.072	0.099	-0.555	-0.574
Kurtosis	0.074	0.024	-0.358	-0.402
Coefficient of variability	0.133	0.131	0.243	0.254
Mean Standard Error	0.890	0.070	2.264	0.177
Correlation	Original Data		Simulated data	
Porosity VS. Water Sat.	-0.3415		-0.6443	

However, the correlation coefficient between simulated porosity and water saturation increases in comparison to the original statistics. This can be explained that SGCOSIM model takes into account correlation among variables. Hence, there is a possibility that the contribution of secondary variables will change the correlation of the original data especially when the correlation of primary and secondary variables is high. In this case, there is a strong correlation between porosity-permeability and porosity-formation resistivity with the correlation value of 0.811 and 0.604, respectively. A moderate to strong correlation is observed in the correlation between water saturation-permeability and water saturation-formation resistivity with the correlation value of -0.424 and -0.625, respectively.

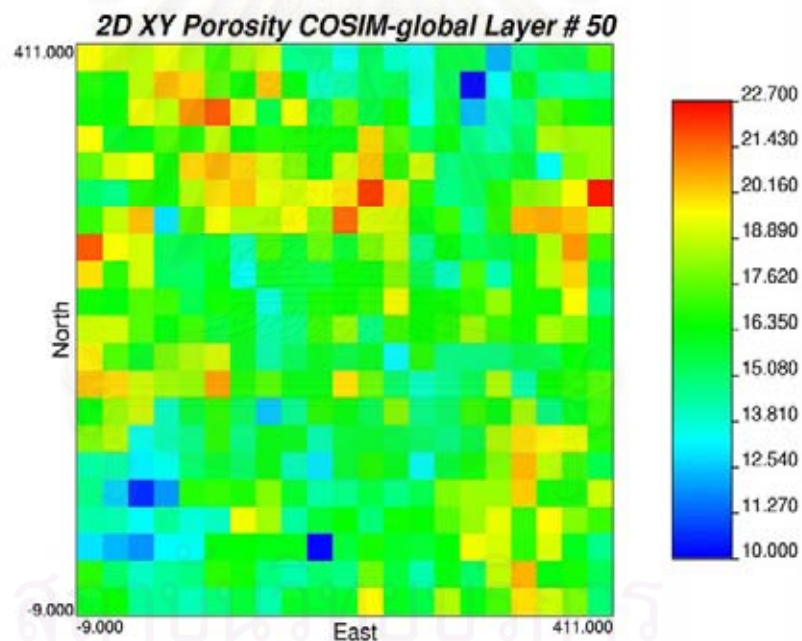


Figure 4.19: Example of porosity realization generated by SGCOSIM-local and global distribution at layer # 50.



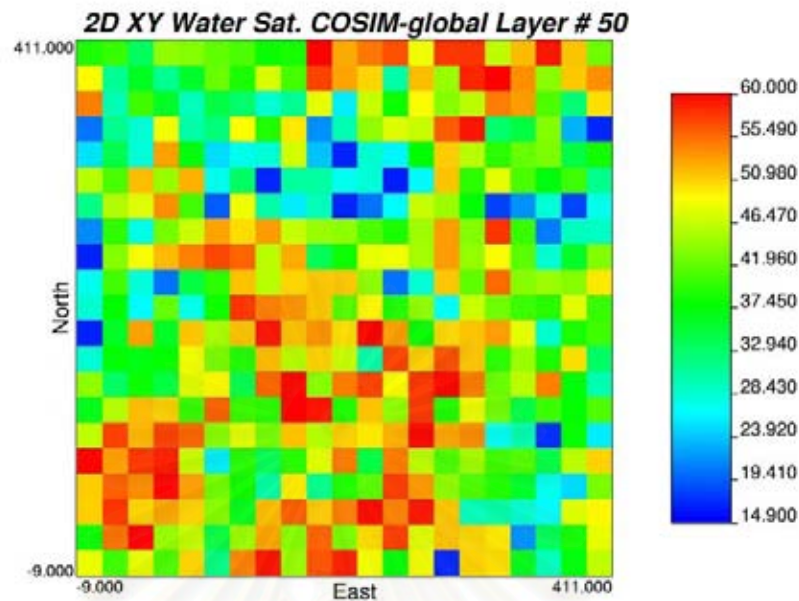


Figure 4.20: Example of water saturation realization generated by SGCOSIM-local and global distribution at layer # 50.

The OGIP were calculated based on simulated variables of each grid block (substituting simulated data into Eq.3.3). The calculated OGIPs resulted from SGCOSIM-local and global distribution of 100 realizations are given in Appendix C.2. Table 4.14 shows summary statistics of OGIP distribution obtained from SGCOSIM-local and global distribution. Histogram of simulated data is illustrated in Figure 4.21. The OGIP ranges from 15.050 to 15.338 Bcf with a mean and variance of 15.186 and 0.003, respectively. Variance of OGIP is shown in good corresponding to coefficient of variation of 0.004. The OGIP distribution is slightly skewed to the left with a skewness of 0.175. The OGIPs at various percentiles obtained from SGCOSIM-local and global distribution are illustrated in Table 4.15.

Table 4.14: The OGIP statistics from SGCOSIM-local and global distribution.

<b>Statistics</b>	<b>OGIP obtained from SGCOSIM-local and global distribution (Bcf)</b>
<b>No. of realizations</b>	<b>100</b>
<b>Mean</b>	<b>15.186</b>
<b>Standard Deviation</b>	<b>0.058</b>
<b>Variance</b>	<b>0.0034</b>
<b>Minimum</b>	<b>15.050</b>
<b>Maximum</b>	<b>15.340</b>
<b>Skewness</b>	<b>0.175</b>
<b>Kurtosis</b>	<b>-0.132</b>
<b>Coefficient of variability</b>	<b>0.004</b>
<b>Mean Standard Error</b>	<b>0.006</b>

Table 4.15: OGIP at various percentiles from SGCOSIM-local and global distribution.

<b>Percentile</b>	<b>OGIP obtained from SGCOSIM-local and global distribution (Bcf)</b>
<b>0%</b>	<b>15.050</b>
<b>10%</b>	<b>15.112</b>
<b>20%</b>	<b>15.137</b>
<b>25%</b>	<b>15.148</b>
<b>30%</b>	<b>15.159</b>
<b>40%</b>	<b>15.172</b>
<b>50%</b>	<b>15.185</b>
<b>60%</b>	<b>15.200</b>
<b>70%</b>	<b>15.211</b>
<b>75%</b>	<b>15.222</b>
<b>80%</b>	<b>15.234</b>
<b>90%</b>	<b>15.264</b>
<b>100%</b>	<b>15.338</b>

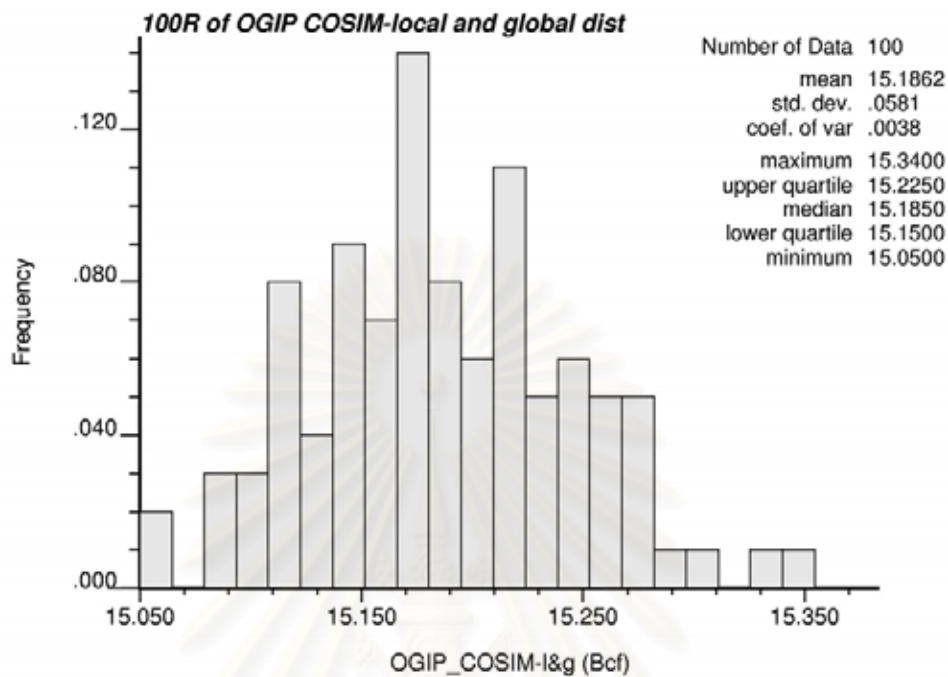


Figure 4.21: Histogram of OGIP obtained from SGCOSIM-local and global distribution variables.

#### 4.4 Comparison of simulation methods

After computing OGIP using MCS, SGS, and SGCOSIM, results from the three simulation methods were evaluated and compared to see which method is the best. The criterion for evaluation is the reproduction of statistics and spatial correlation of porosity and water saturation as well as OGIP statistics results.

In the comparison, statistics of a particular simulated porosity and water saturation realization obtained from MCS, SGS, and SGCOSIM were evaluated. In MCS, a total of 15,000 simulated porosity and water saturation realizations were generated based on global statistics which assumes the formation to be homogeneous. This approach is called Conventional MCS in this study. To compare in term of spatial statistics of the formation with SGS and SGCOSIM, Modified MCS was performed. In this approach, the formation was divided into 57,330 blocks

(the same number of blocks as in the case of SGS and SGCOSIM); then, MCS was used to simulate porosity and water saturation for each block.

Tables 4.16 and 4.17 provide a comparison of the statistics and correlation between porosity and water saturation for the four simulation methods. The statistics of the 50<sup>th</sup> simulated porosity and water saturation realizations from Modified MCS, SGS, and SGCOSIM and 15,000 realizations of simulated porosity and water saturation from Conventional MCS were used to compare with the original statistics to check the reproduction of statistics and correlation coefficient between porosity and water saturation. Simulated porosity and water saturation values obtained from the four methods have good correspondence in term of statistics when compared with the original data except for the correlation coefficient. The mean of simulated porosities obtained from SGCOSIM is almost the same as the mean of the original data but slightly higher than that obtained by SGS. The mean of simulated porosities obtained from Conventional MCS and Modified MCS are almost the same and are higher than the mean of the original data. Moreover, the mean of simulated water saturations obtained from SGCOSIM is closest to the mean of the original data. The means of simulated water saturations obtained from Conventional and Modified MCS are the highest. The variance of simulated porosities obtained from SGS is the lowest compared with the variances obtained by other methods and the variance of the original data. The variance of simulated water saturations obtained from SGCOSIM is the highest compared with the variances obtained by other methods; however, it is closest to the variance of the original data. In addition, the medians of porosity and water saturation obtained by SGCOSIM are closest to those of the original data.

Figures 4.22 and 4.23 illustrate the histograms of simulated porosity and water saturation obtained from the four methods, respectively. These plots reveal that the distributions of simulated variables are similar to the distributions of the original variables. Figure 4.24 shows the cumulative distribution of simulated porosity and water saturation obtained from four simulation methods. The cumulative distributions of simulated porosity and water saturation of SGCOSIM is almost the same as those of the original data. SGS provides a good correspondence

to the original data for simulated porosity. On the other hand, the method yields a lot of deviations for simulated water saturation. Furthermore, Conventional and Modified MCS show large deviation of porosity and water saturation from the original data.

Table 4.16: Statistics of simulated porosity by Conventional MCS, Modified MCS, SGS, and SGCOSIM.

Statistics of Porosity	Original Data	Conventional MCS (15,000 realizations)	50th Realization Simulated Porosity		
			Modified MCS	SGS	SGCOSIM
Mean	16.63	16.90	16.91	16.59	16.64
Standard Deviation	2.21	2.19	2.19	2.05	2.18
Variance	4.88	4.80	4.81	4.21	4.74
Minimum	10.00	10.00	10.00	10.00	10.00
Maximum	22.62	22.62	22.62	22.69	22.70
Median (P50)	16.40	16.62	16.62	16.33	16.41
Skewness	0.072	0.093	0.084	0.154	0.099
Kurtosis	0.074	-0.079	-0.079	0.061	0.024
Coefficient of variability	0.133	0.130	0.130	0.124	0.131
Mean Standard Error	0.890	0.018	0.071	0.069	0.070
Correlation coefficient: Porosity VS. Water saturation	-0.3415	0.0135	-0.0047	-0.0339	-0.6443

Table 4.17: Statistics of simulated water saturation by Conventional MCS, Modified MCS, SGS, and SGCOSIM.

Statistics of Water Saturation	Original Data	Conventional MCS (15,000 realizations)	50th Realization Simulated Water Saturation		
			Modified MCS	SGS	SGCOSIM
Mean	42.29	44.66	44.66	43.87	42.39
Standard Deviation	10.26	9.19	9.22	9.29	10.78
Variance	105.18	84.41	84.95	86.35	116.11
Minimum	14.90	14.90	14.90	14.90	14.90
Maximum	60.00	60.00	60.00	60.00	60.00
Median (P50)	43.80	46.10	46.20	45.40	44.10
Skewness	-0.555	-0.721	-0.716	-0.664	-0.574
Kurtosis	-0.358	0.172	0.138	-0.020	-0.402
Coefficient of variability	0.243	0.206	0.206	0.212	0.254
Mean Standard Error	2.264	0.075	0.187	0.183	0.177
Correlation coefficient: Porosity VS. Water saturation	-0.3415	0.0135	-0.0047	-0.0339	-0.6443

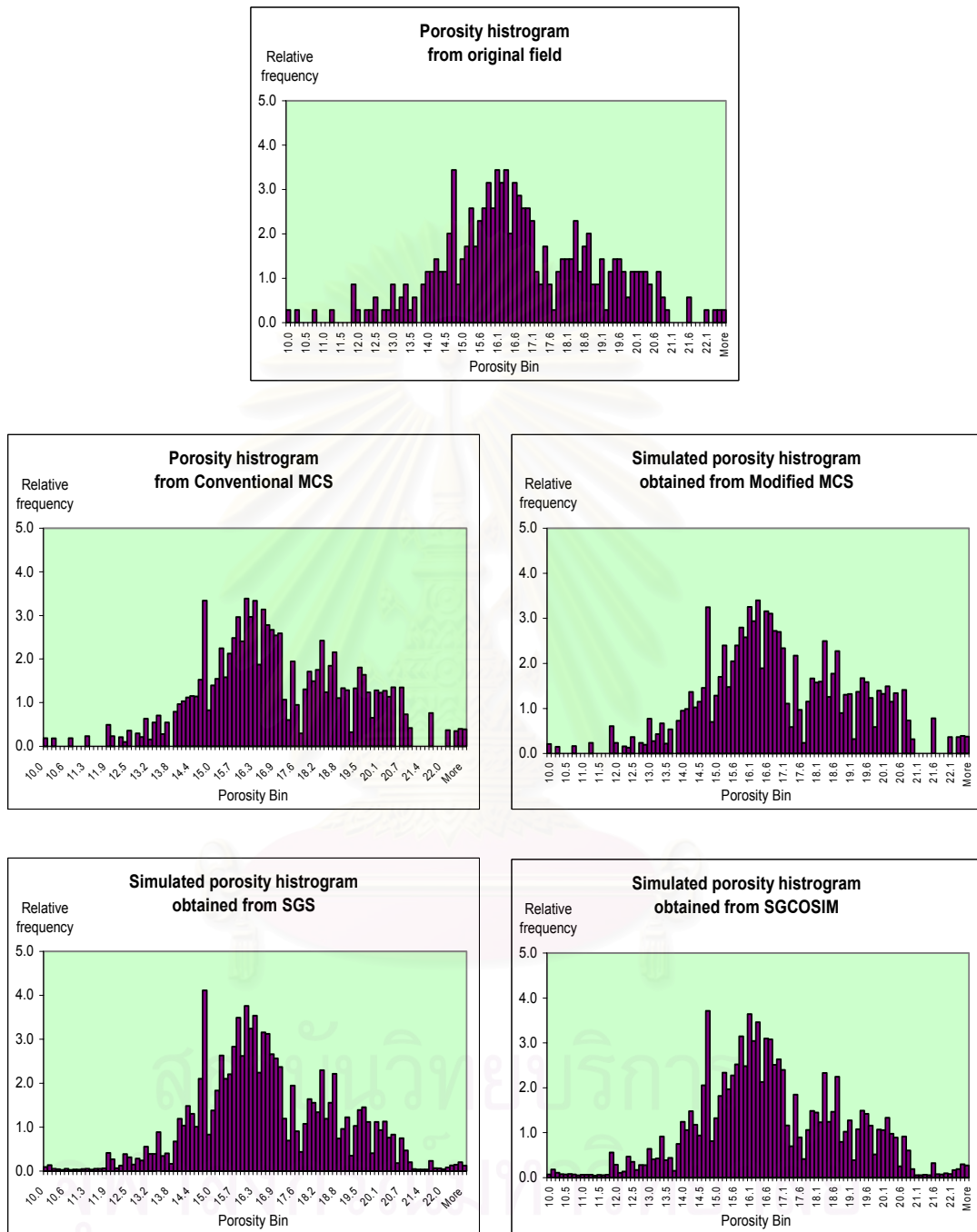


Figure 4.22: Histogram of simulated porosity by Conventional MCS, Modified MCS, SGS, and SGCOSIM.



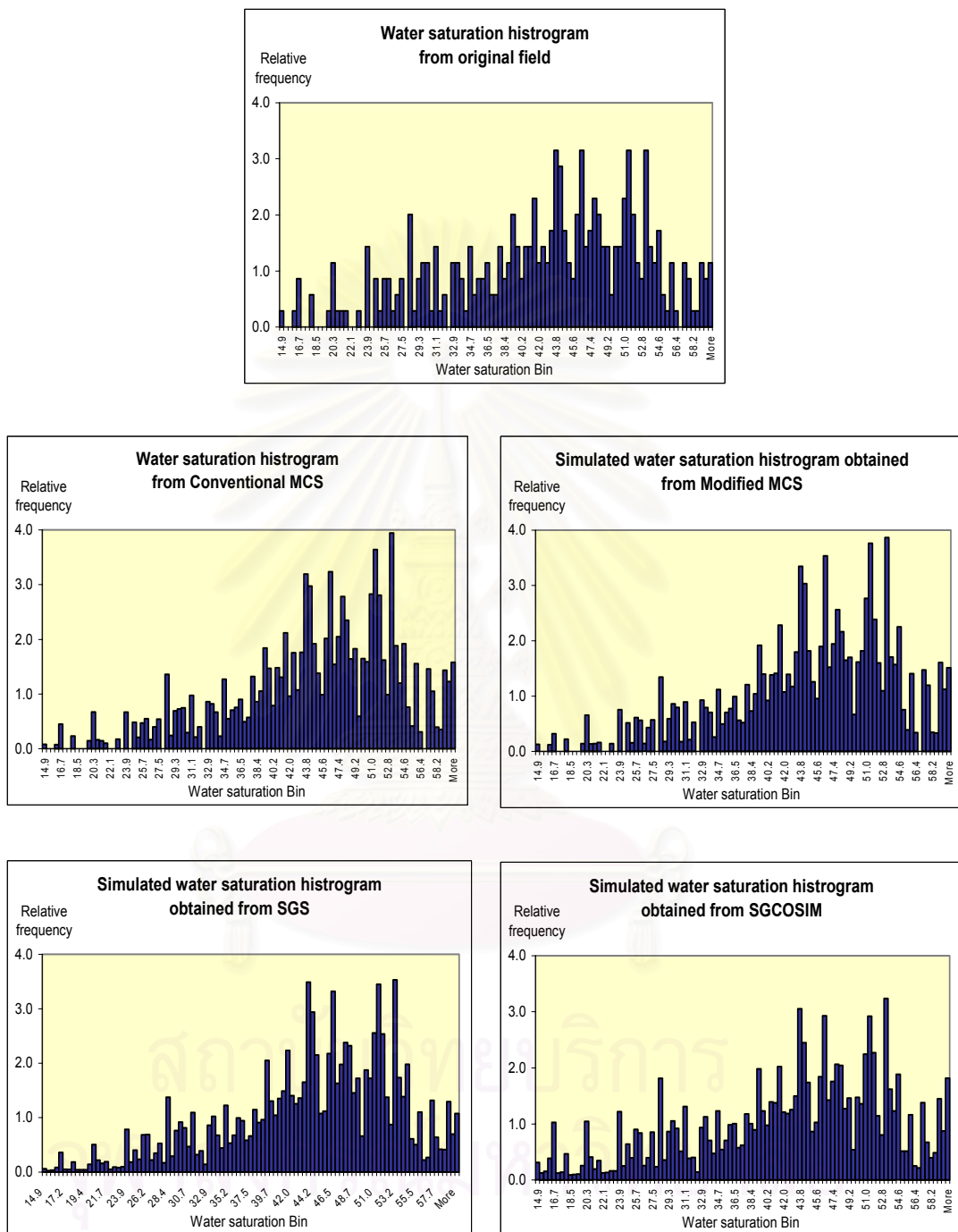


Figure 4.23: Histogram of simulated water saturation by Conventional MCS, Modified MCS, SGS, and SGCOSIM.

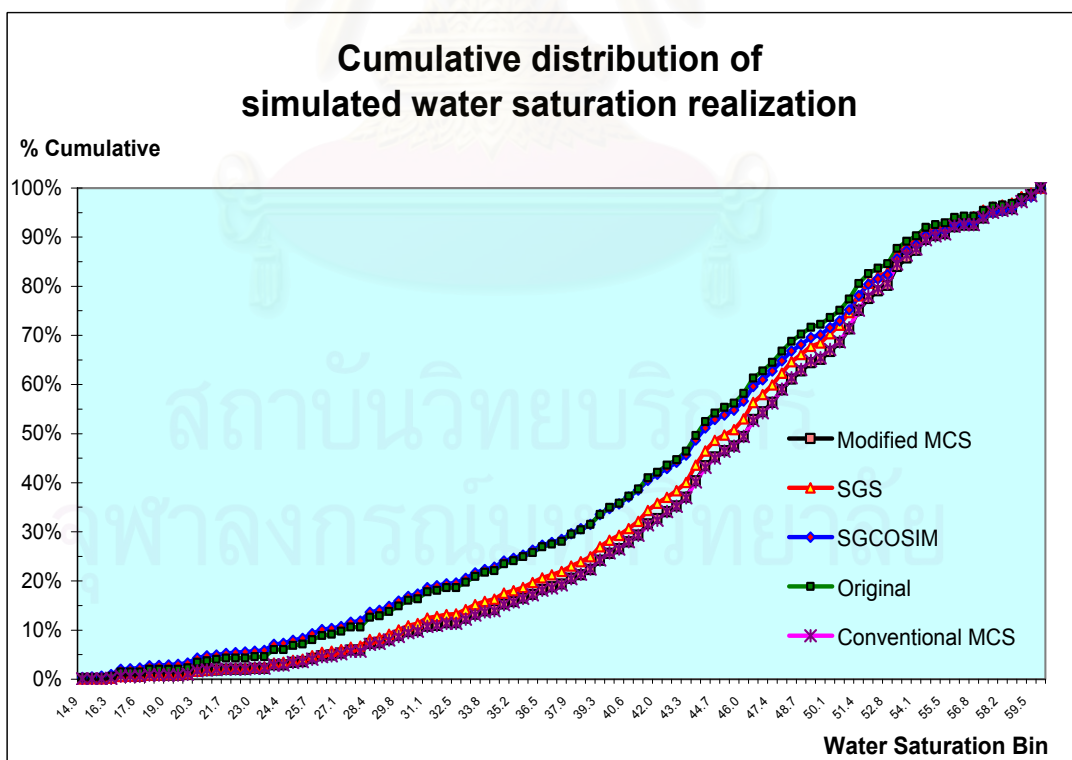
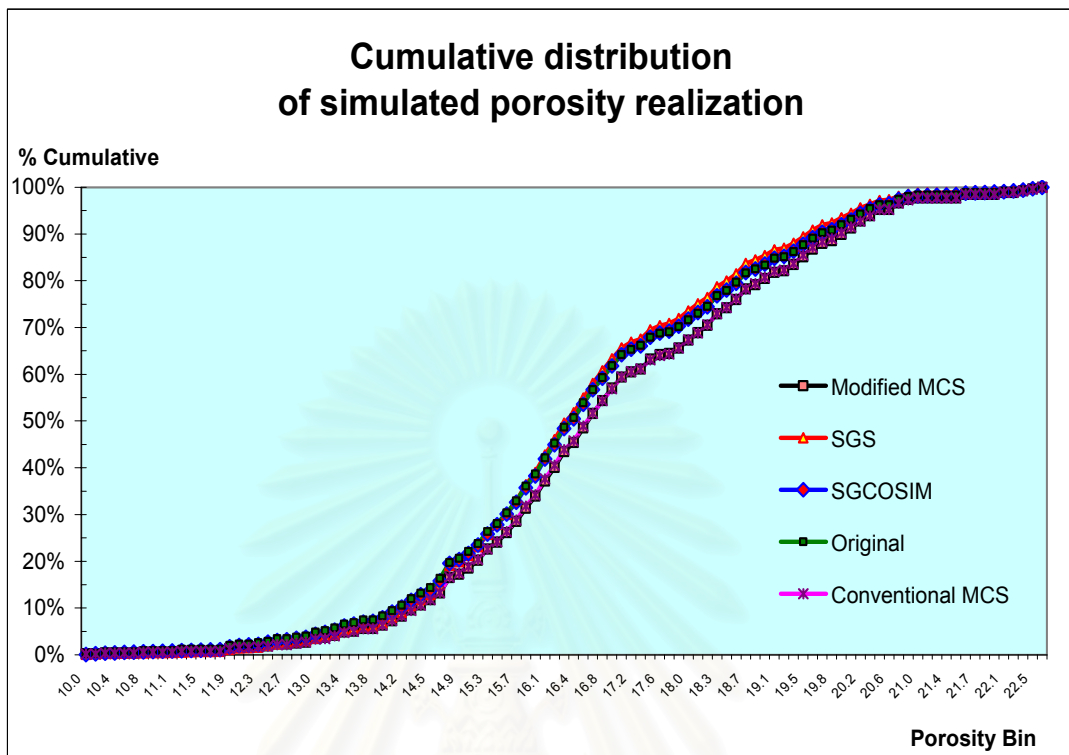


Figure 4.24: Cumulative distribution of simulated porosity and water saturation by Conventional MCS, Modified MCS, SGS, and SGCOSIM.

Apart from correlation coefficient, it is obviously seen that SGCOSIM provides the closest statistics of simulated variables to statistics of the original data. This reflects the ability of SGCOSIM to preserve both the statistics and the distribution of variables. This implies that SGCOSIM does not only well reproduce statistical data and spatial structure of input variables but also provides equiprobable realizations of input variables, each comprising more realistic level of heterogeneity. However, the correlation coefficient obtained from SGCOSIM is not in good agreement with the original data. The reason for this poor correlation is, possibility, the high nugget effect (the nugget of about 30%) used in the simulation which makes the realizations too erratic.

After comparing the input variables, we now proceed to compare the output obtained from the four methods. The porosity and water saturation which were generated from the four methods were used to calculate the OGIP. The multiple of the realizations provide valuable information to assess the uncertainty of OGIP output. Table 4.18 illustrates the statistics of OGIP results obtained from different simulation methods.

Table 4.18: Statistics of OGIP obtained from Conventional MCS, Modified MCS, SGS, and SGCOSIM.

Statistics of OGIP	Conventional MCS (15,000 realizations)	Modified MCS (100 realizations)	SGS (100 realizations)	SGCOSIM (100 realizations)
Mean	14.53	14.57	14.84	15.19
Standard deviation	3.05	0.3351	0.2818	0.0582
Variance	9.32	0.1123	0.0794	0.0034
Minimum	6.52	13.83	14.26	15.05
Maximum	29.17	15.56	15.56	15.34
Skewness	0.667	0.901	0.279	0.175
Kurtosis	0.572	2.767	-0.229	-0.132
Coefficient of variability	0.2100	0.0230	0.0190	0.0038
Mean Standard Error	0.0249	0.0335	0.0282	0.0058
<b>Percentile</b>				
0%	6.52	13.83	14.26	15.05
25%	12.33	14.53	14.68	15.15
50%	14.14	14.54	14.81	15.19
75%	16.35	14.56	15.02	15.22
100%	29.17	15.56	15.56	15.34

Practically, it is impossible to know the real OGIP value. Thus, the criterion to evaluate simulation methods should be uncertainty of the output regardless of the real OGIP value. A simulation method that reduces the output uncertainty is considered to be the best method. According to this criterion SGS and SGCOSIM give very low variance of OGIP estimate whereas Modified MCS gives slightly higher variance than SGS and Conventional MCS gives the highest variance. Simulated porosity and water saturation variables from Conventional MCS were generated from global statistical distribution. A randomly drawn value represents the variable for the entire field. When MCS was modified (Modified MCS), it is apparently seen that variance of OGIP is significantly improved over Conventional MCS. However, Modified MCS still does not take into account spatial correlation. On the other hand, SGS and SGCOSIM consider local relationship imposed by spatial structure (variogram) of each variable. SGS and SGCOSIM characterize uncertainty of OGIP through the spatial structure of variables. For this reason, any conditional simulation approach whether it is SGS or SGCOSIM obviously show better results over Conventional and Modified MCS.

Comparing between SGS and SGCOSIM, the variance from SGS is 0.0794 compared to variance of 0.0034 from SGCOSIM. This is possible because SGCOSIM method incorporates permeability and formation resistivity as secondary variables into the model. In summary, SGCOSIM appears to provide the best result and can be used to represent the realistic heterogeneity of the reservoir being studied.

#### **4.5 Sensitivity analysis**

One of the main objectives of this study is to understand the influence of geostatistical parameters on the calculation of OGIP. Therefore, sensitivity analysis of OGIP under varying spatial parameters was performed. The OGIP results obtained in Section 4.4 reveal that SGCOSIM is the best simulation method. SGCOSIM was then selected to be the simulation method for the sensitivity analysis. Note that the purpose of this analysis is to evaluate the OGIP results under varying spatial parameters, not the simulation method.

In order to carry out the sensitivity analysis of spatial behaviors, porosity which is considered to be one of the most important variables for OGIP in the volumetric method was selected as a studied variable. Its spatial behaviors were subjectively varied when the remaining statistics of variables such as the initial water saturation, permeability, and resistivity were kept unchanged. The spatial parameters that were varied in the sensitivity analysis are nugget value, search distance, and correlation coefficient.

#### **4.5.1 Nugget value**

The spatial structure with various nugget values of porosity was synthetically created using SGCOSIM. The original porosity data were used to simulate the porosity field data conditioned to the defined spatial structure. In a nutshell, the required nugget value was specified in the spatial structure. The simulated porosity field data represent a new spatial structure. Then, a total of 2,210 samples from 17 wells was drawn from this simulated field data and used as data for the SGCOSIM. The number of drawn sample is justified for sensitivity analysis since each sample point is covered by the range imposed in porosity variogram. Therefore, simulated porosity values can be drawn from constructed probability distribution function or called local distribution block. The well locations and positions of drawn sample are depicted in Figure 4.25. Finally, the SGCOSIM used to create a realization of porosity distribution. Repeating the same procedure using different nugget values provides a mean to evaluate the sensitivity of nugget parameters on OGIP results.

In this study, porosity nugget values of 0.0, 0.10, 0.20, and 0.30 were used. It is important to note that one realization was generated for each nugget value and the OGIP was calculated for all simulated blocks called “block-OGIP”. A summation of block-OGIP gives the formation OGIP.

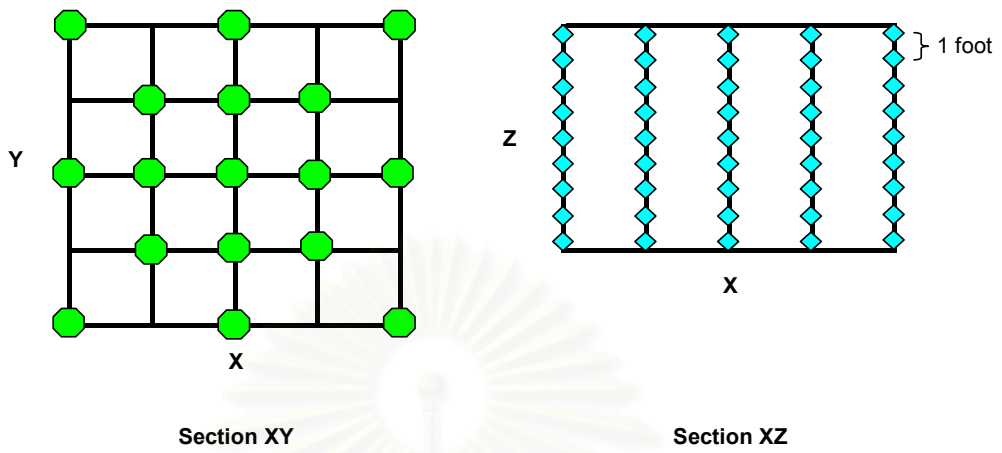


Figure 4.25: The well locations and positions of drawn sample for sensitivity analysis.

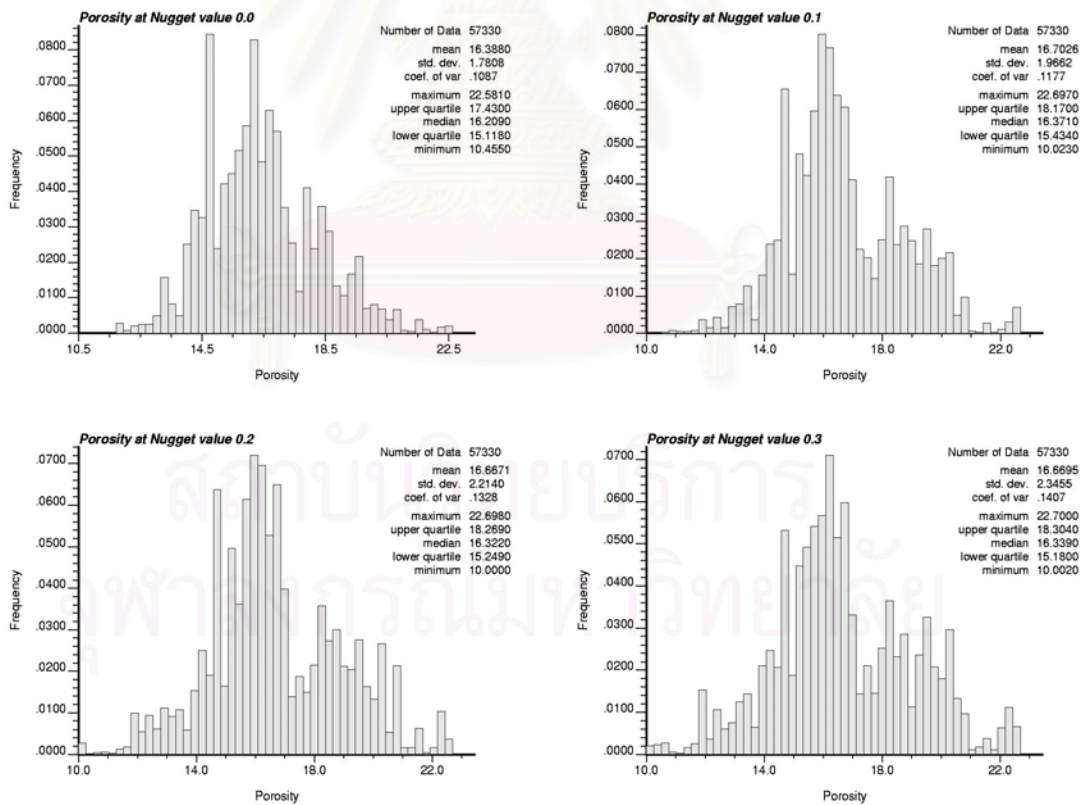


Figure 4.26: Histogram of porosity in block for different nugget values.



Histograms of porosity under varying nugget values are shown in Figure 4.26. The mean values of porosity are slightly different: 16.388, 16.703, 16.667, and 16.670 for nugget values of 0.0, 0.1, 0.2, and 0.3, respectively. However, the standard deviations are gradually larger as the nugget value increases. Their values are 1.781, 1.966, 2.214, and 2.346 for nugget values of 0.0, 0.1, 0.2, and 0.3, respectively. As a matter of fact, the variance of simulated data increases when increasing nugget value. The summary statistics of block-OGIPs and the value of formation OGIP are provided in Table 4.19. The numbers of simulated block are 57,330. The simulated data set was used to calculate block-OGIP.

Table 4.19: Statistical data of block-OGIP under various nugget values.

Statistical Data	Nugget Value (Fraction)			
	0.00	0.10	0.20	0.30
<b>Formation OGIP (bcf)</b>	<b>14.93</b>	<b>15.36</b>	<b>15.12</b>	<b>15.34</b>
<b>Block-OGIP statistics</b>				
<b>Mean</b>	<b>0.2604</b>	<b>0.2679</b>	<b>0.2638</b>	<b>0.2675</b>
<b>Standard deviation</b>	<b>0.0706</b>	<b>0.0768</b>	<b>0.0770</b>	<b>0.0830</b>
<b>Variance</b>	<b>0.0050</b>	<b>0.0059</b>	<b>0.0059</b>	<b>0.0069</b>
<b>Minimum</b>	<b>0.1146</b>	<b>0.1092</b>	<b>0.1085</b>	<b>0.1085</b>
<b>Maximum</b>	<b>0.5208</b>	<b>0.5236</b>	<b>0.5237</b>	<b>0.5238</b>
<b>Skewness</b>	<b>0.797</b>	<b>0.772</b>	<b>0.872</b>	<b>0.745</b>
<b>Kurtosis</b>	<b>0.289</b>	<b>0.117</b>	<b>0.483</b>	<b>0.088</b>
<b>Coefficient of variance</b>	<b>0.2710</b>	<b>0.2867</b>	<b>0.2920</b>	<b>0.3104</b>
<b>Mean Standard Error</b>	<b>0.0003</b>	<b>0.0003</b>	<b>0.0003</b>	<b>0.0003</b>
<b>No. of simulated blocks</b>	<b>57,330</b>	<b>57,330</b>	<b>57,330</b>	<b>57,330</b>
<b>Percentile 0% (P0)</b>	<b>0.1146</b>	<b>0.1092</b>	<b>0.1085</b>	<b>0.1085</b>
<b>Percentile 25% (P25)</b>	<b>0.2081</b>	<b>0.2106</b>	<b>0.2089</b>	<b>0.2064</b>
<b>Percentile 50% (P50)</b>	<b>0.2472</b>	<b>0.2516</b>	<b>0.2480</b>	<b>0.2509</b>
<b>Percentile 75% (P75)</b>	<b>0.3014</b>	<b>0.3139</b>	<b>0.3052</b>	<b>0.3168</b>
<b>Percentile 100% (P100)</b>	<b>0.5208</b>	<b>0.5236</b>	<b>0.5237</b>	<b>0.5238</b>

It can be seen that there is an influence on the variance of block-OGIP by changing the nugget value while the mean values are comparable. The standard deviation and variance of block-OGIP slightly increases when increasing nugget values. Block-OGIP could be varied for many reasons. First, an increase in nugget value will add an additional uncertainty to the porosity data set in such a way that the more nugget value, the more uncertainty introduced to the simulation model.

Second, the simulated realization map will lose locality structure when increasing the nugget value. However, loss in local structure is considered a small effect due to the conditional simulation subroutine that randomly draws simulated value from the probability distribution function. It can be said that an increase in the nugget value slightly changes the block-OGIP statistics. It seems that the random drawing of simulated data reduces the influence of nugget effects.

#### 4.5.2 Search distance

The range defines a spatial correlation with distance and direction. Synthesizing the original data set with a new range value involves the relocation of the entire data set until the spatial structure with a specific range is found. This data location adjustment is considered impractical because these petrophysical data are taken at the borehole along only 3 wells. Therefore, an alternative is to search distance instead of spatial correlation structure. The search distances of 70, 100, 150, 200, and 250 ft were used in the SGCOSIM to evaluate the impact on block-OGIP.

It is evident that the number of simulated blocks that uses local distribution increases when increasing the search distance, and almost all blocks were simulated when the search distance is 250 ft. A small change on the mean and standard deviation of simulated porosity is found when varying the search distance from 70 to 250 ft although the number of simulated blocks increases significantly. The mean value of simulated porosity ranges from 16.594 to 17.137, and standard deviation ranges from 2.121 to 2.214. Histograms of porosity for different search distances are shown in Figure 4.27.

The statistics of block-OGIP and the value of formation OGIP are provided in Table 4.20. The statistics of block-OGIP change in accordance with the change in search distance. The mean approaches the global mean of 0.266 as the search distance increases. Their mean values are 0.342, 0.317, 0.290, 0.270, and 0.266 for search distance of 70, 100, 150, 200, and 250 ft, respectively. A similar trend is observed for the variance which has the value of 0.0132, 0.0101, 0.0074, 0.0068, and 0.0061 for search distances of 70, 100, 150, 200, and 250 ft, respectively. An

extension of search distance gives more possibility in finding a nearby conditioned data value of both primary and secondary variables, and thus maintains Kriging matrix stability.

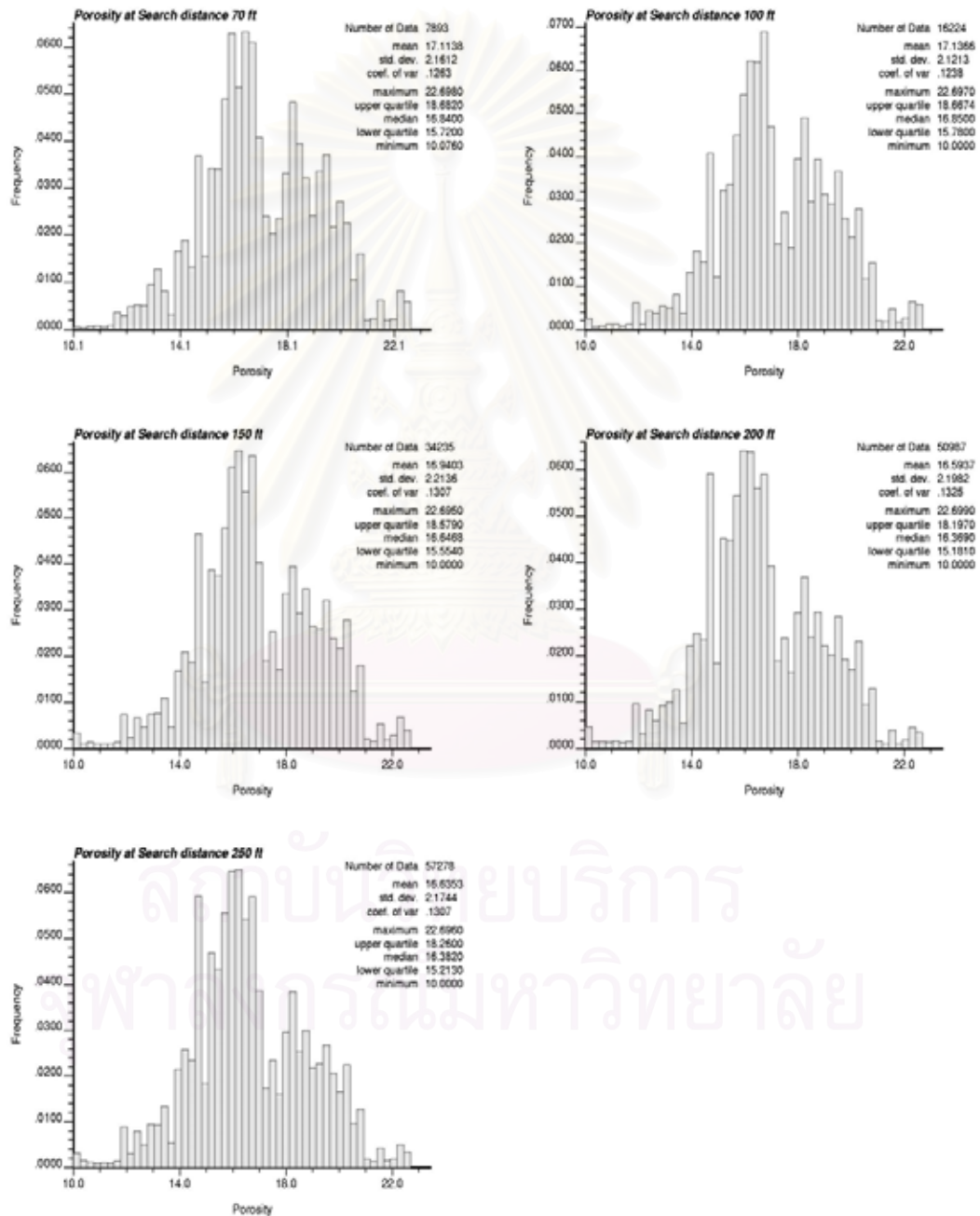


Figure 4.27: Histogram of porosity for different search distances.

Table 4.20: Statistical data of block-OGIP under various search distances.

Statistical Data	Search Distance (ft)				
	70	100	150	200	250
Formation OGIP (bcf)	2.70	5.14	9.93	13.76	15.21
<b>Block-OGIP statistics</b>					
Mean	0.3418	0.3168	0.2901	0.2698	0.2656
Standard deviation	0.1149	0.1005	0.0862	0.0824	0.0784
Variance	0.0132	0.0101	0.0074	0.0068	0.0061
Minimum	0.1136	0.1085	0.1085	0.1085	0.1085
Maximum	0.6149	0.6083	0.6098	0.6153	0.6094
Skewness	0.146	0.387	0.507	0.726	0.791
Kurtosis	-1.043	-0.765	-0.420	0.099	0.356
Coefficient of variance	0.3361	0.3173	0.2973	0.3055	0.2951
Mean Standard Error	0.0005	0.0004	0.0004	0.0003	0.0003
No. of simulated blocks	7,893	16,224	34,235	50,987	57,278
No. of nonsimulated blocks	49,437	41,106	23,095	6,343	52
Percentile 0% (P0)	0.1136	0.1085	0.1085	0.1085	0.1085
Percentile 25% (P25)	0.2465	0.2365	0.2232	0.2087	0.2085
Percentile 50% (P50)	0.3309	0.2997	0.2757	0.2532	0.2504
Percentile 75% (P75)	0.4387	0.3962	0.3497	0.3200	0.3106
Percentile 100% (P100)	0.6149	0.6083	0.6098	0.6153	0.6094

The ultimate aim is to select the simulation model that is able to simulate values for all blocks. However, this depends on many conditions imposed on simulation subroutines such as minimum and maximum number of variables and search method. Practically, the search distance is restricted within the range distance. For petrophysical data, samples are mostly available in the vertical direction (along the borehole) but sparsely located in the horizontal plane (between boreholes). It is likely that there is a greater influence of vertical data than horizontal data on the calculated range.

#### 4.5.3 Correlation coefficient

In this step, the correlation coefficient between porosity and water saturation is varied while other statistics of input parameters remain the same. Similar to synthesis nugget values in section 4.5.1, the generation of a synthetic data set with a specific correlation coefficient was done. The original porosity data were used to simulate the porosity and water saturation field data conditioned to the defined correlation coefficient. The simulated porosity and water saturation field

data represent a new spatial structure. Then, a total of 2,210 samples from 17 wells which is the same method used with nugget was drawn from these simulated field data and used as data for the SGCOSIM. The correlation coefficient was varied from 0.00 to -0.20, -0.40, -0.60, and -0.80. Realization maps of porosity and water saturation were generated for each correlation coefficient. Figure 4.28 shows the histogram of porosity under varying correlation coefficients between porosity and water saturation. Mean values of simulated porosity are 16.615, 16.587, 16.596, 16.600, and 16.628 while standard deviations are 2.013, 1.987, 1.988, 2.000, and 1.870 for the correlation coefficient of 0.00, -0.20, -0.40, -0.60, and -0.80, respectively.

A summary statistics of block-OGIP and formation OGIP under various correlation coefficients are given in Table 4.21. As shown in the table, the correlation coefficient has a greater influence on the variance than on the mean value. The block-OGIP mean values are almost the same at 0.260 for all correlation values. However, the block-OGIP variance is steadily increasing as the correlation becomes more negative. Their values are 0.0023, 0.0027, 0.0034, 0.0054, and 0.0055 for correlation coefficient of 0.00, -0.20, -0.40, -0.60, and -0.80, respectively. A strong correlation means that there is a lot of information of one variable being translated into an estimation of another variable. Thus, more information is incorporated in the simulation model. As a matter of fact, an increase in correlation coefficient results in more pairs of large and small values of porosity and water saturation. Then, this results in more extreme values of block-OGIP output. This explains why variance of block-OGIP significantly increases. It is noted that the standard deviation increases by as much as 49% from no correlation to correlation of 80%. Therefore, the correlation coefficient has a significant impact on block-OGIP output.



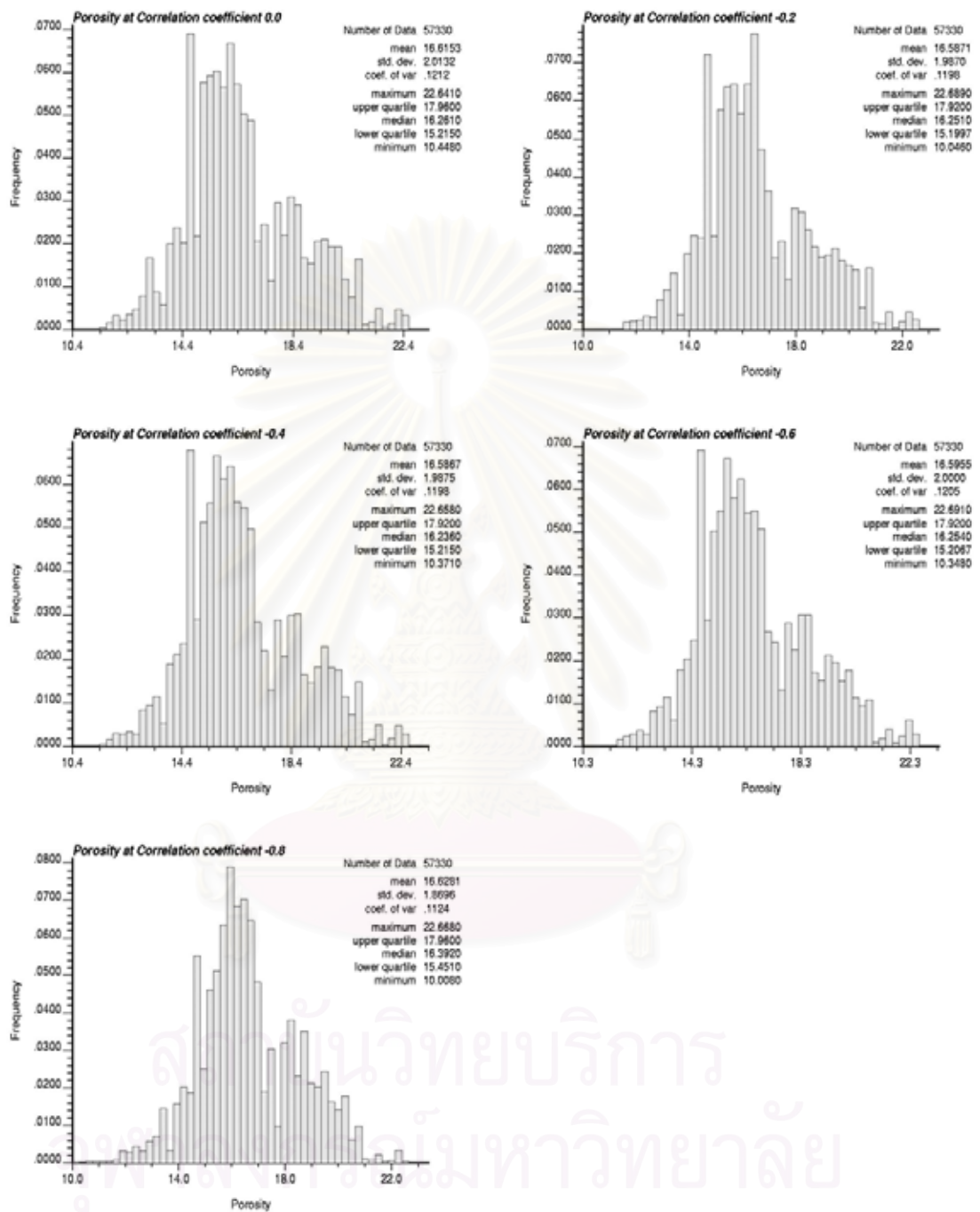


Figure 4.28: Histogram of porosity in block for different correlation coefficients.



Table 4.21: Statistical data of block-OGIP under various correlation coefficients.

Statistical Data	Correlation Coefficient				
	0.00	-0.20	-0.40	-0.60	-0.80
Formation OGIP (bcf)	14.89	14.92	14.98	15.15	15.14
<b>Block-OGIP statistics</b>					
Mean	0.2598	0.2602	0.2612	0.2642	0.2641
Standard deviation	0.0484	0.0519	0.0584	0.0734	0.0739
Variance	0.0023	0.0027	0.0034	0.0054	0.0055
Minimum	0.1314	0.1147	0.1248	0.1130	0.1085
Maximum	0.5079	0.5085	0.5192	0.5226	0.5230
Skewness	0.703	0.737	0.779	0.839	0.748
Kurtosis	0.596	0.580	0.559	0.405	0.131
Coefficient of variance	0.1862	0.1996	0.2237	0.2780	0.2798
Mean Standard Error	0.0002	0.0002	0.0002	0.0003	0.0003
No. of simulated blocks	57,330	57,330	57,330	57,330	57,330
Percentile 0% (P0)	0.1314	0.1147	0.1248	0.1130	0.1085
Percentile 25% (P25)	0.2249	0.2231	0.2193	0.2099	0.2099
Percentile 50% (P50)	0.2533	0.2523	0.2514	0.2507	0.2497
Percentile 75% (P75)	0.2888	0.2906	0.2955	0.3054	0.3073
Percentile 100% (P100)	0.5079	0.5085	0.5192	0.5226	0.5230

The impact of spatial structure variables on block-OGIP output is shown in Table 4.22. In order to quantify the impact of spatial structures, change of statistics of block-OGIP which are mean and standard deviation were compared among spatial structure variables. When considering absolute percentage of block-OGIP's mean, the search distance has the most impact, a reduction of 22% when the search distance is 250 ft. The variation of nugget value and correlation coefficient has a small impact on block-OGIP's mean. The block-OGIP's mean increases by 2-3% for both spatial structure variables.

Table 4.22: Comparison impact of spatial structures to block-OGIP.

Statistics	Nugget Value				Search Distance					Correlation Coefficient				
	0.00	0.10	0.20	0.30	70	100	150	200	250	0.00	-0.20	-0.40	-0.60	-0.80
Mean	0.2604	0.2679	0.2638	0.2675	0.3418	0.3168	0.2901	0.2698	0.2656	0.2598	0.2602	0.2612	0.2642	0.2641
Stdv	0.0706	0.0768	0.0770	0.0830	0.1149	0.1005	0.0862	0.0824	0.0784	0.0484	0.0519	0.0584	0.0734	0.0739
% Variation		10%	20%	30%		43%	114%	186%	257%		20%	40%	60%	80%
% Mean change		2.9%	1.3%	2.7%		-7%	-15%	-21%	-22%		0.2%	0.6%	1.7%	1.7%
% Stdv change		8.8%	9.1%	17.6%		-13%	-25%	-28%	-32%		7%	21%	52%	53%

The percentage change of block-OGIP's standard deviation is quite significant for all variables. Nugget value variation records the highest change of block-OGIP's standard deviation. Block-OGIP's standard deviation increases as much as 18% when the nugget value was varied by 30%. When varying the correlation coefficient by 80%, the block-OGIP's standard deviation increases by 53%. The search distance variation gives the smallest change of block-OGIP's standard deviation. Block-OGIP's standard deviation decreases about 32% on 257% increase of the magnitude of search distances. Taking all aspects into account, the most sensitive parameter is the nugget value followed by correlation coefficient and search distance.



สถาบันวิทยบริการ  
จุฬาลงกรณ์มหาวิทยาลัย

## CHAPTER V

### CONCLUSIONS AND RECOMMENDATIONS

Different stochastic simulation methods were used to simulate petrophysical parameters, i.e., porosity and water saturation. The simulated data were then used to calculate the original gas-in-place (OGIP) using the volumetric method. Three different stochastic simulation models which are Monte Carlo Simulation (MSC), Sequential Gaussian Simulation (SGS), and Sequential Gaussian Cosimulation (SGCOSIM) had been applied on real field data.

First, Monte Carlo Simulation (MCS) was performed. The simulations were conducted via 15,000 random numbers based on global distribution of porosity and water saturation data. OGIPs were calculated based on those simulated parameters, and the results follow lognormal distribution.

Important remarks on MCS are presented as follows:

1. Defining range and distribution of variable is important since randomly simulated values are solely based on the input information. However, it is costly to accurately define the range and shape of the input distribution because it requires a substantial amount of available data. For the data used in this study, porosity behaves like normal distribution while water saturation is clearly lognormal distribution.
2. The main assumption of traditional MCS is that variables are independent. In this case, porosity and water saturation were simulated independently regardless of their correlation coefficient (correlation coefficient between porosity and water saturation calculated from field data is -0.3415). This assumption definitely adds on additional uncertainty to the calculated OGIP. For a better representation of simulated variables, the real condition has to be taken into account in the MCS model.

3. Regarding to Law of large number, very large number of realizations is required to yield a small variation in mean and variance of OGIP. Large number can cause computation burden such that the full MCS analysis can be prohibitive.
4. The distribution of OGIP output appears to be log-normally distributed following the Central Limit Theorem. This proves that the product of distributions gives approximately lognormal distribution.
5. MCS methodology allows incorporation of model input uncertainties, expressed as probability distributions of porosity and water saturation which in turn translates to uncertainty of OGIP output. It is observed that the OGIP variance is high due to the uncertainties of both input variables.

The second stochastic simulation method is Sequential Gaussian Simulation (SGS). Built in multiGaussian framework, SGS requires the input variables to be normally distributed. The simulation process starts with the transformation of porosity and water saturation to standard normal data having zero of mean and unit variance. The checking for bivariate normality on the data shows a good agreement between an experimental and model derived variogram at median cutoff. The variogram models of both variables are best fitted with spherical model. These spatial structures were used as the conditioned information along with the original and previously simulated data in SGS process. In this part of the study, 100 realizations of porosity and water saturation were separately simulated, providing 100 of OGIP values. The histogram and statistics of OGIP were constructed in order to assess the variation and to compare with other simulation methods. Using GSLIB program, SGS can be performed in purely local or combining local and global estimate. In the local estimate, porosity and water saturation were generated for blocks located within the search volume. In the global estimate, porosity and water saturation were generated for blocks located within the search volume and from the global statistics or statistics of original data for blocks located outside the search volume. Results from both approaches show significant impact on OGIP calculated value.

The results from SGS can be summarized as follows:

1. Variograms of porosity and water saturation were performed only in the south-east direction due to a limitation of field data along the drilled wells. Since data are obtained from only three wells data located in the study area, variograms of porosity and water saturation may not represent the best spatial structure of the variables.
2. With SGS algorithm, each variable is univariate and independent. In the simulation process, original statistics are preserved but not correlation between porosity and water saturation. This is because each variable was simulated independently.
3. SGS provides simulated values in the local sense referring to its conditioning information which includes the nearest data available comprising both original data and previously simulated data. The quality and quantity of simulated value mainly depend on spatial correlation captured in the variogram model.
4. When neither original data nor previously simulated value exists within search neighborhood, SGS algorithm simulates the value by drawing it from global statistics. In this case, simulated values honor only global statistics. Locality of the estimates reduces when more simulated values are drawn from global statistics.

The third simulation method is Sequential Gaussian Cosimulation (SGCOSIM). It is built on the same assumption as SGS. However, SGCOSIM has special feature over SGS, which is joint conditional simulation. SGCOSIM allows simultaneous joint simulation of several primary variables and incorporation of several secondary variables. Porosity and water saturation are naturally interdependent. In this study, the secondary variables are permeability and resistivity and are correlated with the primary variables. The correlation coefficient among variables was used as an input in the simulation via correlation matrix. The cross-covariance model was inferred from the product of spatial structures of primary variables and the correlation coefficient. The secondary variables were pre-simulated to fill up the secondary data in all blocks. Then, joint simulation was carried out to

generate 100 realizations of primary variables. The OGIPs were then calculated based on these simulation maps and used to determine statistics and histogram of OGIP.

Important remarks on SGCOSIM are presented as follows:

1. SGCOSIM algorithm allows simultaneous joint simulation of porosity and water saturation with incorporation permeability and resistivity data as secondary variables.
2. This study shows that SGCOSIM reproduces both spatial structures of reservoir properties and the correlation between reservoir properties. It is observed that the correlation coefficient between the simulated values of porosity and water saturation is realistically high as well as correlation coefficient between primary and secondary variables.
3. In order to apply SGCOSIM, secondary variables have to be available for all blocks. In this study, the amount of secondary data is the same as primary data. Therefore, a pre-simulation of secondary variables had to be carried out. However, certain amount of uncertainty was added into the data set during the pre-simulation process. It is better to have secondary data available for all study area. In practice, the secondary data may be found from seismic data.
4. OGIP obtained from porosity and water saturation simulated by SGCOSIM gives in a very low standard deviation and variance.

In addition, the stochastic simulations were evaluated by considering the simulated porosity, water saturation, and OGIP estimate. The criterion for evaluation is a reproduction of the histogram and spatial correlation structure of real field data of Formation I and spread of OGIP statistics. Conclusions from comparison of these stochastic simulations can be drawn as follows:

1. Regarding to the above criteria, SGCOSIM is the best simulation method followed by SGS, Modified MCS, and Conventional MCS.



2. SGS and SGCOSIM preserve the true nature of studied variables such as their statistics and local variability. Moreover, they produce a number of statistically equivalent realizations which capture local uncertainty as well as the global patterns of uncertainty. This is definitely different from MCS which provides only the global estimate.
3. When MCS was modified (Modified MCS), it is seen that variance of OGIP is significantly improved over Conventional MCS. This implies that by increasing numbers of realization, the uncertainty of variables can be reduced.
4. It was found that in accounting for secondary variables in SGCOSIM simulation method, the uncertainty of OGIP output significantly reduces.

Furthermore, sensitivity analysis of spatial behaviors was carried out as porosity was a studied variable. The spatial parameters that were varied are nugget value, search distance, and correlation coefficient. Conclusions from evaluation of the impact to statistics of OGIP can be drawn as follows:

1. The mean and standard deviation of OGIP increase as porosity nugget increases due to higher variation in the data value. On the other hand, the variation of OGIP decreases when increasing the search distance. And, a higher correlation value between variables causes more dispersion of OGIP output.
2. In the comparison the impact of spatial structures, i.e., nugget value, search distance, and correlation coefficient on OGIP output, it is found that the search distance has the most influence on the mean of OGIP while the nugget value has the most influence on variance of OGIP. The shift of the mean when varying the search distance can be explained by the fact that there are more blocks simulated as the search distance increase. Thus, the mean value approaches the global mean.

The following points are recommended for future study:

1. Although MCS was found to give inferior result compared to conditional Geostatistics, it is worth to point out that sensitivity analysis helps defining the most sensitive parameters and a greater detail study should focus on that variable in order to reduce variation in the simulation model and improve the uncertainties of output. Also, interdependent relationship between variables must be included in the simulation to avoid overestimate or underestimate of OGIP in the volumetric method.

2. In this study, many parameters were considered as deterministic in the volumetric method, i.e., area, thickness, and gas formation volume factor. Therefore, in order to apply the simulations to cover full scale of the problem, future study should be conducted to include these variables in the stochastic simulations.

3. Geostatistical Simulations are proven to provide a good OGIP result. They are dramatically improved the uncertainties of OGIP calculation for real field. However, the study area in this study was adjusted to accommodate the simulation process. For the real reservoir, geostatistical simulations can be applied to the reservoirs when there are enough primary and secondary variables in order to define their spatial correlation structures.

## References

1. A. Bahar and M. Kelkar. "*Journey From Well Logs/Cores to Integrated Geological and Petrophysical Properties Simulation: A Methodology and Application*", SPE 66284, SPE India Oil and Gas Conference and Exhibition, New Delhi, 17-19 February 2000.
2. Anuar Bitanov. "*Uncertainty in N/G Ratio in Early Reservoir Development*", Master of Science Thesis, Stanford University, Stanford CA.
3. A. Sahin, A.A. Al-Salem. "*Stochastic Modeling of porosity Distribution in a Multi-Zonal Carbonate Reservoir*", SPE 68113, SPE Middle East Oil Show, Bahrain, 17-20 March, 2001.
4. A.S. Almeida. "*Joint Simulation of Multiple Variables with a Markov-Type Coregionalization Model*", Doctoral. Dissertation, Stanford University, Stanford CA.
5. Christopher J. Murray. "*Stochastic Simulation of Hydrocarbon Pore Volume for Risk Assessment and Economic Planning*", SPE 25527, Stanford University, Stanford CA.
6. C.V. Deutsch and A.G. Journel. "*GSLIB Geostatistic Software Library User's Guide*", Oxford University, Stanford, CA, 1992.
7. F.M. Petit *et al.* "*Early Quantification of Hydrocarbon In Place Through Geostatistical Object Modelling and Connectivity Computations*", SPE 28416, SPE 69<sup>th</sup> Annual Technical Conference and Exhibition. New Orleans, 25-29 September 1994.
8. Hohn, Michael. "*Geostatistics and Petroleum Geology*". New York: Van Nostrand Reinhold, 1988.

9. J.A. Murtha. "*Monte Carlo Simulation: Its Status and Future*", SPE 37932, SPE Distinguished Author Series: Dec 1981-Dec 1983.
10. Jorge L. Landa and Sebastien Strebelle. "*Sensitivity Analysis of Petrophysical Properties Spatial Distributions, and Flow Performance Forecasts to Geostatistical Parameters Using Derivative Coefficients*", SPE 77430, SPE Annual Technical Conference and Exhibition, Texas, 29 September-2 October 2002.
11. Kazuo Nakayama. "*Estimation of Reservoir Properties by Monte Carlo Simulation*", SPE 59408, 2000 SPE Asia Pacific Conference, Yokohama, 25-26 April 2000.
12. M. Ayoub *et al.* "*Identification, Quantification and Analysis of Subsurfaces Uncertainties Associated with Reservoir Description*", 10<sup>th</sup> Abu Dhabi International Petroleum Conference and Exhibition, 13-16 October 2002.
13. P. Behrenbruch, G.J. Turner, and A.R. Backhouse. "*Probabilistic Hydrocarbon Hydrocarbon in place Estimation: A Novel Monte Carlo Approach*", SPE 13982, Offshore Europe 85<sup>th</sup> Conference, Aberdeen, 10-13 September 1985.
14. Srikanta Mishra. "*Alternatives to Monte Carlo Simulation for Probabilistic Reserves Estimation and Production Forecasting*", SPE 49313, SPE Annual and Technical Conference and Exhibition, Louisiana, 27-30 September, 1998.
15. Truong Truong Thanh. "*An Improved Method for Reserves Estimation*", SPE International Student Paper Contest, SPE Asia Pacific Oil and Gas Conference and Exhibition, Melbourne, Australia, October 2002.
16. Wenlong Xu and T.T. Tran. "*Integrating Seismic Data in Reservoir Modeling: The Collocated Cokriging Alternative*", SPE 24742, SPE 67<sup>th</sup> Annual Technical Conference and Exhibition, Washington, 4-7 October 1992.



**APPENDICES**

สถาบันวิทยบริการ  
จุฬาลงกรณ์มหาวิทยาลัย

## APPENDIX A

A-1: SGS-local and global distribution parameter file for porosity.

START OF PARAMETERS:

N3.dat	\Data File in GEOEAS format
1 2 3 4 0	\column: x,y,z,variable,wt
-1.0e21 1.0e21	\data trimming limits
0	\0=transform the data, 1=don't
sgsim_P.trn	\Transf. table(for each var.)
10.0 22.62	\Min. and Max. val. for tails var.1
1 1.0	\Lower tail option and parameter
1 1.0	\Upper tail option and parameter
100R_SGS_N3_Pg.out	\Output File for simulation
2	\Debugging level: 1,2,3
100R_SGS_N3_Pg.dbg	\Output File for Debugging
591405	\Random number seed
0	\Kriging type
100	\Number of simulations
21 1.0 20.0	\nx,xmn,xsiz
21 1.0 20.0	\ny,ymn,ysiz
130 1.0 1.0	\nz,zmn,zsiz
0	\0=two part search, 1=data-nodes
0	\max per octant (0 -> not used)
130.0	\maximum search radius
0.0 0.0 0.0 1.0 1.0	\sang1,sang2,sang3,sanis1,sanis2
0 20	\min (0:global,>0:local), max data for simulation
5	\number simulated nodes to use
1 0.10	\nst, nugget effect
1 100 0.90	\it,aa,cc: STRUCTURE
0.0 0.0 0.0 1.0 1.0	\ang1,ang2,ang3,anis1,anis2:



## A.2: SGS-local and global distribution parameter file for water saturation.

## START OF PARAMETERS:

```

N3.dat          \Data File in GEOEAS format
1 2 3 5 0      \column: x,y,z, variable,wt
-1.0e21 1.0e21 \data trimming limits
0              \0=transform the data, 1=don't
sgsim_S.trn    \Transf. table(for each var.)
14.9 60.0     \Min. and Max. val. for tails var.1
1 1.0         \Lower tail option and parameter
1 1.0         \Upper tail option and parameter
100R_SGS_N3_S.out \Output File for simulation
2             \Debugging level: 1,2,3
100R_SGS_N3_S.dbg \Output File for Debugging
5440903       \Random number seed
0             \Kriging type
100           \Number of simulations
21 1.0 20.0   \nx,xmn,xsiz
21 1.0 20.0   \ny,ymn,ysiz
130 1.0 1.0   \nz,zmn,zsiz
0             \0=two part search, 1=data-nodes
0             \max per octant (0 -> not used)
130.0        \maximum search radius
0.0 0.0 0.0 1.0 1.0 \sang1,sang2,sang3,sanis1,sanis2
0 20         \min (0:global,>0:local), max data for simulation
5            \number simulated nodes to use
1 0.30       \nst, nugget effect
1 120 0.70   \it,aa,cc: STRUCTURE
0.0 0.0 0.0 1.0 1.0 \ang1,ang2,ang3,anis1,anis2:

```

## A.3: SGS-local and global distribution parameter file for resistivity.

START OF PARAMETERS:

N3.dat	\Data File in GEOEAS format
1 2 3 7 0	\column: x,y,z, variable,wt
-1.0e21 1.0e21	\data trimming limits
0	\0=transform the data, 1=don't
sgsim_R.trn	\Transf. table(for each var.)
11.5 113.1	\Min. and Max. val. for tails var.1
1 1.0	\Lower tail option and parameter
1 1.0	\Upper tail option and parameter
SGS_N3_R.out	\Output File for simulation
2	\Debugging level: 1,2,3
SGS_N3_R.dbg	\Output File for Debugging
5903545	\Random number seed
0	\Kriging type
1	\Number of simulations
21 1.0 20.0	\nx,xmn,xsiz
21 1.0 20.0	\ny,ymn,ysiz
130 1.0 1.0	\nz,zmn,zsiz
0	\0=two part search, 1=data-nodes
0	\max per octant (0 -> not used)
130.0	\maximum search radius
0.0 0.0 0.0 1.0 1.0	\sang1,sang2,sang3,sanis1,sanis2
0 20	\min (0:global,>0:local), max data for simulation
5	\number simulated nodes to use
1 0.10	\nst, nugget effect
1 110 0.90	\it,aa,cc: STRUCTURE
0.0 0.0 0.0 1.0 1.0	\ang1,ang2,ang3,anis1,anis2:

## A.4: SGS-local and global distribution parameter file for permeability.

## START OF PARAMETERS:

N3.dat	\Data File in GEOEAS format
1 2 3 6 0	\column: x,y,z, variable,wt
-1.0e21 1.0e21	\data trimming limits
0	\0=transform the data, 1=don't
sgsim_K.trn	\Transf. table(for each var.)
0.483 233.5	\Min. and Max. val. for tails var.1
1 1.0	\Lower tail option and parameter
1 1.0	\Upper tail option and parameter
SGS_N3_KwRt.out	\Output File for simulation
2	\Debugging level: 1,2,3
SGS_N3_KwRt.dbg	\Output File for Debugging
5389545	\Random number seed
5	\Kriging type
NS_SGS_N3_Rt.dat	\Gridded Secondary Variable (nscore)
2	\columns for secondary variable
0.7456	\Correlation valve
1	\Number of simulations
21 1.0 20.0	\nx,xmn,xsiz
21 1.0 20.0	\ny,ymn,ysiz
130 1.0 1.0	\nz,zmn,zsiz
0	\0=two part search, 1=data-nodes
0	\max per octant (0 -> not used)
130.0	\maximum search radius
0.0 0.0 0.0 1.0 1.0	\sang1,sang2,sang3,sanis1,sanis2
0 20	\min (0:global,>0:local), max data for simulation
5	\number simulated nodes to use
1 0.30	\nst, nugget effect
1 130 0.70	\it,aa,cc: STRUCTURE
0.0 0.0 0.0 1.0 1.0	\ang1,ang2,ang3,anis1,anis2:

### A.5: SGCOSIM-local and global distribution parameter file for porosity and water saturation.

#### START OF PARAMETERS:

```

N3.dat          \Data File in GEOEAS format
2 2            \Number of hard and soft var.
1 2 3 4 5 0    \column: x,y,z,vhard(i:1,2),wt
0              \0=transform the data, 1=don't
nscoreP.trn     \Transf. table var1(for each var.)
nscoreS.trn     \Transf. table var2(for each var.)
-99.00 99.00    \min./max. value(can't sim) for var.1
10 22.7        \Min. and Max. val. for tails var.1
1 1            \Lower tail option and parameter var.1(if not linear(1))
1 1            \Upper tail option and parameter var.1(if not linear(1))
-99.00 99.00    \min./max. value(can't sim) for var.2
14.9 60        \Min. and Max. val. for tails var.2
1 1            \Lower tail option and parameter var.2(if not linear(1))
1 1            \Upper tail option and parameter var.2(if not linear(1))
N3CO_PS.out     \Output File for simulation
1              \Debugging level: 1low,2,3high
N3CO_PS.dbg     \Output File for Debugging
26703494        \Random number seed
N3CO_Kw&Rt.dat  \Gridded nscore Secondary Variable(Soft var.)
2 4            \columns for Soft variables:1,2,..etc.
N3CO.cal        \Calibration parameter file (correlation matrix table)
100            \Number of realizations
21 1 20        \nx,xmn,xsiz
21 1 20        \ny,ymn,ysiz
130 1 1        \nz,zmn,zsiz
0              \0=two part search, 1=data-nodes
0              \max per octant (0 -> not used)
130            \maximum search radius
0.0 0.0 0.0 1.0 1.0 \sang1,sang2,sang3,sanis1,sanis2
0 20           \min, max data for simulation
5             \number simulated nodes to use
1 0.10        \nst, nugget effect VARIAB. 1
1 100 0.90    \it,aa,cc: STRUCTURE 1
0.0 0.0 0.0 1.0 1.0 \ang1,ang2,ang3,anis1,anis2:
1 0.30        \nst, nugget effect VARIAB. 2
1 120 0.70    \it,aa,cc: STRUCTURE 1
0.0 0.0 0.0 1.0 1.0 \ang1,ang2,ang3,anis1,anis2:

```

## A.6: Correlation coefficient matrix required by SGCOSIM.

Correlation coefficient matrix

4

Porosity

Water Saturation

Permeability

Resistivity

1.000	-0.3415	0.8108	0.6043
	1.000	-0.4240	-0.6250
		1.000	0.7456
			1.000



สถาบันวิทยบริการ  
จุฬาลงกรณ์มหาวิทยาลัย

# APPENDIX B

## B.1: Statistics of porosity and water saturation for each of 100 realizations from SGS-local and global distribution.

Realization Number #	1		2		3		4		5		6		7		8		9		10	
Statistical Data	Simulated		Simulated		Simulated		Simulated		Simulated		Simulated		Simulated		Simulated		Simulated		Simulated	
	Porosity	Water Sat.	Porosity	Water Sat.	Porosity	Water Sat.	Porosity	Water Sat.	Porosity	Water Sat.	Porosity	Water Sat.	Porosity	Water Sat.	Porosity	Water Sat.	Porosity	Water Sat.	Porosity	Water Sat.
No. of realization	57,330	57,330	57,330	57,330	57,330	57,330	57,330	57,330	57,330	57,330	57,330	57,330	57,330	57,330	57,330	57,330	57,330	57,330	57,330	57,330
No. of simulated	57,330	57,330	57,330	57,330	57,330	57,330	57,330	57,330	57,330	57,330	57,330	57,330	57,330	57,330	57,330	57,330	57,330	57,330	57,330	57,330
No. of unsimulated	0	0	0	0	0	0	0	0	0	0	0	0	0	0	0	0	0	0	0	0
Mean	16.70	42.19	16.33	42.52	16.43	42.50	16.82	42.37	16.59	42.62	16.75	40.91	16.59	43.38	16.16	41.75	16.41	42.45	16.25	43.16
Std. Deviation	2.03	9.63	2.14	9.47	2.09	9.81	1.93	9.96	2.10	9.53	2.04	10.01	2.11	9.54	1.96	9.83	2.10	9.74	1.94	9.65
Variance	4.12	92.66	4.59	89.62	4.36	96.26	3.71	99.17	4.39	90.87	4.17	100.19	4.45	91.06	3.83	96.63	4.40	94.83	3.78	93.18
Minimum	10.00	14.90	10.00	14.90	10.00	14.90	10.00	14.90	10.00	14.90	10.00	14.90	10.00	14.90	10.00	14.90	10.00	14.90	10.00	14.90
Maximum	22.70	60.00	22.70	60.00	22.66	60.00	22.69	60.00	22.69	60.00	22.70	60.00	22.70	60.00	22.68	60.00	22.69	60.00	22.70	60.00
Median	16.45	43.70	16.19	43.90	16.23	43.98	16.55	43.89	16.33	43.90	16.45	42.79	16.41	44.58	16.03	43.43	16.20	43.85	16.10	44.30
Skewness	0.133	-0.576	0.013	-0.596	0.024	-0.602	0.197	-0.581	0.138	-0.582	0.240	-0.468	0.008	-0.657	0.126	-0.494	0.095	-0.555	0.201	-0.597
Kurtosis	0.163	-0.248	0.184	-0.207	0.178	-0.253	-0.047	-0.292	0.091	-0.241	0.025	-0.497	0.214	-0.098	0.476	-0.397	0.258	-0.309	0.313	-0.202
Coefficient of variability	0.122	0.228	0.131	0.223	0.127	0.231	0.114	0.235	0.126	0.224	0.122	0.245	0.127	0.220	0.121	0.235	0.126	0.229	0.120	0.224
Mean Standard Error	0.070	0.176	0.068	0.178	0.069	0.178	0.070	0.177	0.069	0.178	0.070	0.171	0.069	0.181	0.068	0.174	0.069	0.177	0.068	0.180
Correlation	Porosity	Water Sat.	Porosity	Water Sat.	Porosity	Water Sat.	Porosity	Water Sat.	Porosity	Water Sat.	Porosity	Water Sat.	Porosity	Water Sat.	Porosity	Water Sat.	Porosity	Water Sat.	Porosity	Water Sat.
Porosity	1.0000	0.0064	1.0000	-0.0237	1.0000	-0.0407	1.0000	-0.0405	1.0000	-0.0367	1.0000	0.0466	1.0000	0.0531	1.0000	0.0141	1.0000	-0.0717	1.0000	-0.0329
Water Saturation	1.0000	1.0000	1.0000	1.0000	1.0000	1.0000	1.0000	1.0000	1.0000	1.0000	1.0000	1.0000	1.0000	1.0000	1.0000	1.0000	1.0000	1.0000	1.0000	1.0000





## B.2: Statistics of porosity and water saturation for each of 100 realizations from SGCOSIM-local and global distribution.

Realization Number #	1		2		3		4		5		6		7		8		9		10	
	Simulated		Simulated		Simulated		Simulated		Simulated		Simulated		Simulated		Simulated		Simulated		Simulated	
Statistical Data	Porosity	Water Sat.	Porosity	Water Sat.	Porosity	Water Sat.	Porosity	Water Sat.	Porosity	Water Sat.	Porosity	Water Sat.	Porosity	Water Sat.	Porosity	Water Sat.	Porosity	Water Sat.	Porosity	Water Sat.
No. of realization	57.330	57.330	57.330	57.330	57.330	57.330	57.330	57.330	57.330	57.330	57.330	57.330	57.330	57.330	57.330	57.330	57.330	57.330	57.330	57.330
No. of simulated	57.330	57.330	57.330	57.330	57.330	57.330	57.330	57.330	57.330	57.330	57.330	57.330	57.330	57.330	57.330	57.330	57.330	57.330	57.330	57.330
No. of unsimulated	0	0	0	0	0	0	0	0	0	0	0	0	0	0	0	0	0	0	0	0
Mean	16.60	42.11	16.61	42.03	16.61	42.26	16.63	42.06	16.61	42.27	16.65	42.21	16.59	42.08	16.66	42.19	16.69	42.13	16.62	42.06
Std. Deviation	2.18	10.85	2.19	10.79	2.18	10.90	2.23	10.89	2.15	10.83	2.21	10.71	2.18	10.85	2.16	10.77	2.19	10.79	2.18	10.97
Variance	4.74	117.85	4.80	114.47	4.75	118.74	4.97	118.85	4.64	117.22	4.89	114.81	4.75	117.78	4.68	115.93	4.79	116.36	4.74	120.28
Minimum	10.00	14.80	10.00	14.80	10.00	14.80	10.00	14.80	10.00	14.80	10.00	14.80	10.00	14.80	10.00	14.80	10.00	14.80	10.00	14.80
Maximum	22.70	60.00	22.69	60.00	22.70	60.00	22.70	60.00	22.70	60.00	22.70	60.00	22.70	60.00	22.69	60.00	22.70	60.00	22.70	60.00
Median	16.37	43.82	16.39	43.74	16.36	44.00	16.39	43.80	16.36	44.00	16.41	43.86	16.33	43.86	16.44	43.80	16.45	43.85	16.38	43.80
Skewness	0.132	-0.539	0.096	-0.523	0.109	-0.554	0.100	-0.525	0.097	-0.559	0.069	-0.549	0.123	-0.551	0.061	-0.565	0.073	-0.537	0.100	-0.535
Kurtosis	-0.031	-0.484	-0.001	-0.500	0.094	-0.468	0.040	-0.506	0.080	-0.438	0.022	-0.428	0.104	-0.468	0.057	-0.414	0.021	-0.472	0.086	-0.501
Coefficient of variability	0.131	0.258	0.132	0.257	0.131	0.258	0.134	0.259	0.130	0.256	0.133	0.254	0.131	0.258	0.130	0.255	0.131	0.256	0.131	0.261
Mean Standard Error	0.069	0.176	0.069	0.176	0.069	0.176	0.069	0.176	0.069	0.176	0.069	0.176	0.070	0.176	0.069	0.176	0.070	0.176	0.069	0.176
Correlation	Porosity	Water Sat.	Porosity	Water Sat.	Porosity	Water Sat.	Porosity	Water Sat.	Porosity	Water Sat.	Porosity	Water Sat.	Porosity	Water Sat.	Porosity	Water Sat.	Porosity	Water Sat.	Porosity	Water Sat.
Porosity	1.0000	-0.6276	1.0000	-0.6276	1.0000	-0.6438	1.0000	-0.6374	1.0000	-0.6392	1.0000	-0.6400	1.0000	-0.6359	1.0000	-0.6284	1.0000	-0.6243	1.0000	-0.6367
Water Saturation		1.0000		1.0000		1.0000		1.0000		1.0000		1.0000		1.0000		1.0000		1.0000		1.0000
Permeability	0.6676	-0.5452	0.6670	-0.5393	0.6756	-0.5524	0.6686	-0.5414	0.6718	-0.5453	0.6633	-0.5454	0.6712	-0.5472	0.6623	-0.5426	0.6704	-0.5416	0.6715	-0.5520
Resistivity	0.6357	-0.6234	0.6388	-0.6222	0.6442	-0.6380	0.6407	-0.6248	0.6403	-0.6305	0.6412	-0.6306	0.6449	-0.6270	0.6370	-0.6282	0.6379	-0.6256	0.6384	-0.6310

Realization Number #	11		12		13		14		15		16		17		18		19		20	
	Simulated		Simulated		Simulated		Simulated		Simulated		Simulated		Simulated		Simulated		Simulated		Simulated	
Statistical Data	Porosity	Water Sat.	Porosity	Water Sat.	Porosity	Water Sat.	Porosity	Water Sat.	Porosity	Water Sat.	Porosity	Water Sat.	Porosity	Water Sat.	Porosity	Water Sat.	Porosity	Water Sat.	Porosity	Water Sat.
No. of realization	57.330	57.330	57.330	57.330	57.330	57.330	57.330	57.330	57.330	57.330	57.330	57.330	57.330	57.330	57.330	57.330	57.330	57.330	57.330	57.330
No. of simulated	57.330	57.330	57.330	57.330	57.330	57.330	57.330	57.330	57.330	57.330	57.330	57.330	57.330	57.330	57.330	57.330	57.330	57.330	57.330	57.330
No. of unsimulated	0	0	0	0	0	0	0	0	0	0	0	0	0	0	0	0	0	0	0	0
Mean	16.65	42.28	16.63	42.05	16.60	42.13	16.62	41.77	16.61	41.84	16.56	42.17	16.66	42.12	16.68	42.09	16.64	42.30	16.63	42.08
Std. Deviation	2.19	10.83	2.18	10.79	2.23	10.86	2.20	11.09	2.17	10.97	2.19	10.97	2.19	10.84	2.16	10.97	2.19	10.87	2.19	10.77
Variance	4.79	117.34	4.75	114.49	4.97	119.86	4.84	123.06	4.71	118.69	4.70	119.02	4.78	117.50	4.68	116.05	4.84	119.00	4.79	116.02
Minimum	10.00	14.80	10.00	14.80	10.00	14.80	10.00	14.80	10.00	14.80	10.00	14.80	10.00	14.80	10.00	14.80	10.00	14.80	10.00	14.80
Maximum	22.69	60.00	22.70	60.00	22.70	60.00	22.69	60.00	22.70	60.00	22.70	60.00	22.70	60.00	22.69	60.00	22.70	60.00	22.70	60.00
Median	16.41	44.10	16.37	43.78	16.38	43.87	16.38	43.70	16.37	43.70	16.30	43.90	16.40	43.85	16.32	43.85	16.40	44.10	16.40	43.80
Skewness	0.088	-0.573	0.116	-0.541	0.064	-0.543	0.117	-0.522	0.096	-0.519	0.101	-0.562	0.144	-0.539	0.091	-0.551	0.094	-0.470	0.077	-0.558
Kurtosis	0.021	-0.433	0.068	-0.466	0.076	-0.479	0.026	-0.540	-0.015	-0.625	0.112	-0.462	0.044	-0.481	0.094	-0.467	0.019	-0.426	0.032	-0.436
Coefficient of variability	0.131	0.256	0.131	0.257	0.134	0.258	0.132	0.266	0.131	0.260	0.131	0.259	0.131	0.258	0.131	0.258	0.132	0.258	0.132	0.256
Mean Standard Error	0.070	0.177	0.069	0.176	0.069	0.176	0.069	0.174	0.069	0.175	0.069	0.176	0.070	0.176	0.069	0.176	0.070	0.177	0.069	0.176
Correlation	Porosity	Water Sat.	Porosity	Water Sat.	Porosity	Water Sat.	Porosity	Water Sat.	Porosity	Water Sat.	Porosity	Water Sat.	Porosity	Water Sat.	Porosity	Water Sat.	Porosity	Water Sat.	Porosity	Water Sat.
Porosity	1.0000	-0.6360	1.0000	-0.6197	1.0000	-0.6343	1.0000	-0.6490	1.0000	-0.6372	1.0000	-0.6316	1.0000	-0.6413	1.0000	-0.6356	1.0000	-0.6483	1.0000	-0.6302
Water Saturation		1.0000		1.0000		1.0000		1.0000		1.0000		1.0000		1.0000		1.0000		1.0000		1.0000
Permeability	0.6692	-0.5454	0.6668	-0.5410	0.6665	-0.5430	0.6688	-0.5383	0.6649	-0.5487	0.6664	-0.5506	0.6744	-0.5444	0.6656	-0.5440	0.6678	-0.5363	0.6668	-0.5419
Resistivity	0.6396	-0.6318	0.6377	-0.6257	0.6379	-0.6300	0.6405	-0.6331	0.6321	-0.6313	0.6331	-0.6321	0.6453	-0.6252	0.6387	-0.6267	0.6416	-0.6379	0.6385	-0.6309

Realization Number #	21		22		23		24		25		26		27		28		29		30	
	Simulated		Simulated		Simulated		Simulated		Simulated		Simulated		Simulated		Simulated		Simulated		Simulated	
Statistical Data	Porosity	Water Sat.	Porosity	Water Sat.	Porosity	Water Sat.	Porosity	Water Sat.	Porosity	Water Sat.	Porosity	Water Sat.	Porosity	Water Sat.	Porosity	Water Sat.	Porosity	Water Sat.	Porosity	Water Sat.
No. of realization	57.330	57.330	57.330	57.330	57.330	57.330	57.330	57.330	57.330	57.330	57.330	57.330	57.330	57.330	57.330	57.330	57.330	57.330	57.330	57.330
No. of simulated	57.330	57.330	57.330	57.330	57.330	57.330	57.330	57.330	57.330	57.330	57.330	57.330	57.330	57.330	57.330	57.330	57.330	57.330	57.330	57.330
No. of unsimulated	0	0	0	0	0	0	0	0	0	0	0	0	0	0	0	0	0	0	0	0
Mean	16.60	42.23	16.59	42.40	16.59	42.19	16.59	42.24	16.59	42.30	16.60	42.30	16.60	42.30	16.59	42.29	16.56	42.29	16.58	42.29
Std. Deviation	2.17	10.90	2.17	10.92	2.16	10.91	2.20	10.60	2.20	10.69	2.19	10.90	2.19	10.95	2.18	10.90	2.17	10.88	2.10	10.81
Variance	4.70	118.81	4.73	118.54	4.68	118.76	4.86	112.27	4.83	114.25	4.75	118.88	4.80	119.87	4.76	116.81	4.72	117.99	4.75	116.79
Minimum	10.00	14.80	10.00	14.80	10.00	14.80	10.00	14.80	10.00	14.80	10.00	14.80	10.00	14.80	10.00	14.80	10.00	14.80	10.00	14.80
Maximum	22.70	60.00	22.70	60.00	22.70	60.00	22.70	60.00	22.70	60.00	22.70	60.00	22.70	60.00	22.70	60.00	22.70	60.00	22.70	60.00
Median	16.39	44.00	16.33	44.10	16.33	44.01	16.35	43.85	16.35	44.00	16.36	43.70	16.35	43.80	16.35	43.91	16.35	43.91	16.44	43.70
Skewness	0.107	-0.559	0.108	-0.563	0.130	-0.561	0.117	-0.540	0.088	-0.567	0.116	-0.517	0.132	-0.540	0.136	-0.520	0.101	-0.551	0.069	-0.542
Kurtosis	0.110	-0.454	0.088	-0.452	0.048	-0.466	0.070	-0.430	0.092	-0.421	0.082	-0.489	0.085	-0.505	0.053	-0.489	0.030	-0.460	0.058	-0.454
Coefficient of variability	0.130	0.258	0.13																	

B.2: Statistics of porosity and water saturation for each of 100 realizations from SGCOSIM-local and global distribution (continued).

Realization Number #	51		52		53		54		55		56		57		58		59		60	
	Simulated		Simulated		Simulated		Simulated		Simulated		Simulated		Simulated		Simulated		Simulated		Simulated	
Statistical Data	Porosity	Water Sat.	Porosity	Water Sat.	Porosity	Water Sat.	Porosity	Water Sat.	Porosity	Water Sat.	Porosity	Water Sat.	Porosity	Water Sat.	Porosity	Water Sat.	Porosity	Water Sat.	Porosity	Water Sat.
No. of realization	57.330	57.330	57.330	57.330	57.330	57.330	57.330	57.330	57.330	57.330	57.330	57.330	57.330	57.330	57.330	57.330	57.330	57.330	57.330	57.330
No. of simulated	57.330	57.330	57.330	57.330	57.330	57.330	57.330	57.330	57.330	57.330	57.330	57.330	57.330	57.330	57.330	57.330	57.330	57.330	57.330	57.330
No. of unsimulated	0	0	0	0	0	0	0	0	0	0	0	0	0	0	0	0	0	0	0	0
Mean	16.64	41.98	16.62	42.09	16.59	42.03	16.60	41.81	16.65	42.11	16.68	42.02	16.67	42.07	16.61	42.10	16.68	41.76	16.63	41.85
Std. Deviation	2.23	10.87	2.16	10.93	2.16	10.99	2.18	11.00	2.17	10.89	2.15	10.86	2.18	10.86	2.18	10.77	2.20	11.02	2.17	10.87
Variance	4.96	118.08	4.65	119.46	4.65	120.67	4.73	120.93	4.70	118.99	4.64	118.04	4.73	117.84	4.77	116.00	4.85	121.33	4.71	118.20
Minimum	10.00	14.90	10.00	14.90	10.00	14.90	10.00	14.90	10.00	14.90	10.00	14.90	10.00	14.90	10.00	14.90	10.00	14.90	10.00	14.90
Maximum	22.70	60.00	22.70	60.00	22.70	60.00	22.70	60.00	22.70	60.00	22.70	60.00	22.70	60.00	22.70	60.00	22.70	60.00	22.70	60.00
Median	16.41	43.80	16.40	43.88	16.34	43.80	16.33	43.70	16.40	43.88	16.43	43.79	16.44	43.80	16.37	43.80	16.44	43.70	16.41	43.70
Skewness	0.076	-0.543	0.071	-0.568	0.068	-0.545	0.117	-0.505	0.112	-0.543	0.108	-0.534	0.068	-0.538	0.067	-0.563	0.069	-0.523	0.050	-0.529
Kurtosis	0.043	-0.489	0.087	-0.437	0.130	-0.486	0.051	-0.538	0.005	-0.487	0.049	-0.492	0.065	-0.485	0.043	-0.436	0.004	-0.528	0.062	-0.484
Coefficient of variability	0.134	0.259	0.130	0.260	0.130	0.261	0.131	0.263	0.130	0.259	0.129	0.259	0.131	0.258	0.131	0.256	0.132	0.264	0.131	0.260
Mean Standard Error	0.069	0.175	0.069	0.176	0.069	0.176	0.069	0.175	0.070	0.176	0.070	0.175	0.069	0.176	0.069	0.176	0.070	0.174	0.069	0.175
Correlation	Porosity	Water Sat.	Porosity	Water Sat.	Porosity	Water Sat.	Porosity	Water Sat.	Porosity	Water Sat.	Porosity	Water Sat.	Porosity	Water Sat.	Porosity	Water Sat.	Porosity	Water Sat.	Porosity	Water Sat.
Porosity	1.0000	-0.6458	1.0000	-0.6253	1.0000	-0.6430	1.0000	-0.6335	1.0000	-0.6370	1.0000	-0.6456	1.0000	-0.6419	1.0000	-0.6327	1.0000	-0.6449	1.0000	-0.6371
Water Saturation		1.0000		1.0000		1.0000		1.0000		1.0000		1.0000		1.0000		1.0000		1.0000		1.0000
Permeability	0.6681	-0.5494	0.6627	-0.5497	0.6688	-0.5577	0.6687	-0.5420	0.6632	-0.5509	0.6675	-0.5471	0.6658	-0.5475	0.6638	-0.5517	0.6660	-0.5493	0.6623	-0.5550
Resistivity	0.6436	-0.6312	0.6328	-0.6328	0.6404	-0.6400	0.6388	-0.6275	0.6342	-0.6309	0.6419	-0.6278	0.6384	-0.6337	0.6338	-0.6340	0.6378	-0.6311	0.6336	-0.6305

Realization Number #	61		62		63		64		65		66		67		68		69		70	
	Simulated		Simulated		Simulated		Simulated		Simulated		Simulated		Simulated		Simulated		Simulated		Simulated	
Statistical Data	Porosity	Water Sat.	Porosity	Water Sat.	Porosity	Water Sat.	Porosity	Water Sat.	Porosity	Water Sat.	Porosity	Water Sat.	Porosity	Water Sat.	Porosity	Water Sat.	Porosity	Water Sat.	Porosity	Water Sat.
No. of realization	57.330	57.330	57.330	57.330	57.330	57.330	57.330	57.330	57.330	57.330	57.330	57.330	57.330	57.330	57.330	57.330	57.330	57.330	57.330	57.330
No. of simulated	57.330	57.330	57.330	57.330	57.330	57.330	57.330	57.330	57.330	57.330	57.330	57.330	57.330	57.330	57.330	57.330	57.330	57.330	57.330	57.330
No. of unsimulated	0	0	0	0	0	0	0	0	0	0	0	0	0	0	0	0	0	0	0	0
Mean	16.67	42.00	16.63	42.12	16.60	42.15	16.61	41.98	16.61	42.80	16.63	41.82	16.62	42.13	16.61	42.14	16.64	41.98	16.59	42.03
Std. Deviation	2.23	10.95	2.20	10.96	2.16	11.03	2.20	10.93	2.18	10.71	2.21	10.93	2.20	10.80	2.21	10.98	2.19	10.96	2.18	10.86
Variance	4.96	120.00	4.84	120.05	4.77	121.59	4.85	117.16	4.74	114.65	4.93	119.45	4.82	116.81	4.90	118.04	4.77	119.87	4.73	116.34
Minimum	10.00	14.90	10.00	14.90	10.00	14.90	10.00	14.90	10.00	14.90	10.00	14.90	10.00	14.90	10.00	14.90	10.00	14.90	10.00	14.90
Maximum	22.70	60.00	22.70	60.00	22.70	60.00	22.70	60.00	22.70	60.00	22.70	60.00	22.70	60.00	22.70	60.00	22.70	60.00	22.70	60.00
Median	16.43	43.70	16.38	43.90	16.39	43.86	16.40	43.70	16.37	44.18	16.40	43.70	16.40	43.90	16.36	43.90	16.41	43.80	16.32	43.74
Skewness	0.076	-0.531	0.125	-0.548	0.084	-0.535	0.040	-0.542	0.084	-0.584	0.078	-0.497	0.062	-0.561	0.112	-0.560	0.065	-0.545	0.121	-0.540
Kurtosis	0.009	-0.489	0.019	-0.489	0.057	-0.507	0.093	-0.468	0.050	-0.362	0.038	-0.536	0.000	-0.446	0.058	-0.466	0.068	-0.495	0.098	-0.473
Coefficient of variability	0.134	0.261	0.132	0.260	0.132	0.262	0.133	0.258	0.131	0.251	0.133	0.261	0.132	0.256	0.133	0.258	0.131	0.261	0.131	0.259
Mean Standard Error	0.070	0.175	0.069	0.176	0.069	0.176	0.069	0.175	0.069	0.178	0.069	0.175	0.069	0.176	0.069	0.176	0.069	0.176	0.069	0.176
Correlation	Porosity	Water Sat.	Porosity	Water Sat.	Porosity	Water Sat.	Porosity	Water Sat.	Porosity	Water Sat.	Porosity	Water Sat.	Porosity	Water Sat.	Porosity	Water Sat.	Porosity	Water Sat.	Porosity	Water Sat.
Porosity	1.0000	-0.6437	1.0000	-0.6481	1.0000	-0.6445	1.0000	-0.6252	1.0000	-0.6314	1.0000	-0.6472	1.0000	-0.6383	1.0000	-0.6430	1.0000	-0.6387	1.0000	-0.6363
Water Saturation		1.0000		1.0000		1.0000		1.0000		1.0000		1.0000		1.0000		1.0000		1.0000		1.0000
Permeability	0.6675	-0.5492	0.6717	-0.5493	0.6669	-0.5520	0.6598	-0.5460	0.6644	-0.5475	0.6679	-0.5518	0.6643	-0.5459	0.6737	-0.5510	0.6653	-0.5532	0.6710	-0.5470
Resistivity	0.6411	-0.6343	0.6404	-0.6277	0.6386	-0.6323	0.6326	-0.6253	0.6357	-0.6342	0.6354	-0.6281	0.6366	-0.6286	0.6349	-0.6336	0.6363	-0.6325	0.6438	-0.6290

Realization Number #	71		72		73		74		75		76		77		78		79		80	
	Simulated		Simulated		Simulated		Simulated		Simulated		Simulated		Simulated		Simulated		Simulated		Simulated	
Statistical Data	Porosity	Water Sat.	Porosity	Water Sat.	Porosity	Water Sat.	Porosity	Water Sat.	Porosity	Water Sat.	Porosity	Water Sat.	Porosity	Water Sat.	Porosity	Water Sat.	Porosity	Water Sat.	Porosity	Water Sat.
No. of realization	57.330	57.330	57.330	57.330	57.330	57.330	57.330	57.330	57.330	57.330	57.330	57.330	57.330	57.330	57.330	57.330	57.330	57.330	57.330	57.330
No. of simulated	57.330	57.330	57.330	57.330	57.330	57.330	57.330	57.330	57.330	57.330	57.330	57.330	57.330	57.330	57.330	57.330	57.330	57.330	57.330	57.330
No. of unsimulated	0	0	0	0	0	0	0	0	0	0	0	0	0	0	0	0	0	0	0	0
Mean	16.60	42.34	16.60	42.23	16.62	41.91	16.64	42.15	16.61	42.24	16.61	42.18	16.63	42.24	16.62	42.22	16.60	42.16	16.58	42.15
Std. Deviation	2.16	10.85	2.21	10.71	2.21	10.98	2.20	10.93	2.16	10.75	2.17	10.83	2.19	10.82	2.22	10.71	2.19	10.71	2.20	10.81
Variance	4.73	117.80	4.89	114.75	4.85	119.28	4.84	119.40	4.74	115.58	4.69	117.25	4.79	116.87	4.92	114.73	4.78	114.70	4.85	116.92
Minimum	10.00	14.90	10.00	14.90	10.00	14.90	10.00	14.90	10.00	14.90	10.00	14.90	10.00	14.90	10.00	14.90	10.00	14.90	10.00	14.90
Maximum	22.70	60.00	22.70	60.00	22.70	60.00	22.70	60.00	22.70	60.00	22.70	60.00	22.70	60.00	22.70	60.00	22.70	60.00	22.70	60.00
Median	16.33	44.10	16.34	43.87	16.40	43.70	16.41	43.88	16.34	43.84	16.37	43.90	16.40	44.28	16.35	43.94	16.36	43.80	16.34	43.84
Skewness	0.142	-0.581	0.109	-0.565	0.043	-0.533	0.109	-0.540	0.130	-0.544	0.115	-0.555	0.106	-0.602	0.135	-0.564	0.104	-0.548	0.065	-0.529
Kurtosis	0.089	-0.412	0.013	-0.398	0.092	-0.504	0.041	-0.499	0.056	-0.429	0.010	-0.453	0.061	-0.370	0.002	-0.437	0.146	-0.452	0.078	-0.468
Coefficient of variability	0.131	0.256</																		

## APPENDIX C

C.1: OGIP resulted from SGS-local and global distribution for 100 realizations of variables.

Realization Number	OGIP from SGS-local and global distribution (Bcf)	Realization Number	OGIP from SGS-local and global distribution (Bcf)	Realization Number	OGIP from SGS-local and global distribution (Bcf)
1	15.01	35	15.22	68	15.42
2	14.60	36	14.81	69	14.38
3	14.70	37	15.10	70	14.82
4	15.08	38	14.86	71	14.82
5	14.81	39	15.20	72	15.13
6	15.37	40	15.46	73	15.29
7	14.58	41	15.56	74	14.50
8	14.63	42	14.73	75	14.74
9	14.70	43	15.17	76	14.79
10	14.36	44	14.26	77	14.71
11	15.17	45	14.74	78	14.87
12	15.25	46	14.30	79	14.87
13	14.73	47	14.42	80	14.69
14	14.92	48	15.21	81	14.61
15	14.42	49	14.79	82	14.62
16	15.38	50	14.49	83	14.60
17	14.61	51	15.19	84	14.92
18	14.79	52	15.04	85	14.81
19	14.79	53	15.35	86	14.86
20	14.75	54	14.99	87	14.92
21	14.80	55	14.77	88	15.07
22	15.04	56	14.99	89	14.89
23	14.63	57	15.21	90	14.41
24	14.82	58	14.76	91	14.85
25	14.89	59	15.28	92	14.72
26	14.74	60	14.35	93	14.92
27	15.05	61	14.66	94	14.85
28	14.45	62	14.79	95	14.84
29	14.48	63	14.59	96	14.86
30	14.51	64	14.98	97	15.30
31	14.78	65	14.62	98	14.70
32	14.33	66	14.73	99	14.83
33	14.94	67	14.69	100	15.07
34	14.93				

C.2: OGIP resulted from SGCOSIM-local and global distribution for 100 realizations of variables.

Realization Number	OGIP from SGCOSIM-local and global distribution (Bcf)	Realization Number	OGIP from SGCOSIM-local and global distribution (Bcf)	Realization Number	OGIP from SGCOSIM-local and global distribution (Bcf)
1	15.17	35	15.23	68	15.18
2	15.20	36	15.12	69	15.25
3	15.15	37	15.23	70	15.18
4	15.22	38	15.19	71	15.11
5	15.14	39	15.11	72	15.13
6	15.19	40	15.16	73	15.24
7	15.17	41	15.16	74	15.20
8	15.19	42	15.21	75	15.15
9	15.24	43	15.10	76	15.16
10	15.20	44	15.18	77	15.06
11	15.17	45	15.19	78	15.16
12	15.20	46	15.18	79	15.15
13	15.17	47	15.10	80	15.14
14	15.29	48	15.09	81	15.13
15	15.25	49	15.11	82	15.26
16	15.12	50	15.14	83	15.23
17	15.23	51	15.25	84	15.21
18	15.16	52	15.19	85	15.27
19	15.17	53	15.19	86	15.30
20	15.21	54	15.26	87	15.28
21	15.16	55	15.22	88	15.15
22	15.09	56	15.26	89	15.18
23	15.14	57	15.24	90	15.22
24	15.13	58	15.18	91	15.11
25	15.10	59	15.34	92	15.11
26	15.21	60	15.26	93	15.20
27	15.22	61	15.27	94	15.12
28	15.20	62	15.21	95	15.13
29	15.09	63	15.17	96	15.18
30	15.26	64	15.21	97	15.19
31	15.21	65	15.05	98	15.23
32	15.28	66	15.28	99	15.16
33	15.33	67	15.19	100	15.17
34	15.15				

## Vitae

Patchalalai Isarangkura was born on November 7, 1973 in Bangkok, Thailand. She received her B. Eng. in Chemical Engineering from Faculty of Engineering, Rangsit University in 1993. She also received her MBA from School of Business Administration, National Institute of Development and Administration in 1997. She has been a graduate student in the Master's Degree Program in Petroleum Engineering of the Department of Mining and Petroleum Engineering, Chulalongkorn University since 2002.



สถาบันวิทยบริการ  
จุฬาลงกรณ์มหาวิทยาลัย